

# Average Scattered Field From a PEMC Cylinder With Random Radius



**Fahad Masood**

A Thesis Submitted in Partial Fulfillment of the Requirements  
for the Degree of  
Doctor of Philosophy  
At  
Department of Electronics  
Quaid-i-Azam University  
Islamabad, Pakistan  
September 2021

© Copyright by Fahad Masood, 2021



**QUAID-I-AZAM UNIVERSITY**  
**Department of Electronics**

**Author's Declaration**

I, **Fahad Masood** hereby state that my PhD thesis titled  
**"Average scattered field from a PEMC cylinder with random  
radius"** is my own work and has not been submitted previously by  
me for taking degree from **Department of Electronics, Quaid-i-  
Azam University** Or anywhere else in the country/world.

At any time if my statement is found to be incorrect even after my  
graduation, the university has the right to withdraw my PhD  
degree.

A handwritten signature in black ink, appearing to read 'Fahad Masood'.

**Fahad Masood**

**Date: 20-09-2021**



**QUAID-I-AZAM UNIVERSITY**  
**Department of Electronics**

**Plagiarism Undertaking**

I solemnly declare that research work presented in the thesis titled

**"Average scattered field from a PEMC cylinder with random radius."**

is solely my research work with no significant contribution from any other person. Small contribution/help wherever taken has been duly acknowledged and that complete thesis has been written by me.

I understand the zero tolerance policy of the HEC and Quaid-i-Azam University towards plagiarism. Therefore, I as an Author of the above titled thesis, declare that no portion of my thesis has been plagiarized and any material used as reference is properly referred/cited.

I undertake that if I am found guilty of any formal plagiarism in the above titled thesis even after award of PhD degree, the University reserves the rights to withdraw/revoke my PhD degree and that HEC and the University has the right to publish my name on the HEC/University Website on which names of students are placed who submitted plagiarized thesis.

Student/Author Signature: \_\_\_\_\_

A handwritten signature in black ink, appearing to read 'Fahad Masood', written over a horizontal line.

Name: **Fahad Masood**




**QUAID-I-AZAM UNIVERSITY**  
**Department of Electronics**

**Certificate of Approval**

This is to certify that the research work presented in this thesis, entitled "Average scattered field from a PEMC cylinder with random radius" was conducted by Mr. Fahad Masood under the supervision of Dr. Muhammad Arshad Fiaz and under the co-supervision of Dr. Muhammad Aqueel Ashraf. No part of this thesis has been submitted anywhere else for any other degree. This thesis is submitted to the Department of Electronics, Quaid-i-Azam University in partial fulfillment of the requirements for the degree of Doctor of Philosophy in Field of Electronics, Department of Electronics, Quaid-i-Azam University.

Student Name: Mr. Fahad Masood

Signature: 

**Examination Committee:**

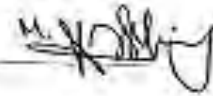
A. Dr. Akhtar Hussain  
General Manager,  
National Development Complex (NDC),  
P.O.Box 1702, Islamabad.

Signature: 

B. Dr. Khuram Saleem Alimgier  
Assistant Professor  
Department of Electrical and Computer Engineering,  
COMSATS University, Park Road, Chak Shahzad,  
Islamabad.

Signature: 

C. Dr. Muhammad Arshad Fiaz  
Assistant Professor & Supervisor  
Department of Electronics  
Quaid-i-Azam University, Islamabad.

Signature: 

D. Dr. Muhammad Aqueel Ashraf  
Associate Professor & Co-Supervisor  
Department of Electronics  
Quaid-i-Azam University, Islamabad.

Signature: 

Supervisor Name: Dr. Muhammad Arshad Fiaz

Signature: 

Co-Supervisor Name: Dr. Muhammad Aqueel Ashraf

Signature: 

Name of Chairman: Prof. Dr. Syed Aqeel A. Bukhari

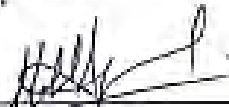
Signature: 

**DEPARTMENT OF ELECTRONICS  
QUAID-I-AZAM UNIVERSITY  
ISLAMABAD**

It is certified that the work contained in the dissertation titled "**Average Scattered Field From a PEMC Cylinder With Random Radius**" is carried out and completed by **Mr. Fahad Musood** under my supervision at Quaid-i-Azam University, Islamabad, Pakistan.

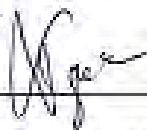


**Advisor**  
Dr. Muhammad Arshad Fiaz  
Assistant Professor  
Department of Electronics  
Quaid-i-Azam University, Islamabad  
Pakistan



**Co Supervisor**  
Dr. Muhammad Aqueel Ashraf  
Associate Professor  
Department of Electronics  
Quaid-i-Azam University, Islamabad  
Pakistan

Submitted through:



**Chairman**  
Prof. Dr. Syed Aqeel Abbas Bukhari  
Department of Electronics  
Quaid-i-Azam University, Islamabad  
Pakistan

*To my parents and family.*

# Table of Contents

<b>Table of Contents</b>	<b>vi</b>
<b>List of Figures</b>	<b>viii</b>
<b>Acknowledgements</b>	<b>xiii</b>
<b>List of publications included in the thesis</b>	<b>xiv</b>
<b>List of publications not included in the thesis</b>	<b>xv</b>
<b>1 Introduction</b>	<b>1</b>
1.1 Realization of a PEMC boundary . . . . .	2
1.2 Scattering from deterministic boundaries . . . . .	3
1.3 Scattering from random boundaries . . . . .	4
1.4 RC models . . . . .	5
1.5 Thesis overview and scientific contribution . . . . .	6
<b>2 Average scattered field from a PEC cylinder with random radius</b>	<b>9</b>
2.1 Problem description and formulation . . . . .	9
2.2 Evaluation of average scattered field . . . . .	11
2.2.1 Uniform Distribution . . . . .	13
2.2.2 Normal Distribution . . . . .	14
2.3 Numerical results . . . . .	15
<b>3 Average scattered field from a PEMC cylinder with random size</b>	<b>25</b>
3.1 Problem description and formulation . . . . .	25
3.1.1 Uniform Distribution . . . . .	28
3.1.2 Normal Distribution . . . . .	30
3.2 Numerical results . . . . .	31

<b>4</b>	<b>Scattered field from a random PEC cylinder with arbitrary shape using the perturbation theory</b>	<b>44</b>
4.1	Problem formulation . . . . .	44
4.1.1	Solution for TM Polarization . . . . .	46
4.1.2	Solution for TE Polarization . . . . .	47
4.2	RC Generation and Results . . . . .	49
<b>5</b>	<b>Scattered field from a random PEMC cylinder with arbitrary shape using the perturbation theory</b>	<b>61</b>
5.1	Problem formulation . . . . .	61
5.1.1	TM polarization . . . . .	62
5.1.2	TE polarization . . . . .	68
5.2	Numerical Results . . . . .	72
<b>6</b>	<b>Conclusion</b>	<b>90</b>
<b>7</b>	<b>Appendix</b>	<b>92</b>
7.1	Taylor series of $\frac{1}{z(a^2)}$ about $a = \langle a \rangle$ . . . . .	92
7.2	Evaluation of integral $I_1$ . . . . .	92
7.3	Evaluation of integral $I_2$ . . . . .	93
	<b>References</b>	<b>94</b>



# List of Figures

1.1	Flow chart of the thesis. . . . .	8
2.1	Geometry of the scattering problem. . . . .	10
2.2	Average scattering cross section of a very small PEC cylinder of random radius with uniform distribution where $a_1 = 0.01\lambda$ , $a_2 = 0.06\lambda$ . Results are shown using both analytic and numerical average. . . . .	16
2.3	Scattering cross section (normalized) of a small PEC cylinder of random radius with uniform distribution for TM polarization where $a_1 = 0.1\lambda$ and $a_2 = 0.6\lambda$ . . . . .	17
2.4	Scattering cross section (normalized) of a large PEC cylinder of random radius with uniform distribution for TM polarization where $a_1 = 1\lambda$ and $a_2 = 6\lambda$ . . . . .	18
2.5	Scattering cross section (normalized) of a small PEC cylinder of random radius with uniform distribution for TE polarization where $a_1 = 0.1\lambda$ and $a_2 = 0.6\lambda$ . . . . .	19
2.6	Scattering cross section (normalized) of a large PEC cylinder of random radius with uniform distribution for TE polarization where $a_1 = 1\lambda$ and $a_2 = 6\lambda$ . . . . .	20
2.7	Same as Figure (2.3) except that normal distribution with $s_a = 0.25$ is considered. . . . .	21
2.8	Same as Figure (2.4) except that normal distribution with $s_a = 0.25$ is considered. . . . .	22

2.9	Same as Figure (2.5) except that normal distribution with $s_a = 0.25$ is considered. . . . .	23
2.10	Same as Figure (2.6) except that normal distribution with $s_a = 0.25$ is considered. . . . .	24
3.1	A linearly polarized plane wave is incident upon a random PEMC cylinder. . . . .	26
3.2	Co and cross polarized scattered field from a PEMC cylinder. . . . .	33
3.3	Cross polarized scattering cross section (normalized) of a very small PEMC cylinder of random radius with uniform distribution where $a_1 = 0.01\lambda$ and $a_2 = 0.06\lambda$ . . . . .	33
3.4	Co polarized scattering cross section (normalized) of a small PEMC cylinder of random radius with uniform distribution where $a_1 = 0.1\lambda$ and $a_2 = 0.6\lambda$ . . . . .	34
3.5	Cross polarized scattering cross section (normalized) of a small PEMC cylinder of random radius with uniform distribution where $a_1 = 0.1\lambda$ and $a_2 = 0.6\lambda$ . . . . .	35
3.6	Co polarized scattering cross section (normalized) of a large PEMC cylinder of random radius with uniform distribution where $a_1 = 1\lambda$ and $a_2 = 6\lambda$ . . . . .	36
3.7	Cross polarized scattering cross section (normalized) of a large PEMC cylinder of random radius with uniform distribution where $a_1 = 1\lambda$ and $a_2 = 6\lambda$ . . . . .	37
3.8	Same as Figure (3.4) except that normal distribution with $s_a = 0.25$ is considered. . . . .	38
3.9	Same as Figure (3.5) except that normal distribution with $s_a = 0.25$ is considered. . . . .	39
3.10	Same as Figure (3.6) except that normal distribution with $s_a = 0.25$ is considered. . . . .	40

3.11	Same as Figure (3.7) except that normal distribution with $s_a = 0.25$ is considered. . . . .	41
3.12	Co polarized scattering cross section (normalized) of a PEMC cylinder of random radius with normal distribution for different values of standard deviation. . . . .	42
3.13	Cross polarized scattering cross section (normalized) of a PEMC cylinder of random radius with normal distribution for different values of standard deviation. . . . .	43
4.1	A circular random PEC cylinder illuminated by TM/TE polarized incident field. . . . .	45
4.2	Generation of the random cylinder with $a = 0.5\lambda$ . . . . .	52
4.3	Comparison of scattered field from a perturbed PEC cylinder using the PT with that obtained using the MoM where $a = 0.5\lambda$ , $B = 0.005$ and $N = 5$ . . . . .	53
4.4	Same as figure (4.3) except that radius $a = 1\lambda$ is assumed. . . . .	53
4.5	Scattered field from a perturbed PEC cylinder with mean radius $a = 0.5\lambda$ and $N = 5$ . . . . .	54
4.6	Same as Figure (4.5) except that $a = 1\lambda$ is assumed. . . . .	55
4.7	Scattered field from a perturbed PEC cylinder for TM polarization where $a = 0.5\lambda$ and $B = 0.005$ . . . . .	56
4.8	Same as Figure (4.7) except that TE polarization is assumed. . . . .	56
4.9	Scattered field from a perturbed PEC cylinder for TM polarization where $a = 1\lambda$ and $B = 0.005$ . . . . .	57
4.10	Same as Figure (4.9) except that TE polarization is assumed. . . . .	57
4.11	Scattered field from a perturbed PEC cylinder for different values of B where $a = 0.5\lambda$ and TM polarized incident field is assumed. . . . .	58
4.12	Same as Figure (4.11) except that TE polarized incident field is assumed. . . . .	58
4.13	Scattered field from a perturbed PEC cylinder for different values of N where $a = 0.5\lambda$ and TM polarized incident field is assumed. . . . .	59

4.14	Same as Figure (4.13) except that TE polarized incident field is assumed.	59
4.15	Scattered field from a perturbed PEC cylinder for different values of 'a' where $B = 0.005$ , $N = 5$ and TM polarized incident field is assumed.	60
4.16	Same as Figure (4.15) except that TE polarized incident field is assumed.	60
5.1	A random PEMC cylinder with radius $a = 0.5\lambda$ .	62
5.2	Scattered field from a perturbed PEMC cylinder with mean radius $a = 0.5\lambda$ , $B=0.005$ , $M\eta_0 = 2$ and $N=5$ .	74
5.3	Same as Figure (5.2) except that a perturbed PEMC cylinder with mean radius $a = 1\lambda$ is assumed.	75
5.4	Two dimensional filed map of the scattered field from a perturbed PEMC cylinder with mean radius $a = 0.5\lambda$ , $N = 5$ and $M\eta_0 = 2$ . A TM polarized field is normally incident on the cylinder.	76
5.5	Same as Figure (5.4) except that a perturbed PEMC cylinder with mean radius $a = 1\lambda$ is assumed.	77
5.6	Two dimensional filed map of the scattered field from a perturbed PEMC cylinder with mean radius $a = 0.5\lambda$ , $N = 5$ and $M\eta_0 = 2$ . A TE polarized field is normally incident on the cylinder.	78
5.7	Same as Figure (5.6) except that a perturbed PEMC cylinder with mean radius $a = 1\lambda$ is considered.	79
5.8	Scattered field from a perturbed PEMC cylinder for different values of the perturbation parameter $B$ with mean radius $a = 0.5\lambda$ , $M\eta_0 = 2$ and $N=5$ .	80
5.9	Same as Figure (5.8) except that a perturbed PEMC cylinder with mean radius $a = 1\lambda$ is considered.	81
5.10	Two dimensional filed map of the scattered field from a perturbed PEMC cylinder for different values of $B$ with mean radius $a = 0.5\lambda$ , $N = 5$ and $M\eta_0 = 2$ . A TM polarized field is normally incident on the cylinder.	82

5.11	Same as figure (5.10) except that a TE polarized field is incident on the cylinder. . . . .	83
5.12	Scattered field from a perturbed PEMC cylinder for different values of $N$ with mean radius $a = 0.5\lambda$ , $M\eta_0 = 2$ and $B=0.005$ . . . . .	84
5.13	Same as Figure (5.12) except that a perturbed PEMC cylinder with mean radius $a = 1\lambda$ is considered. . . . .	85
5.14	Two dimensional field map of the scattered field from a perturbed PEMC cylinder for different values of $N$ with mean radius $a = 0.5\lambda$ , $B = 0.005$ and $M\eta_0 = 2$ . A TM polarized field is normally incident on the cylinder. . . . .	86
5.15	Same as figure (5.14) except that a TE polarized field is normally incident on the cylinder. . . . .	87
5.16	Scattered field from a perturbed PEMC cylinder for different values of $M\eta_0$ with mean radius $a = 0.5\lambda$ , $B = 0.005$ and $N=5$ . . . . .	88
5.17	Same as Figure (5.16) except that a perturbed PEMC cylinder with mean radius $a = 1\lambda$ is considered. . . . .	89

# Acknowledgements

With the grace of Almighty ALLAH who is the creator and guider of the universe. I would pay my acknowledgments to the Holy Prophet Mohammad (SAW), to whom this work is a humble dedication. I would like to thank those people who motivated and encouraged me to complete this work. I would like to thank my honorable and caring advisor Dr. M. Arshad Fiaz. Without his guidance and direction I am not able to complete this dissertation. I am thankful for consenting me precious suggestions. I could not have imagined having a better advisor for my Ph.D. other than Dr Muhammad Arshad Fiaz. I think this work would have not been possible without his kind supervision. I am also thankful to my co advisor Dr Muhammad Aqueel Ashraf for his guidance and cooperation throughout the studies.

I thank my friends Tehreem Qasim, Shahzad Hameed, Ashfaq Ahmad and Awais Ahmad for giving me company in this tenure. Moreover, I would like to thank my brother, sisters and every member of my family especially my wife for the continuous encouragement, prayers and support in my studies. Finally, I would like to dedicate this work to my parents, especially my father Mr. Masood Ahmad who motivated me at every stage of my studies.

Fahad Masood  
September 2021

# List of publications included in the thesis

1. F. Masood and M.A. Fiaz, “Evaluation of average cross-polarised scattered field from a PEMC cylinder of the random radius with uniform/normal distribution”, IET Microwaves, Antennas and propagation, Vol. 13, 804-812, 2019.
2. F. Masood, U. Amin, M.A. Fiaz and M.A. Ashraf, “On relating the perturbation theory and random cylinder generation to study scattered field”, Physical Communication, Vol. 39, 101003, 2020.
3. F. Masood, M.A. Fiaz and M.A Ashraf, “On applying the perturbation theory for the evaluation of near zone scattering properties of a perturbed PEMC cylinder”, Optik, Vol. 243, 166844, October 2021. .

## List of publications not included in the thesis

1. F. Masood and M.A. Fiaz, “On computing the average scattering cross section of a buried PEMC cylinder with uniformly/normally distributed radius”, Submitted for the publication, 2020.



## Abstract

Average scattered field from a perfect electric conductor (PEC) cylinder and perfect electromagnetic conductor (PEMC) cylinder with random radius is investigated. Uniform and normal distributions of the radius are considered. First, a very small cylinder is considered and analytical expressions for average scattered field can be written using small approximation of cylindrical wave functions. Co polarized average scattered field from a very small PEMC cylinder depends upon only zeroth order scattering coefficient while higher order coefficients contribute in cross polarized average scattered field. Zeroth order scattered field of a very small PEMC cylinder can be written as sum of zeroth and first order scattered field of a PEC cylinder. For a small and large cylinder, it is not possible to write down analytical expressions for average field so numerical average is done. Average scattered field from a small PEC cylinder of random radius differs from the scattered field from a PEC cylinder with mean radius for both transverse magnetic (TM) and transverse electric (TE) polarizations respectively. For a small PEMC cylinder it has been observed that the average co polarized scattered field is equal to scattered field from a cylinder with mean radius. This is not true in case of cross polarized scattered field and difference can be seen for most of the scattering angles. In case of large PEC/ PEMC cylinders it is worth mentioning that the average scattered field is almost equal to the scattered field from a cylinder with mean radius.

In the second problem, the perturbation theory (PT) is used to calculate the scattered field from a slightly perturbed PEC/PEMC cylinder for shape perturbation. Both transverse magnetic (TM) and transverse electric (TE) polarized incidence fields are considered. A relation between the PT and the model for random cylinder (RC) generation is developed which is important for the PT to remain valid during the numerical simulations. The scattered field expressions obtained using the PT are verified using the result obtained by method of moments (MoM) in case of a

PEC cylinder. The solution obtained by using the PT is more efficient in terms of simplicity and computational time. The scattering cross section for both the PEC and PEMC random cylinders is analyzed by varying the perturbation parameter  $B$  and the parameter describing the RC generation  $N$ . In particular, the distinctions due to perturbation are pronounced in the forward and backward scattering. It is noticeable that both  $B$  and  $N$  control the roughness of the cylinder and hence affect the scattering pattern.

# Chapter 1

## Introduction

Scattering from random boundaries and structures is an area of special interest for remote sensing and it can be applied in tropospheric wave propagation, wireless communication and radar technology, etc. Scattering is also very important phenomenon in modelling the channel for wireless communication. Owing to the random nature of the channel, it is difficult to predict the behaviour of the channel. The randomness could arise in two ways, either in the shape of the cylinder i.e., non circular/arbitrarily shaped structures or in the parameters such as radius, location etc. The applications also include semi deterministic wideband propagation for urban environments. Scattering properties of the structure depend on the physical and geometrical parameters such as size, material and shape of the object. Moreover, the hosting medium also affects the scattering pattern in cylindrical structures.

The interaction of electromagnetic waves with the scatterer depends upon the material of the scatterer. The scattering response varies a lot with the change of the material properties. It is hard to predict the behavior of the scattered field. In general, forward and backward scattering properties are of interest in many applications which have widely being investigated for many available naturally materials. With the advancement in science many artificial materials are engineered named metamaterials. Researchers took the challenge to explore the electromagnetic interaction with such materials.

In the literature, very little work has been found to study scattering from random

boundaries. In this research work, electromagnetic scattering from a perfect electromagnetic conductor (PEMC) random cylinder is studied. The aim is to calculate the analytical solution of the average field scattered from a PEMC cylinder for both random size and random shape. This chapter includes motivation of the research work and introduction to the main problem, literature review of the current research work for regular and irregular structures, contribution and outline of the thesis.

## 1.1 Realization of a PEMC boundary

Electromagnetic boundary conditions play an important role to describe the wave interaction of field and objects. For a perfect electric conductor (PEC) object, the tangential components of the electric field must be continuous [1], i.e.,

$$\vec{n} \times \vec{E} = 0 \quad (1.1.1)$$

where  $\vec{n}$  is the unit vector normal to the surface of the cylinder. The boundary condition for a perfect magnetic conductor (PMC) is often written in terms of magnetic field as,

$$\vec{n} \times \vec{H} = 0 \quad (1.1.2)$$

The boundary conditions described in equations (1.1.1) and (1.1.2) can be combined using the admittance parameter  $M$  as [2],

$$\vec{n} \times (M\vec{E} + \vec{H}) = 0 \quad (1.1.3)$$

For  $M \rightarrow \infty$ , boundary condition for PEC is extracted while the boundary condition for PMC is retrieved for  $M = 0$ . PEMC boundary is proposed by Lindell and Sihvola [3, 4]. It is reported that a layer of bi-isotropic Tellegen medium or gyrotropic anisotropic medium when added with a guiding structure acts as a PEMC boundary. Montaseri [5] et al. proposed the realization of the curved PEMC boundary. A PEMC boundary has been practically realized in [6]. Also, PEMC structure has been proposed using graphene sheet deposited onto a PEC backed dielectric layer in [7].

## 1.2 Scattering from deterministic boundaries

Scattered field from a PEC cylinder is investigated in [1]. Scattering width (SW) is observed for small as well as large radius of the object. For small radius of the object, it is observed that SW does not vary too much for all scattering angles. On the other hand, scattering width for large radius varies rapidly as a function of scattered angle. Scattering by dielectric cylinders is reported in [8]-[9] where scattered as well as transmitted field exists. Due to the presence of transmitted field, the radar cross section (RCS) may be small. Scattering by two nearby conducting cylinders is discussed in [10]. Scattered field from multiple cylinders have been reported in [11]-[12]. Yin et al. [13] studied the scattered field from an array of circular bi anisotropic cylinders for normal incidence while an oblique incidence is discussed in [14].

Scattering from a metamaterial object such as PEMC cylinder has been reported in [2]. For a special case  $M = 1/\eta_0$ , maximum cross polarized scattered field is observed where  $\eta_0$  is the impedance of the free space. It is also observed that for an unpolarized incident wave, scattering width is independent of the parameter  $M$ . Scattering by a PEMC elliptic cylinder is investigated in [15]. The analytical solution for the field is obtained using the method of separation of variables. Scattered field from parallel metamaterial cylinders is discussed in [16]. It is reported that the scattering cross section increases in forward direction for an array of cylinders which can be used for increasing the directivity of the antennas. Later on, many researchers discussed the various scattering scenarios such as PEMC cylinder coated with metamaterial [17]-[21].

Scattering from buried objects is another important class of the problem. In [22], scattering from a PEC cylinder under a dielectric half space is studied using spectral domain solution. Scattered field from a finite set of buried PEC cylinders is reported in [23] while dielectric circular cylinders are discussed in [24]. A semi analytical cylindrical wave approach is used to calculate the scattered field for both near and far zones. In [25], PEC cylinders buried below a dielectric slab is studied. Scattered field from a PEMC cylinder buried under a flat interface is reported in [26] while

rough interface is assumed in [27, 28].

### 1.3 Scattering from random boundaries

Scattering from the random media has been discussed as early as 1950 by Rice and Cartwright [29, 30]. Their main focus was on planar random surfaces. Liang et al. [31] reported the scattering by rough surfaces with large heights and slopes. Further, scattering from a three dimensional arbitrary layered media having periodic rough interfaces was presented in [32, 33]. A small amount of effort has been made to study the scattered field from cylindrical objects with random shape and radius as compared with the random planar surface scattering.

In [34], scattering from a PEC cylinder of an arbitrary shape is discussed using the perturbation theory (PT) while a dielectric cylinder is reported in [35]. It is shown that acoustically vibrating an object at its resonant frequencies can provide an effective method to measure the Doppler scattered response monostatically or bistatically. Scattered field from an object of arbitrary shaped cylindrical structures is discussed in [36, 37]. Ashraf and Rizvi [38] reported the electromagnetic scattering from a random cylinder of arbitrary shape by the method of moments (MoM). It is reported that the coherent scattering cross-section increases in the forward direction as the randomness increases and decreases in a backward direction. In [39], both the studies of [34] and [38] are combined to relate the PT with the random cylinder (RC) generation. The PT requires small surface variations as compared to wavelength of incident field and it is a computationally efficient method while the MoM is shape dependent and the computational time increases manifolds if the scatterer size is large. Scattering from a PEC cylinder with random radius placed under a slightly rough surface was studied by Fiaz et al. [40]. This work has been done analytically using the PT for rough surface scattering. Average cross polarized scattering from a random PEMC cylinder with uniform and normal distribution of the radius has been reported in [41].

## 1.4 RC models

Random cylindrical structures can be defined in three different types in cylindrical coordinate system  $(r, \theta, z)$  i.e., a circular RC, an axially corrugated RC and an angularly corrugated RC. In circular RC, the radius 'r' is a random variable. The ensemble of this type of RCs will have circular cylinders with different radii. In axially corrugated RC, the radius 'r(z)' of the RCs is a stochastic process with parameter z. The cross section of these cylinders will be circular having different radius at different 'z' values. In an angularly corrugated RC, the radius, which is a stochastic function of azimuthal angle ' $\theta$ ', will be different at different angles. The cross section of the angularly corrugated RC does not vary along cylindrical axis. The modeling of angularly corrugated RC is most difficult because of a periodic random process needed to generate it.

In literature, three different models for angularly corrugated RC generation are discussed [43, 44, 38]. In [43], RC is defined by a stationary stochastic process with zero mean, obtained with its correlation function  $\exp\{-2\alpha \sin^2(\theta/2)\}$ . This correlation function should be even, translationally invariant and periodic with period  $2\pi$ . Hence, this model is restricted by its correlation function. The second model reported in [44] is defined in terms of an infinite Fourier series where the coefficients are independently complex Gaussian random variables. The above two RC models possess various disadvantages. In the first model, the shape of the cylinder cannot be controlled directly by the correlation function. In the second model, the complex Gaussian coefficients of the infinite Fourier series describe a noisy random process and the electromagnetic boundary conditions are difficult to satisfy.

In [38], the finite Fourier series is used to generate a random cylinder and it is given by

$$p(\theta) = \sum_{n=1}^N Y_n \cos(n\theta + \psi_n) \quad (1.4.1)$$

It is assumed that the random amplitude  $Y_n$  and phase  $\psi_n$  are independent and identically distributed uniformly between  $[-B, B]$  and  $[-\pi, \pi]$  respectively. In this

model,  $p(\theta)$  is zero mean and its variance is  $NB^2/6$  where  $N$  denotes the number of terms. The maximum value of the sum of the series is  $|NB|$ . By adding the mean radius  $r_0$ , a random cylinder can be realized whose radius cannot be negative if  $r_0 > NB$ .

In this research, a random cylinder has been generated using the model reported in [38]. This model is not limited by the choice of correlation function as in [43, 44]. It gives a better control on the shape of the resultant cylinder and the cylinder will have no negative radius at any angle.

## 1.5 Thesis overview and scientific contribution

The flow chart of the thesis is shown in figure 1.1. Chapter 2 presents the scattering from a PEC circular cylinder of random radius with uniform/normal distribution. Assuming that the size of the cylinder is very small, the analytical expressions for average scattered field are written using the small approximation of cylindrical wave functions. It is worth mentioning that the small approximation used in [1, 40] reduces the size of the cylinder to a very thin wire. The approximation used in this work enabled to obtain the analytical expressions for average scattered field for a relatively larger radius. Beyond a certain value of radius, it is not possible to write down analytical expressions for the average field and the numerical average is obtained, i.e., an ensemble average of the field scattered from all the generated RC's. The average field is obtained for 500 realizations of RC. Moreover, scattered field from a cylinder with mean radius is calculated and its difference with the average scattered field is noted. By varying the standard deviation of the normal distribution, its effect on the average scattered field is also analyzed.

In chapter 3, PEMC (metamaterial) circular cylinder with random radius is considered to compute the average co and cross polarized scattered field. To this end, all the average scattering coefficients for a very small PEMC cylinder have been expressed in terms of scattering coefficients for PEC cylinder reported in chapter 2. Moreover, it is observed that only zeroth-order scattering coefficient contributes to



co-polarised average scattered field whereas first order coefficients also contribute to cross-polarised average scattered field. In case of large PEMC cylinders, it is observed that the average scattered field is almost equal to the scattered field from a cylinder with a mean radius. For small PEMC cylinder, it has been observed that average co-polarised scattered field is equal to the scattered field from a cylinder with a mean radius. This is not true in case of cross-polarised scattered field and the difference can be seen for most of the scattering angles. These observations have been reported in a journal publication by the author [41].

In chapter 4, an analytical method based on perturbation theory (PT) has been developed which not only generate the cylinder but also calculate the average scattered field from a perturbed cylinder. To ensure the validity of the PT during the numerical simulations for generating RC and calculating average field, an effort has been made to derive two conditions in terms of perturbation parameter ( $B$ ) and the number of terms ( $N$ ) in the Fourier series representation of RC. It has been concluded that the perturbations must be small and the condition for gentle slope will be automatically satisfied for smaller values of  $N$ . The expressions obtained for the scattered field are also verified with the results obtained through MoM. The developed method is more efficient as compared to MoM in terms of simplicity and computational time. This method allows the efficient evaluation of near zone two dimensional field plots which are very useful to analyze the forward and backscattering properties of perturbed cylinder with reference to that for a circular cylinder. These observations have been reported in a journal publication by the author [39].

In chapter 5, the PT is applied to study the scattering from PEMC perturbed cylinder. It is observed that how the perturbations affect the co and cross polarized components of the scattered field compared with the reference scattered field from the circular PEMC cylinder. In particular, the distinctions due to perturbations are pronounced in the forward and backward scattering. The forward scattering is affected more than the backward scattering due to perturbations. Also, the effect of perturbations for the TE polarization is more evident. Finally, by changing the value

of the admittance of the PEMC cylinder, the variations in the co and cross polarized scattering are noted. This work has been accepted for a journal publication by the author [42]. In chapter 6, final remarks and conclusions are given.

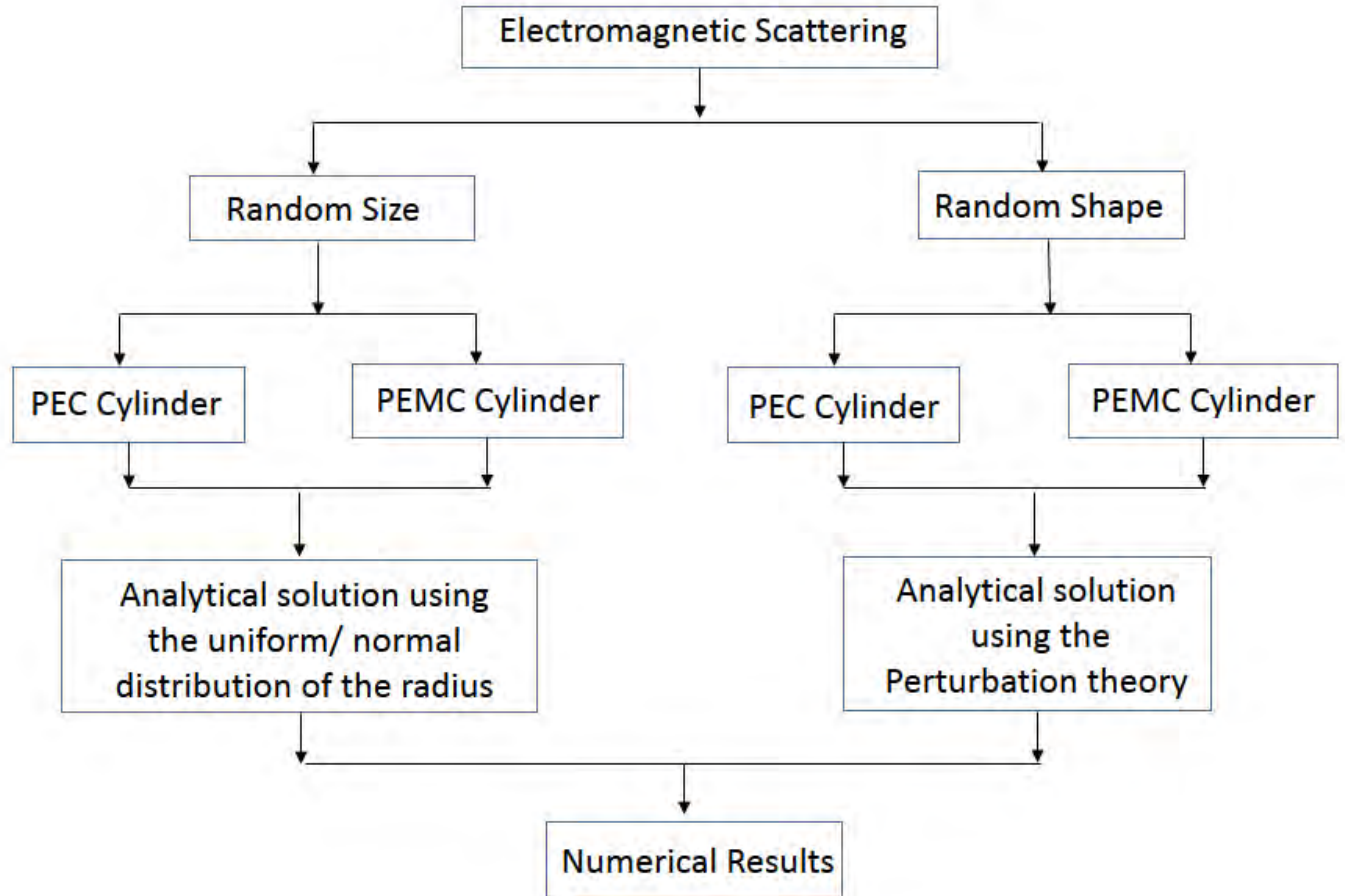


Figure 1.1: Flow chart of the thesis.

## Chapter 2

# Average scattered field from a PEC cylinder with random radius

Average scattered field from a random PEC cylinder is discussed in this chapter. Uniform and normal distributions of the radius are considered due to the random nature of the radius. First, a very small cylinder is considered and analytical expressions for the average scattered field are written using small approximation of cylindrical wave functions. Secondly, a small and large cylinder is considered. In this case, it is not possible to write down analytical expressions for the average field, the numerical average is only done. The problem formulation is given in Section 2.1. In Section 2.2, evaluation of the average scattered field is presented. Numerical results are discussed in Section 2.3. The time dependency is taken as  $e^{j\omega t}$ .

### 2.1 Problem description and formulation

A PEC circular cylinder of radius  $a$  is considered in Figure (2.1) where  $a$  is a random variable. It is assumed that the cylinder is infinite in  $z$ -direction and the problem is two dimensional. All the mediums are linear, homogeneous and isotropic. The incident field can be both TM polarized ( $E$  is parallel to cylinder axis) or TE polarized ( $E$  is perpendicular to cylinder axis). It is expressed in terms of  $V_i$  which represents

electric or magnetic field for TM or TE polarization, respectively. It is given by

$$V_i = V_0 e^{-jk_{ix}x} \quad (2.1.1)$$

where  $V_0$  represents amplitude of incident plane wave and is given by

$$V_0 = \begin{cases} \frac{E_0}{k_0} & \text{TM Polarization} \\ \frac{E_0}{\omega\mu_0} & \text{TE Polarization} \end{cases} \quad (2.1.2)$$

The scattered field in terms of scalar cylindrical functions can be expressed as

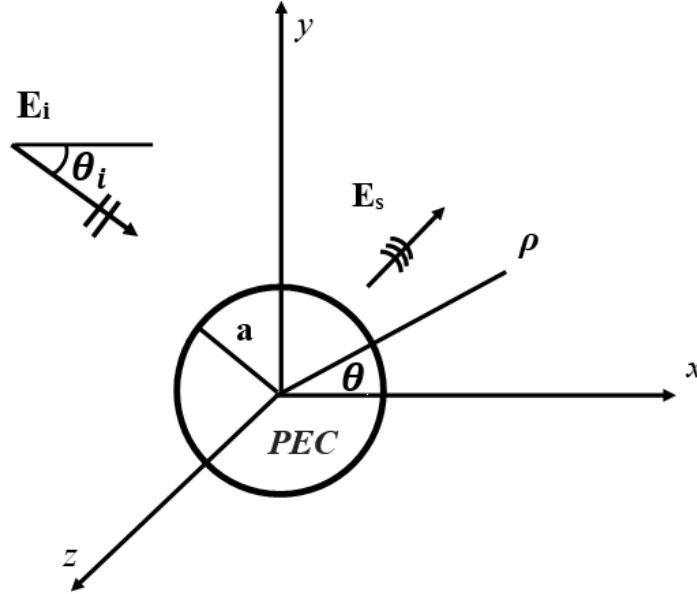


Figure 2.1: Geometry of the scattering problem.

$$V_s = V_0 \sum_{n=-\infty}^{n=\infty} j^{-n} b_n^{TM,TE} H_n^{(2)}(k_0\rho) e^{jn\theta} \quad (2.1.3)$$

where  $H_n^{(2)}(k_0\rho)$  is Hankel function,  $b_n$  is the unknown coefficient and can be found by imposing the following boundary condition at the surface of the cylinder  $\rho = a$  [1]

$$V_z^i + V_z^s = 0 \quad (2.1.4)$$

$$b_n^{TM} = -\frac{J_n(k_0a)}{H_n^{(2)}(k_0a)} \quad (2.1.5)$$

$$b_n^{TE} = -\frac{J'_n(k_0a)}{H_n'^{(2)}(k_0a)} \quad (2.1.6)$$

where  $J_n(k_0a)$  is Bessel function. In case of a cylinder having small radius,  $k_0a \ll 1$  and  $n > 0$ , the following approximations for Bessel and Hankel functions can be used [45].

$$J_n(k_0a) = \frac{(0.5k_0a)^n}{\Gamma(n+1)} \quad (2.1.7)$$

$$H_n^{(2)}(k_0a) = \frac{(0.5k_0a)^n}{\Gamma(n+1)} + j\frac{\Gamma(n)}{\pi}\left(\frac{2}{k_0a}\right)^n \quad (2.1.8)$$

$$F'_n(k_0a) = \frac{n}{k_0a}F_n(k_0a) - F_{n+1}(k_0a) \quad (2.1.9)$$

where  $F_n$  is Bessel or Hankel function of second kind. The scattering width  $\sigma_{2D}$  can be expressed as [1]

$$\sigma_{2D} = \lim_{\rho \rightarrow \infty} \left[ 2\pi\rho \frac{|E_s^z|^2}{|E_i^z|^2} \right] \quad (2.1.10)$$

$$\sigma_{2D} = \frac{4}{\beta} \left| \sum_{n=0}^{\infty} b_n e^{jn\phi} \right|^2 \quad (2.1.11)$$

$$\sigma_{2D} = \frac{2\pi}{\lambda} \left| \sum_{n=0}^{\infty} \epsilon_n b_n \cos(n\theta) \right|^2 \quad (2.1.12)$$

where

$$\epsilon_n = \begin{cases} 1 & n = 0 \\ 2 & n \neq 0 \end{cases} \quad (2.1.13)$$

## 2.2 Evaluation of average scattered field

In this problem, it is assumed that the randomness is due to the radius, i.e., the radius ' $a$ ' is a random variable with a certain distribution. Average scattered field can be calculated analytically when a very small cylinder is considered i.e.,  $k_0a \ll 1$

while for large cylinder only numerical average can be done. In this section, analytical evaluation of the average scattered field is discussed for uniform and normal distribution of the radius. Putting the equations (2.1.7), (2.1.8) and (2.1.9) in the equations (2.1.5) and (2.1.6),  $b_n$  for TM polarization is given by

$$b_0^{TM} = \frac{1}{1 - \frac{2j}{\pi} \ln(k'_0 a)} \quad (2.2.1)$$

$$b_n^{TM} = \frac{j\pi}{\Gamma(n)\Gamma(n+1)} (k_0 a)^{2n} \quad (2.2.2)$$

For TE polarization,  $b_n$  is given by

$$b_0^{TE} = b_1^{TM} = \frac{j\pi(k_0 a)^2}{4} \quad (2.2.3)$$

$$b_1^{TE} = -b_1^{TM} = -\frac{j\pi(k_0 a)^2}{4} \quad (2.2.4)$$

where  $k'_0 = 0.89k_0$ . The higher terms can be ignored as  $k_0 a \ll 1$ .

The analytic average has been done in [40] where

$$H_0^2(k_0 a) = \frac{1}{-\frac{2j}{\pi} \ln(k'_0 a)} \quad (2.2.5)$$

is used instead of

$$H_0^2(k_0 a) = \frac{1}{1 - \frac{2j}{\pi} \ln(k'_0 a)} \quad (2.2.6)$$

which reduces the size of the cylinder to a very thin wire. Balanis [1] has also used the same approximation for the Hankel function as in [40] to calculate scattering by conducting circular cylinder with small radius. Here the approximation of Hankel function defined in equation (2.2.6) is used for which the radius of small cylinder is increased from millimeters to centimeters for the same frequency. The average scattered field can be obtained by taking average

$$\langle V_s \rangle = V_0 \sum_{n=-\infty}^{n=\infty} j^{-n} \langle b_n \rangle H_n^{(2)}(k_0 \rho) e^{jn\phi} \quad (2.2.7)$$

### 2.2.1 Uniform Distribution

For uniformly distributed random radius, the probability density function for the radius  $a$  is defined as [40]

$$P_a(a) = \begin{cases} \frac{1}{a_2 - a_1} = A_c & a_1 \leq a \leq a_2 \\ 0 & \text{Otherwise} \end{cases} \quad (2.2.8)$$

$\langle b_n \rangle$  can be calculated using the following integral

$$\langle b_n \rangle = \int_{-\infty}^{\infty} b_n P_a(a) da \quad (2.2.9)$$

For TM polarization,  $\langle b_n \rangle$  is given by

$$\langle b_0^{TM} \rangle = \int_{a_1}^{a_2} \frac{A_c}{z(a)} da \quad (2.2.10)$$

$$z(a) = 1 - \frac{2j}{\pi} \ln(k'_0 a) \quad (2.2.11)$$

The solution of integral is given in Appendix as,

$$\langle b_0^{TM} \rangle = \frac{j\pi A_c e^{\frac{\pi}{2j}}}{2k'_0} C_z \quad (2.2.12)$$

where

$$C_z = \left\{ E_1[z(a_2)] - E_1[z(a_1)] - \gamma \right\} \quad (2.2.13)$$

$$z(a_1) = 1 - \frac{2j}{\pi} \ln(k'_0 a_1) \quad (2.2.14)$$

$$z(a_2) = 1 - \frac{2j}{\pi} \ln(k'_0 a_2) \quad (2.2.15)$$

$$(2.2.16)$$

and  $\gamma = 1.781$ . The expression for  $b_n^{TM} \forall n \neq 0$  is given by

$$\langle b_n^{TM} \rangle = \frac{j\pi A_c}{\Gamma(n)\Gamma(n+1)k_0(2n+1)} \left[ (k_0 a_2)^{2n+1} - (k_0 a_1)^{2n+1} \right] \quad (2.2.17)$$

For TE polarization,  $\langle b_n \rangle$  is given by

$$\langle b_0 \rangle^{TE} = \langle b_1 \rangle^{TM} \quad (2.2.18)$$

$$\langle b_1 \rangle^{TE} = - \langle b_1 \rangle^{TM} \quad (2.2.19)$$

The covariance function for uniform distribution of the radius is,

$$\langle b_0 b_0 \rangle = \frac{\pi^2 A_c}{4k_0'^2} \int_{a_1}^{a_2} \frac{1}{(z(a))^2} da \quad (2.2.20)$$

$$\langle b_0 b_0 \rangle = \frac{\pi^2 A_c}{4k_0'^2} \left[ \frac{a_2}{z(a_2)} - \frac{a_1}{z(a_1)} - \frac{j\pi e^{\frac{\pi}{2j}}}{2k_0'} C_z \right] \quad (2.2.21)$$

$$\langle b_0 b_1 \rangle = \frac{\pi^2 2A_c}{8k_0'^3} \left[ E_1(1 + \frac{6}{\pi} \ln(k_0' a_2)) - E_1(1 + \frac{6}{\pi} \ln(k_0' a_1)) \right] \quad (2.2.22)$$

$$\langle b_1 b_1 \rangle = \frac{\pi^2 A_c}{20k_0'} \left[ (k_0 a_2)^5 - (k_0 a_1)^5 \right] \quad (2.2.23)$$

## 2.2.2 Normal Distribution

The probability density function for normally distributed random radius is given by

$$P_a(a) = \frac{1}{\sqrt{2\pi}s_a} \exp \left[ - \frac{(a - \langle a \rangle)^2}{2s_a^2} \right] \quad (2.2.24)$$

The average scattering coefficient  $\langle b_n \rangle$  can be calculated using the following integral

$$\langle b_n \rangle = \frac{1}{\sqrt{2\pi}s_a} \int_{-\infty}^{\infty} b_n \exp \left[ - \frac{(a - \langle a \rangle)^2}{2s_a^2} \right] da \quad (2.2.25)$$

The Taylor series given in the Appendix is used to evaluate the above integral. For TM polarization,  $\langle b_n \rangle$  is given by

$$\begin{aligned} \langle b_0^{TM} \rangle &= \frac{j\pi(k_0)^2}{4Q} (\langle a \rangle^2 + s_a^2) - \frac{j\pi M^2 \eta_0^2}{2Q} \left\{ \frac{1}{z(\langle a \rangle)} \right. \\ &\quad \left. + \frac{j s_a^2 \left[ 1 - \frac{2j}{\pi} (2 + \ln(k_0' \langle a \rangle)) \right]}{\pi \langle a \rangle^2 [z(\langle a \rangle)]^3} \right\} \end{aligned} \quad (2.2.26)$$

$$\langle b_1^{TM} \rangle = \frac{j\pi(k_0)^2}{4} (\langle a \rangle^2 + s_a^2) \quad (2.2.27)$$



Since  $k_0 a \ll 1$ , higher terms can be ignored. For TE polarization,  $\langle b_n \rangle$  can be calculated using equations (2.2.18) and (2.2.19). The covariance function for normal distribution of the radius is,

$$\langle b_0 b_0 \rangle = -\frac{\pi^2}{4} \left\{ \frac{1}{[z(\langle a \rangle)]^2} + \frac{4s_a^2 \left[ \ln(k'_0 \langle a \rangle) - \frac{\pi}{j} + 1 \right]}{\pi^2 \langle a \rangle^2 [z(\langle a \rangle)]^4} \right\} \quad (2.2.28)$$

$$\begin{aligned} \langle b_0 b_1 \rangle = \frac{j\pi^2 k_0'^2}{4} \left\{ \frac{\langle a \rangle^2 + \sigma_a^2}{z(\langle a \rangle)} - \frac{2s_a^2}{[z(\langle a \rangle)]^2} \right. \\ \left. - \frac{\frac{2j}{\pi} \left[ 1 - \frac{2j}{\pi} (2 + \ln(k'_0 \langle a \rangle)) \right]}{[z(\langle a \rangle)]^3} \right\} (\langle a \rangle^2 + 5s_a^2) \end{aligned} \quad (2.2.29)$$

$$\langle b_1 b_1 \rangle = \left( \frac{\pi^2 k_0'^2}{2} \right)^2 \left[ (\langle a \rangle^4 + 6 \langle a \rangle^2 s_a^2 + 3s_a^4) \right] \quad (2.2.30)$$

## 2.3 Numerical results

In this section, numerical implementation of the theory is done. Results are reported for three sizes of cylinder.

- Very small cylinder ( $a_1 = 0.01\lambda$ ,  $a_2 = 0.06\lambda$ , frequency (f)=30MHz)
- Small cylinder ( $a_1 = 0.1\lambda$ ,  $a_2 = 0.6\lambda$ , f=300MHz)
- Large cylinder ( $a_1 = 1\lambda$ ,  $a_2 = 6\lambda$ , f=300MHz)

All the results are averaged over 500 realizations.

First, average scattered field from very small PEC cylinder of random radius with uniform distribution is shown in Figure (2.2). It is observed that the results for both analytic average defined in equation (2.2.7) and numerical average (an ensemble

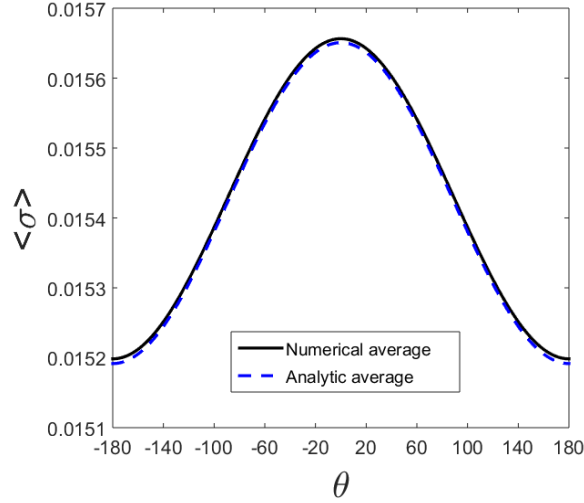
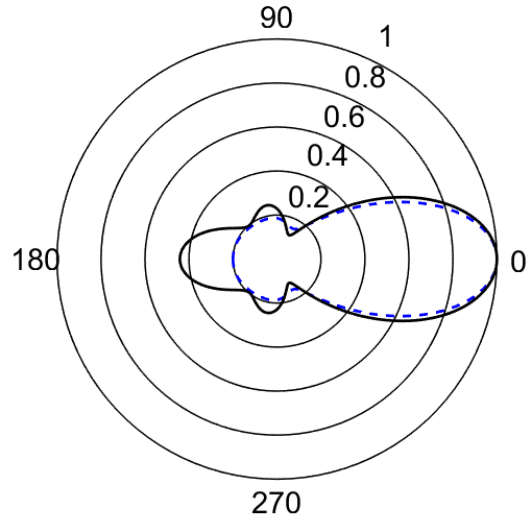


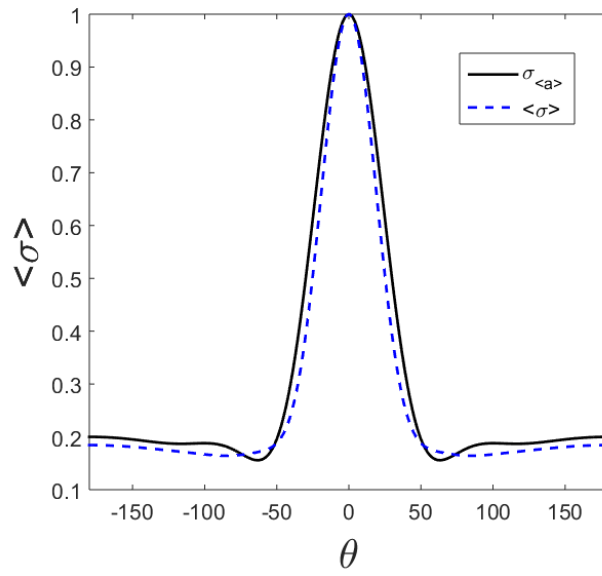
Figure 2.2: Average scattering cross section of a very small PEC cylinder of random radius with uniform distribution where  $a_1 = 0.01\lambda$ ,  $a_2 = 0.06\lambda$ . Results are shown using both analytic and numerical average.

average of the field scattered from all the generated RC's) are in good agreement. Average scattering width  $\langle \sigma \rangle$  of a small PEC cylinder of random radius with uniform distribution is shown in Figure (2.3). Also scattering cross section  $\sigma_{\langle a \rangle}$  of a cylinder with mean radius is shown as reference result for TM polarization. A large PEC cylinder is considered in Figure (2.4). It is noticed that the averaged cross-section is very close to that of a circular cylinder with mean radius having maximum amplitude at  $\theta=0^\circ$ . To better analyze the pattern, polar plots are also given. Results for TE polarization are shown in Figures (2.5) and (2.6) respectively. For large cylinder,  $\langle \sigma \rangle$  is almost equal to  $\sigma_{\langle a \rangle}$  where difference is observed for small cylinder.

Now consider a random cylinder when radius is normally distributed with  $s_a = 0.25$ . Figure (2.7) shows scattering pattern of a small random PEC cylinder for TM polarization while large PEC cylinder is considered in Figure (2.8). Figures (2.9) and (2.10) show results for TE polarization respectively. It is observed that  $\langle \sigma \rangle$  is same as  $\sigma_{\langle a \rangle}$  for large cylinder while difference is observed for small cylinder.

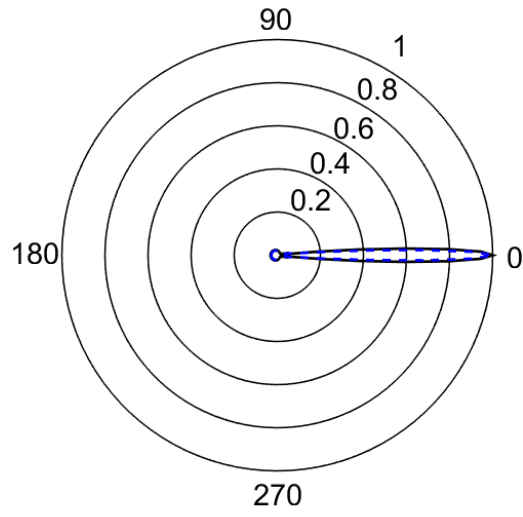


(a)

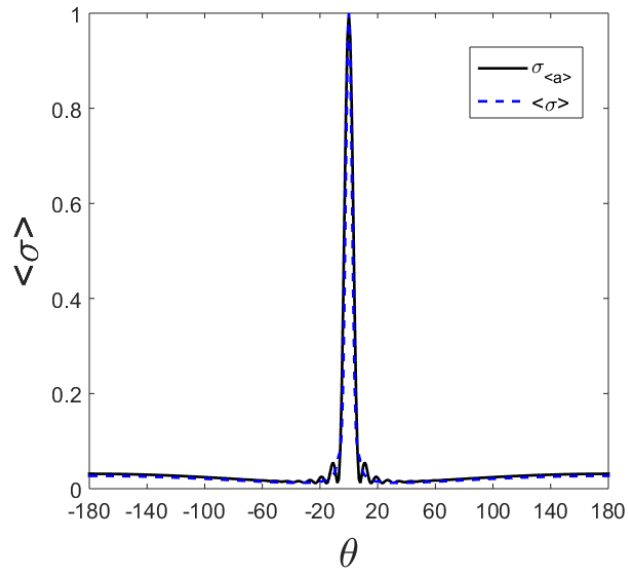


(b)

Figure 2.3: Scattering cross section (normalized) of a small PEC cylinder of random radius with uniform distribution for TM polarization where  $a_1 = 0.1\lambda$  and  $a_2 = 0.6\lambda$ .

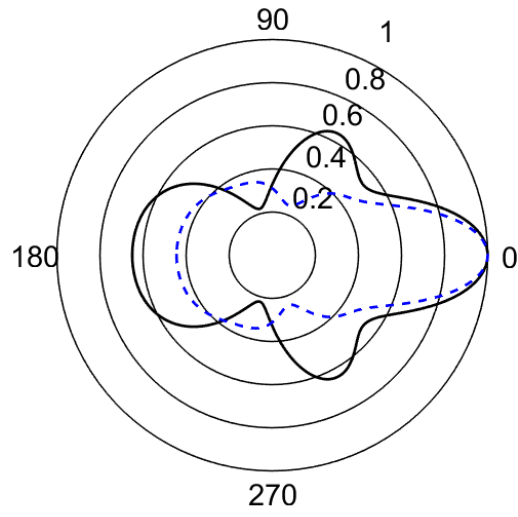


(a)

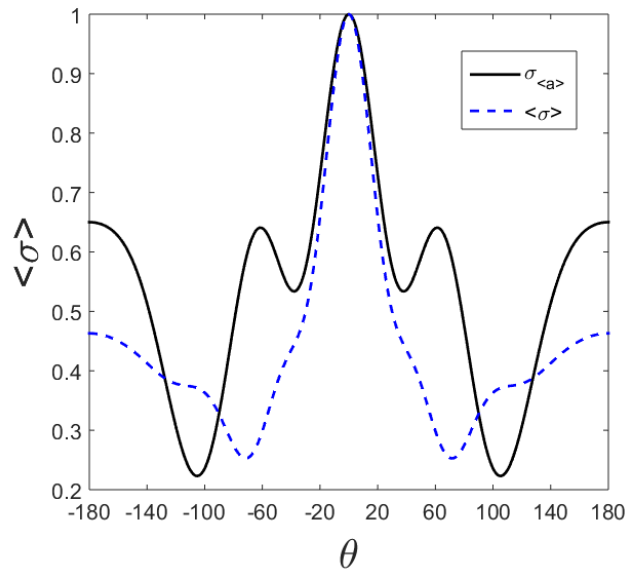


(b)

Figure 2.4: Scattering cross section (normalized) of a large PEC cylinder of random radius with uniform distribution for TM polarization where  $a_1 = 1\lambda$  and  $a_2 = 6\lambda$ .

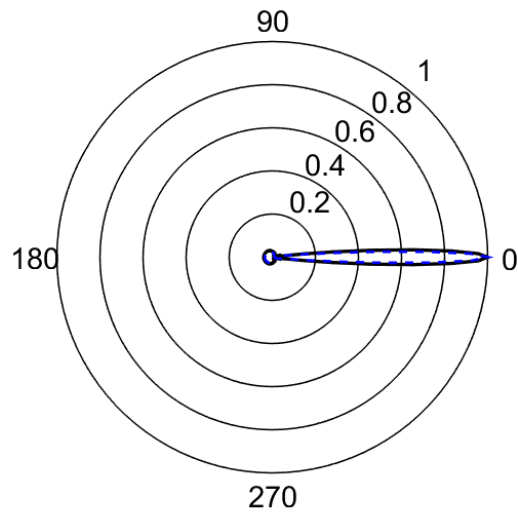


(a)

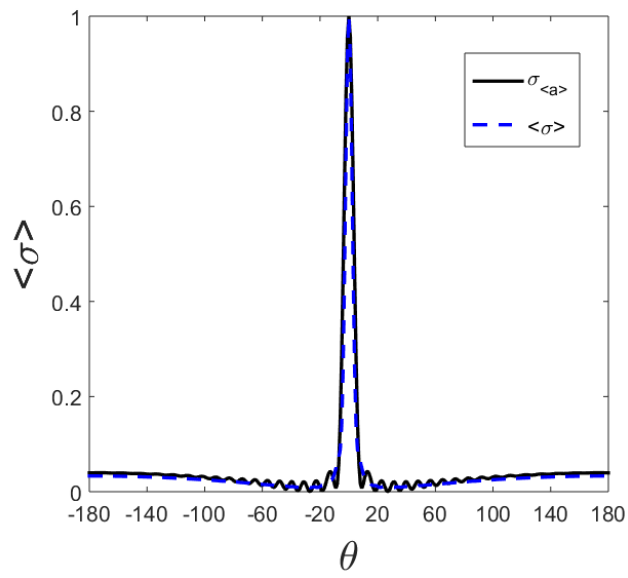


(b)

Figure 2.5: Scattering cross section (normalized) of a small PEC cylinder of random radius with uniform distribution for TE polarization where  $a_1 = 0.1\lambda$  and  $a_2 = 0.6\lambda$ .

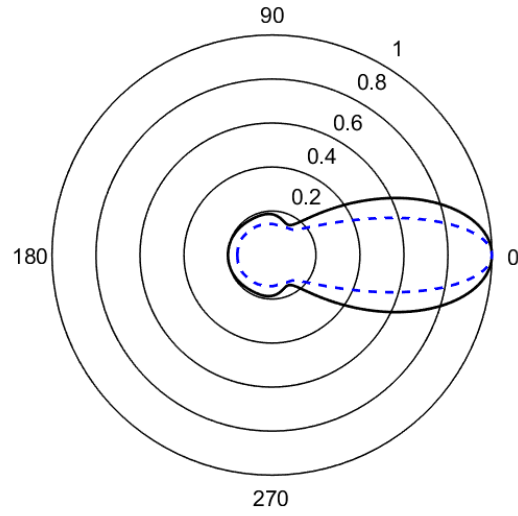


(a)

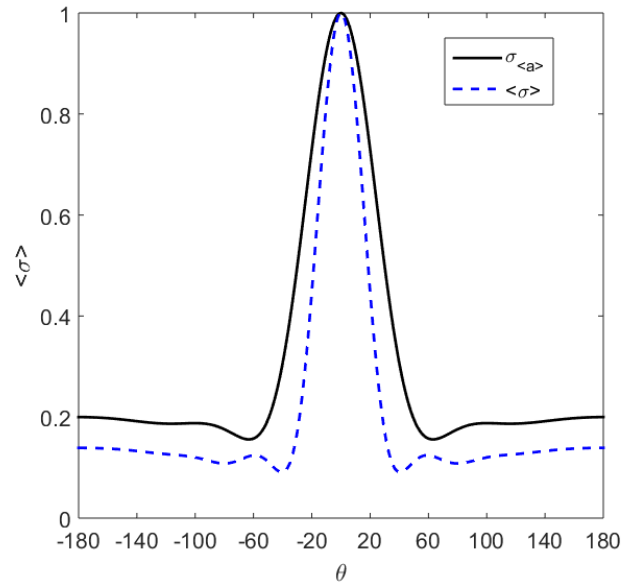


(b)

Figure 2.6: Scattering cross section (normalized) of a large PEC cylinder of random radius with uniform distribution for TE polarization where  $a_1 = 1\lambda$  and  $a_2 = 6\lambda$ .

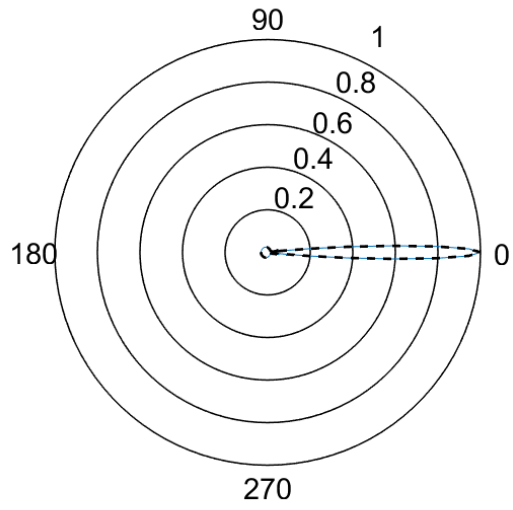


(a)

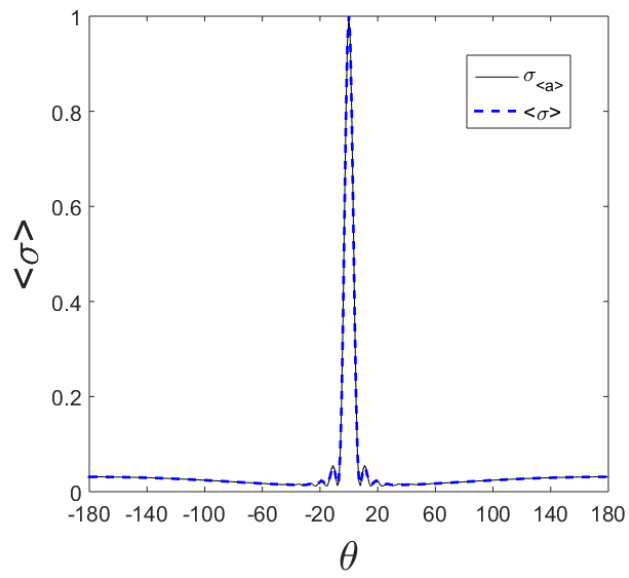


(b)

Figure 2.7: Same as Figure (2.3) except that normal distribution with  $s_a = 0.25$  is considered.



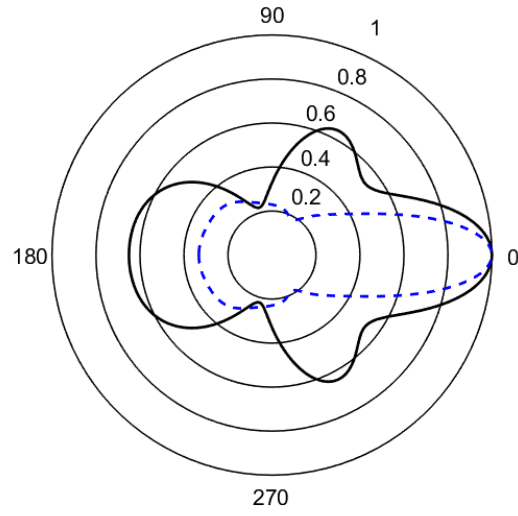
(a)



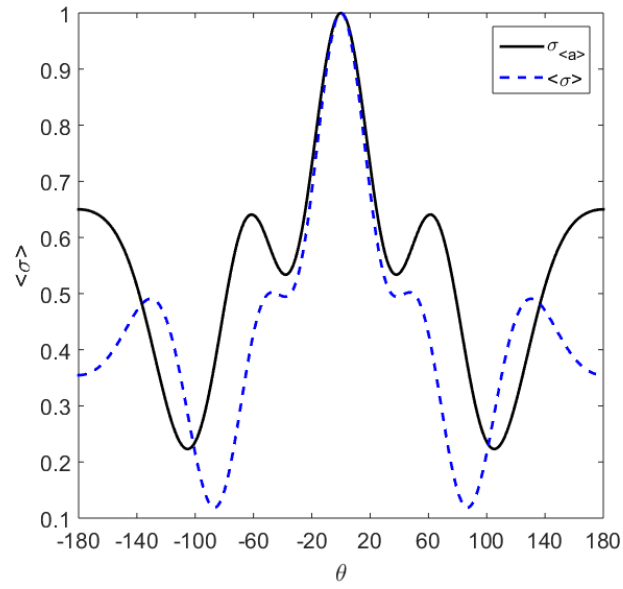
(b)

Figure 2.8: Same as Figure (2.4) except that normal distribution with  $s_a = 0.25$  is considered.



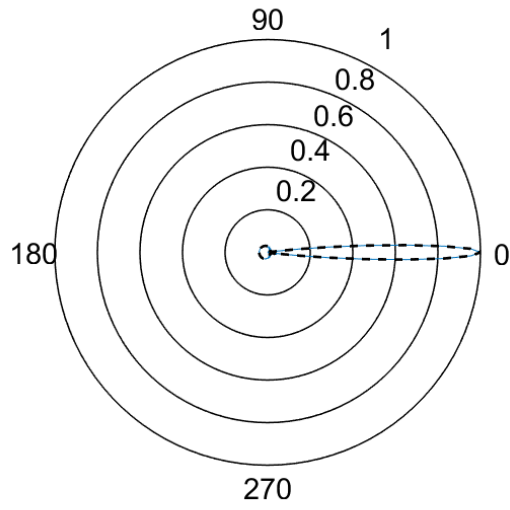


(a)

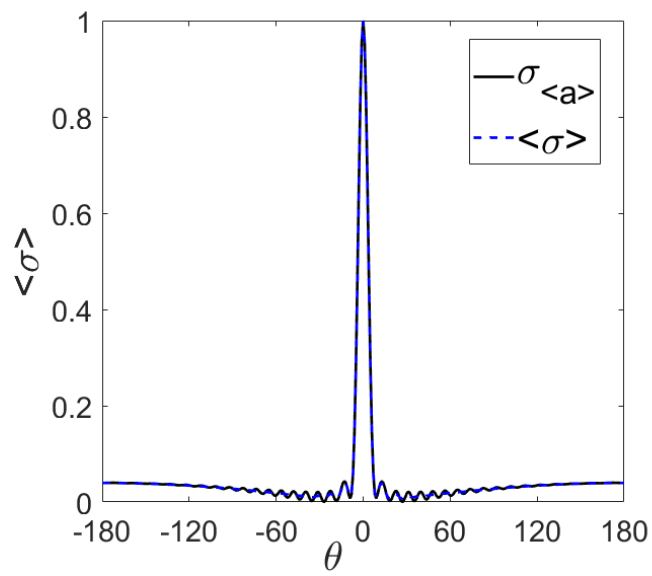


(b)

Figure 2.9: Same as Figure (2.5) except that normal distribution with  $s_a = 0.25$  is considered.



(a)



(b)

Figure 2.10: Same as Figure (2.6) except that normal distribution with  $s_a = 0.25$  is considered.

## Chapter 3

# Average scattered field from a PEMC cylinder with random size

In this chapter, average scattered field from a random PEMC cylinder is discussed. Uniform and normal distribution of the radius is considered for both TM and TE polarizations to evaluate the average scattered field. The time dependency is taken as  $e^{j\omega t}$ . The problem formulation is given in Section 3.1. In Sections 3.1.1 and 3.1.2, solution for the uniform and normal distributions is presented respectively. Numerical results are discussed in Section 3.2.

### 3.1 Problem description and formulation

A PEMC circular cylinder of radius  $a$  is considered in Figure (3.1). It is assumed that the cylinder is infinite in z-direction and the problem is two dimensional. All the mediums are linear, homogeneous and isotropic. The incident field can be both TM polarized or TE polarized expressed in terms of  $V_i$  which represents electric or magnetic field for TM or TE polarization, respectively,

$$V_i = V_0 e^{-jk_{ix}x} \quad (3.1.1)$$

where  $V_0$  represents amplitude of incident plane wave and is given by

$$V_0 = \begin{cases} \frac{E_0}{k_0} & \text{TM Polarization} \\ \frac{E_0}{\omega\mu_0} & \text{TE Polarization} \end{cases} \quad (3.1.2)$$

In case of PEMC cylinder, cross polarized scattered field also exists in addition to

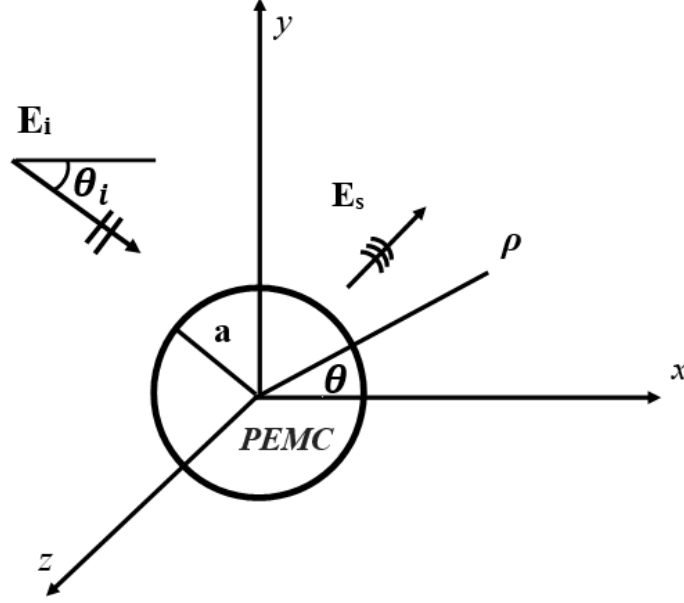


Figure 3.1: A linearly polarized plane wave is incident upon a random PEMC cylinder.

co-polarized scattered field. The co and cross polarized components in terms of scalar cylindrical functions can be expressed as

$$V_s = V_0 \sum_{n=-\infty}^{n=\infty} j^{-n} [b_n^{TM,TE} H_n^{(2)}(k_0 \rho) + c_n^{TM,TE} H_n'^{(2)}(k_0 \rho)] e^{jn\theta} \quad (3.1.3)$$

where  $b_n$  and  $c_n$  are the unknown coefficients. Boundary conditions at the surface of the cylinder  $\rho = a$  are given by [2]

$$ME_t^i + H_t^i + H_t^s + ME_t^s = 0 \quad (3.1.4)$$

$$\epsilon_0 E_\rho^i + \epsilon_0 E_\rho^s - M\mu_0 H_\rho^i - M\mu_0 H_\rho^s = 0 \quad (3.1.5)$$

Unknown coefficients are obtained by imposing the above boundary conditions and are given by [2]

$$b_n^{TM} = -\frac{H_n^{(2)}(k_0 a) J_n'(k_0 a) + M^2 \eta_0^2 J_n(k_0 a) H_n'^{(2)}(k_0 a)}{(1 + M^2 \eta_0^2) H_n^{(2)}(k_0 a) H_n'^{(2)}(k_0 a)} \quad (3.1.6)$$

$$c_n^{TM} = \frac{2M\eta_0}{\pi k_0 a (1 + M^2 \eta_0^2) H_n^{(2)}(k_0 a) H_n'^{(2)}(k_0 a)} \quad (3.1.7)$$

$$b_n^{TE} = -\frac{H_n'^{(2)}(k_0 a) J_n(k_0 a) + M^2 \eta_0^2 J_n'(k_0 a) H_n^{(2)}(k_0 a)}{(1 + M^2 \eta_0^2) H_n^{(2)}(k_0 a) H_n'^{(2)}(k_0 a)} \quad (3.1.8)$$

$$c_n^{TE} = -\frac{2M\eta_0}{\pi k_0 a (1 + M^2 \eta_0^2) H_n^{(2)}(k_0 a) H_n'^{(2)}(k_0 a)} \quad (3.1.9)$$

The scattering width  $\sigma_{2D}$  can be expressed as

$$\sigma_{2D}^{co} = \frac{2\pi}{\lambda} \left| \sum_{n=0}^{\infty} \epsilon_n b_n \cos(n\theta) \right|^2 \quad (3.1.10)$$

$$\sigma_{2D}^{cr} = \frac{2\pi}{\lambda} \left| \sum_{n=0}^{\infty} \epsilon_n c_n \cos(n\theta) \right|^2 \quad (3.1.11)$$

where

$$\epsilon_n = \begin{cases} 1 & n = 0 \\ 2 & n \neq 0 \end{cases} \quad (3.1.12)$$

From equations (3.1.6) to (3.1.9), it can be seen that

$$c_n^{TE} = -c_n^{TM} \quad (3.1.13)$$

Moreover for  $M\eta_0 = 1$ , the above equations are simplified to

$$b_n^{TE} = b_n^{TM} \quad (3.1.14)$$

This gives the idea that SW will be same for both polarizations. Using the approximations for Bessel and Hankel functions as in equations (2.1.7) through (2.1.9),  $b_n$  and  $c_n$  for TM polarization are given by

$$b_0^{TM} = \left( \frac{j\pi}{4Q} \right) (k_0 a)^2 - \left( \frac{M^2 \eta_0^2}{Q} \right) \left( \frac{1}{z(a)} \right) \quad (3.1.15)$$

$$b_1^{TM} = \left( \frac{j\pi(1 - M^2 \eta_0^2)}{4Q} \right) (k_0 a)^2 \quad (3.1.16)$$

$$c_0^{TM} = -\left( \frac{M\eta_0 j}{Q} \right) \frac{1}{z(a)} \quad (3.1.17)$$

$$c_1^{TM} = \left( \frac{\pi M\eta_0}{2Q} \right) (k_0 a)^2 \quad (3.1.18)$$

where  $Q = (1 + M^2\eta_0^2)$  and higher terms can be ignored. From the above equations it can be seen that  $b_n$  and  $c_n$  can be expressed in terms of the expressions obtained for PEC,

$$b_0^{TM} = \left(\frac{1}{Q}\right)b_1^{TM,PEC} - \left(\frac{M^2\eta_0^2}{Q}\right)b_0^{TM,PEC} \quad (3.1.19)$$

$$b_1^{TM} = \frac{(1 - M^2\eta_0^2)}{Q}b_1^{TM,PEC} \quad (3.1.20)$$

$$c_0^{TM} = -\left(\frac{M\eta_0 j}{Q}\right)b_0^{TM,PEC} \quad (3.1.21)$$

$$c_1^{TM} = \left(\frac{2M\eta_0}{jQ}\right)b_1^{TM,PEC} \quad (3.1.22)$$

For TE polarization,  $b_n$  and  $c_n$  satisfy the following relations

$$b_0^{TE} = b_0^{TM} \quad (3.1.23)$$

$$b_1^{TE} = b_1^{TM} \quad (3.1.24)$$

$$c_0^{TE} = -c_0^{TM} \quad (3.1.25)$$

$$c_1^{TE} = -c_1^{TM} \quad (3.1.26)$$

### 3.1.1 Uniform Distribution

The average scattered field can be obtained using equation (2.2.9). For TM polarization,  $\langle b_n \rangle$  and  $\langle c_n \rangle$  are given by

$$\langle b_0^{TM} \rangle = \frac{j\pi Ac}{12Qk_0} \left[ (k_0 a_2)^3 - (k_0 a_1)^3 \right] + \frac{\pi A_c M^2 \eta_0^2 e^{\frac{\pi}{2j}}}{jQk'_0} C_z \quad (3.1.27)$$

$$\langle b_1^{TM} \rangle = \frac{j\pi Ac(1 - M^2\eta_0^2)}{12Qk_0} \left[ (k_0 a_2)^3 - (k_0 a_1)^3 \right] \quad (3.1.28)$$

$$\langle b_n^{TM} \rangle = \frac{j\pi Ac(1 - M^2\eta_0^2)}{4Qk_0(2n + 1)} \left[ (k_0 a_2)^{2n+1} - (k_0 a_1)^{2n+1} \right] \quad (3.1.29)$$

$$\langle c_0^{TM} \rangle = -\frac{\pi M \eta_0 A_c e^{\frac{\pi}{2j}}}{2Q k'_0} C_z \quad (3.1.30)$$

$$\langle c_1^{TM} \rangle = \frac{\pi M \eta_0 A_c}{6Q k_0} \left[ (k_0 a_2)^3 - (k_0 a_1)^3 \right] \quad (3.1.31)$$

$$\langle c_n^{TM} \rangle = \frac{\pi M \eta_0 A_c}{2Q k_0 (2n+1)} \left[ (k_0 a_2)^{2n+1} - (k_0 a_1)^{2n+1} \right] \quad (3.1.32)$$

For TE polarization,  $\langle b_n \rangle$  and  $\langle c_n \rangle$  are given by

$$\langle b_0^{TE} \rangle = \langle b_0^{TM} \rangle \quad (3.1.33)$$

$$\langle b_1^{TE} \rangle = \langle b_1^{TM} \rangle \quad (3.1.34)$$

$$\langle c_0^{TE} \rangle = -\langle c_0^{TM} \rangle \quad (3.1.35)$$

$$\langle c_1^{TE} \rangle = -\langle c_1^{TM} \rangle \quad (3.1.36)$$

The covariance function for uniform distribution of the radius is,

$$\langle c_0 c_0 \rangle = \frac{j\pi^2 M^2 \eta_0^2 A_c}{2Q^2} \int_{a_1}^{a_2} \frac{1}{\left(z(a)\right)^2} da \quad (3.1.37)$$

$$\langle c_0 c_0 \rangle = \frac{j\pi^2 M^2 \eta_0^2 A_c}{2Q^2} \left[ \frac{a_2}{z(a_2)} - \frac{a_1}{z(a_1)} - \frac{j\pi e^{\frac{\pi}{2j}}}{2k'_0} C_z \right] \quad (3.1.38)$$

$$\langle c_0 c_1 \rangle = \frac{j\pi^2 M^2 \eta_0^2 A_c}{8Q^2 k_0^3} \left[ E_1 \left( 1 + \frac{6}{\pi} \ln(k'_0 a_2) \right) - E_1 \left( 1 + \frac{6}{\pi} \ln(k'_0 a_1) \right) \right] \quad (3.1.39)$$

$$\langle c_1 c_1 \rangle = \frac{\pi^2 M^2 \eta_0^2 A_c}{20Q^2 k_0} \left[ (k_0 a_2)^5 - (k_0 a_1)^5 \right] \quad (3.1.40)$$

$$\begin{aligned} \langle b_0 b_0 \rangle &= \frac{\pi (M^2 \eta_0^2)^2 A_c}{2j} \left[ \frac{a_2}{z(a_2)} - \frac{a_1}{z(a_1)} - \frac{j\pi e^{\frac{\pi}{2j}}}{2k'_0} C_z \right] \\ &\quad - \frac{j\pi^2 M^2 \eta_0^2 A_c}{4Q^2 k_0^3} \left[ E_1 \left( 1 + \frac{6}{\pi} \ln(k'_0 a_2) \right) - E_1 \left( 1 + \frac{6}{\pi} \ln(k'_0 a_1) \right) \right] \end{aligned} \quad (3.1.41)$$

$$\begin{aligned} \langle b_0 b_1 \rangle &= \frac{(\pi M^2 \eta_0^2 (1 - M^2 \eta_0^2))^2 A_c}{(4Q)^2 k_0^3} \left[ E_1 \left( 1 + \frac{6}{\pi} \ln(k'_0 a_2) \right) \right. \\ &\quad \left. - E_1 \left( 1 + \frac{6}{\pi} \ln(k'_0 a_1) \right) \right] \end{aligned} \quad (3.1.42)$$

$$\langle b_1 b_1 \rangle = \frac{(\pi (1 - M^2 \eta_0^2))^2 A_c}{(4Q)^2 k_0} \left[ (k_0 a_2)^5 - (k_0 a_1)^5 \right] \quad (3.1.43)$$

### 3.1.2 Normal Distribution

For TM polarization,  $\langle b_n \rangle$  and  $\langle c_n \rangle$  are calculated by using the Taylor series given in Appendix

$$\begin{aligned} \langle b_0^{TM} \rangle = & \frac{j\pi(k_0)^2}{4Q}(\langle a \rangle^2 + s_a^2) - \frac{M^2\eta_0^2}{Q} \left\{ \frac{1}{z(\langle a \rangle)} \right. \\ & \left. + \frac{\frac{2j}{\pi}s_a^2 \left[ 1 - \frac{2j}{\pi}(2 + \ln(k'_0 \langle a \rangle)) \right]}{\langle a \rangle^2 \left[ z(\langle a \rangle) \right]^3} \right\} \end{aligned} \quad (3.1.44)$$

$$\langle b_1^{TM} \rangle = \frac{j\pi(1 - M^2\eta_0^2)}{4Q}(k_0)^2(\langle a \rangle^2 + s_a^2) \quad (3.1.45)$$

$$\langle c_0^{TM} \rangle = \frac{jM\eta_0}{Q} \left\{ \frac{1}{z(\langle a \rangle)} - \frac{\frac{2j}{\pi}s_a^2 \left[ 1 - \frac{2j}{\pi}(2 + \ln(k'_0 \langle a \rangle)) \right]}{2 \langle a \rangle^2 \left[ z(\langle a \rangle) \right]^3} \right\} \quad (3.1.46)$$

$$\langle c_1^{TM} \rangle = \frac{\pi M\eta_0(k_0)^2}{2Q}(\langle a \rangle^2 + s_a^2) \quad (3.1.47)$$

For TE polarization,  $\langle b_n \rangle$  can be calculated using equations (3.1.33) to (3.1.36). The covariance function for normal distribution of the radius is,

$$\begin{aligned} \langle b_0 b_0 \rangle = & \frac{(M^2\eta_0^2)^2}{Q^2} \left\{ \frac{1}{\left[ z(\langle a \rangle) \right]^2} + \frac{\frac{2j}{\pi}s_a^2 \left[ -1 + \frac{2j}{\pi}(3 + \ln(k'_0 \langle a \rangle)) \right]}{\langle a \rangle^2 \left[ z(\langle a \rangle) \right]^4} \right\} \\ & - \frac{j\pi M^2\eta_0^2}{2Q^2} \left\{ \frac{\langle a \rangle^2 + s_a^2}{\left[ z(\langle a \rangle) \right]} - \frac{2s_a^2}{\left[ z(\langle a \rangle) \right]^2} - \frac{\frac{2j}{\pi} \left[ 1 - \frac{2j}{\pi}(2 + \ln(k'_0 \langle a \rangle)) \right]}{\left[ z(\langle a \rangle) \right]^3} \right. \\ & \left. (\langle a \rangle^2 + 5s_a^2) - \frac{\pi^2(k_0)^4}{16Q^2}(\langle a \rangle^4 + 6\langle a \rangle^2 s_a^2 + 3s_a^4) \right\} \end{aligned} \quad (3.1.48)$$



$$\begin{aligned}
\langle b_0 b_1 \rangle = & -\frac{j\pi M^2 \eta_0^2 (1 - M^2 \eta_0^2)}{4Q^2} \left\{ \frac{\langle a \rangle^2 + s_a^2}{[z(\langle a \rangle)]} - \frac{2s_a^2}{[z(\langle a \rangle)]^2} \right. \\
& - \frac{\frac{2j}{\pi} \left[ 1 - \frac{2j}{\pi} (2 + \ln(k'_0 \langle a \rangle)) \right]}{[z(\langle a \rangle)]^3} \left. \right\} (\langle a \rangle^2 + 5s_a^2) \\
& - \frac{\pi^2 (1 - M^2 \eta_0^2) (k_0)^4}{16Q^2} (\langle a \rangle^4 + 6 \langle a \rangle^2 s_a^2 + 3s_a^4) \quad (3.1.49)
\end{aligned}$$

$$\langle b_1 b_1 \rangle = - \left( \frac{\pi (1 - M^2 \eta_0^2) (k_0)^2}{4Q} \right)^2 [\langle a \rangle^4 + 6 \langle a \rangle^2 s_a^2 + 3s_a^4] \quad (3.1.50)$$

$$\langle c_0 c_0 \rangle = -\frac{M^2 \eta_0^2}{Q^2} \left\{ \frac{1}{[z(\langle a \rangle)]^2} + \frac{4s_a^2 [\ln(k'_0 \langle a \rangle) - \frac{\pi}{j} + 1]}{\pi^2 \langle a \rangle^2 [z(\langle a \rangle)]^4} \right\} \quad (3.1.51)$$

$$\begin{aligned}
\langle c_0 c_1 \rangle = & \frac{j\pi M^2 \eta_0^2 (k_0)^2}{2Q^2} \left\{ \frac{\langle a \rangle^2 + s_a^2}{z(\langle a \rangle)} - \frac{2s_a^2}{[z(\langle a \rangle)]^2} \right. \\
& - \frac{\frac{2j}{\pi} \left[ 1 - \frac{2j}{\pi} (2 + \ln(k'_0 \langle a \rangle)) \right]}{[z(\langle a \rangle)]^3} \left. \right\} (\langle a \rangle^2 + 5s_a^2) \quad (3.1.52)
\end{aligned}$$

$$\langle c_1 c_1 \rangle = \left( \frac{\pi M \eta_0 (k_0)^2}{2Q} \right)^2 [\langle a \rangle^4 + 6 \langle a \rangle^2 s_a^2 + 3s_a^4] \quad (3.1.53)$$

## 3.2 Numerical results

In this section, numerical implementation of the theory is done. First the results reported by Ruppini [2] have been reproduced in Figure (3.2) where far zone scattered field is shown for  $k_0 a = 10$  and  $M \eta_0 = \pm 1$ . The cross polarized scattered field is maximum for  $M \eta_0 = \pm 1$  and many side lobes are observed. In the subsequent discussion, results are reported for three sizes of cylinder.

- Very small cylinder ( $a_1 = 0.01\lambda$ ,  $a_2 = 0.06\lambda$ ,  $f=30\text{MHz}$ )

- Small cylinder ( $a_1 = 0.1\lambda$ ,  $a_2 = 0.6\lambda$ ,  $f=300\text{MHz}$ )
- Large cylinder ( $a_1 = 1\lambda$ ,  $a_2 = 6\lambda$ ,  $f=300\text{MHz}$ )

All the results are averaged over 500 realizations. Figure (3.3) shows the result for cross polarized scattered field of a random PEMC cylinder and very little difference is observed. The graphical representation for analytical expression of co polarized scattered field is not shown because for  $M\eta_0 = \pm 1$ ,  $b_n \rightarrow 0, \forall n \neq 0$  and  $b_0$  only contributes. The analytical average is the arithmetic mean of  $b_0$ .

Figures (3.4) and (3.5) show co and cross polarized scattering patterns of a small PEMC cylinder of random radius having uniform distribution. It is noticed that  $\langle \sigma \rangle$  is very closed to  $\sigma_{\langle a \rangle}$  in case of co polarized component. Very small difference can be found for cross polarized scattered field. Large cylinder is considered in Figures (3.6) and (3.7). It is seen that difference can be better analyzed using polar plot in forward and backward scattering directions. Results also show that there is no significant difference between  $\langle \sigma \rangle$  and  $\sigma_{\langle a \rangle}$ . The scattering pattern for large cylinder is more focused in both the cases for co and cross polarized fields while for small cylinder it varies for most of the scattering angles. It is worth mentioning that the plots of co and cross polarized scattered field for TE and TM polarization are same due to  $M\eta_0 = \pm 1$ .

Now consider a random cylinder when radius is normally distributed. Scattering widths for a small PEMC cylinder are shown in Figures (3.8) and (3.9) while a large PEMC cylinder is shown in Figures (3.10) and (3.11) respectively. It is observed that for a small PEMC cylinder,  $\langle \sigma \rangle$  and  $\sigma_{\langle a \rangle}$  are different both co and cross polarized scattered fields. In case of a large PEMC cylinder,  $\langle \sigma \rangle$  and  $\sigma_{\langle a \rangle}$  are same for co polarized scattered field while difference can be noticed for cross polarized scattered field.

Figures (3.12) and (3.13) show co and cross scattering pattern of PEMC cylinder for different values of standard deviation. The mean radius is  $\langle a \rangle = 3.5\lambda$ . Results show that the co polarized scattering pattern does not vary as a function of  $s_a$  while variations can be observed in cross polarized scattering pattern.

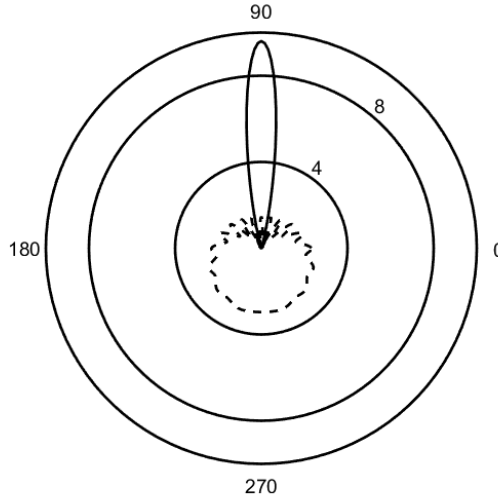


Figure 3.2: Co and cross polarized scattered field from a PEMC cylinder.

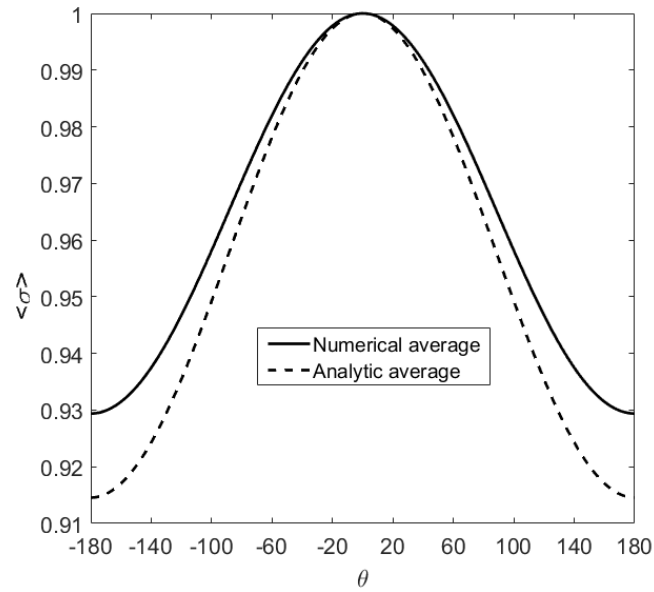


Figure 3.3: Cross polarized scattering cross section (normalized) of a very small PEMC cylinder of random radius with uniform distribution where  $a_1 = 0.01\lambda$  and  $a_2 = 0.06\lambda$ .

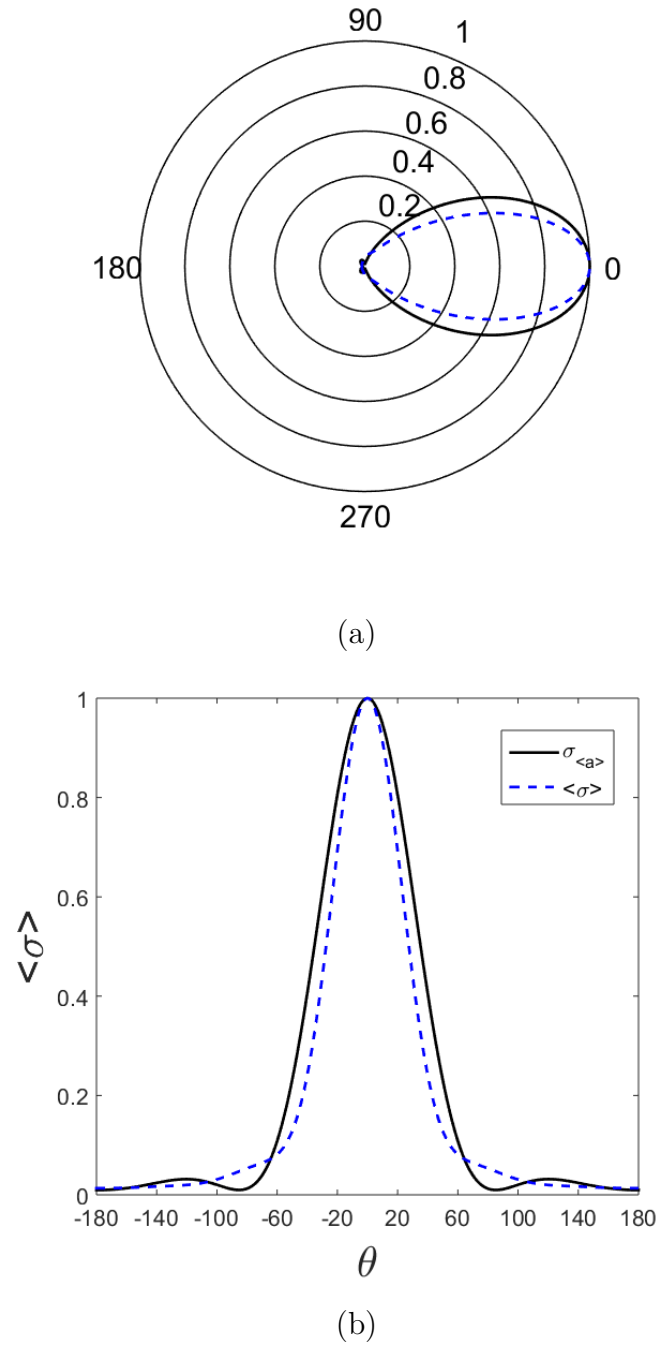
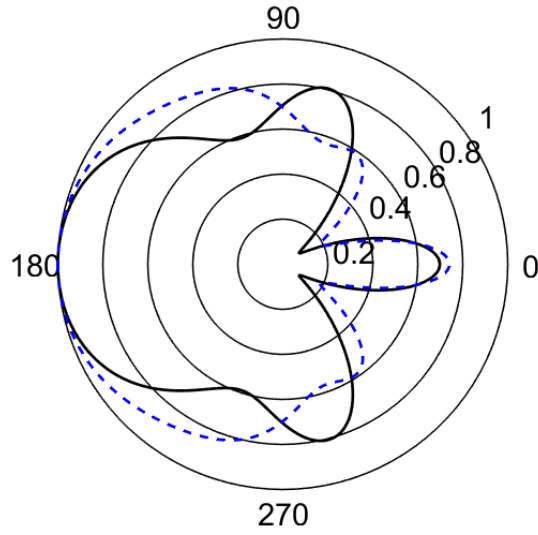
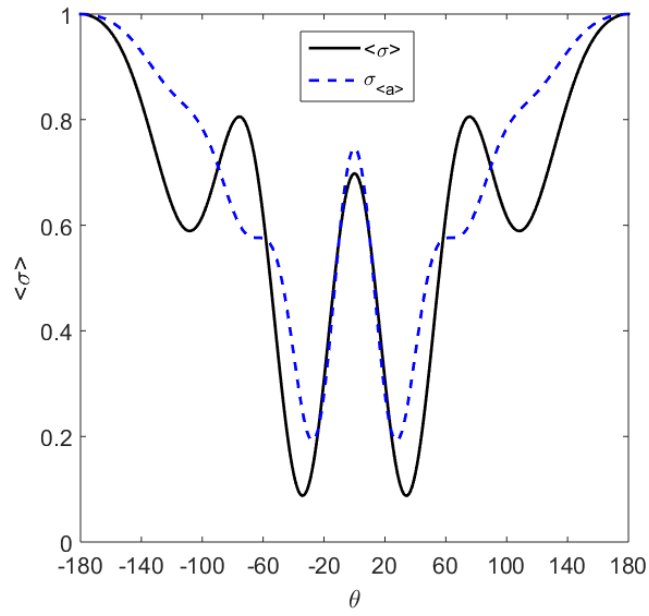


Figure 3.4: Co polarized scattering cross section (normalized) of a small PEMC cylinder of random radius with uniform distribution where  $a_1 = 0.1\lambda$  and  $a_2 = 0.6\lambda$ .

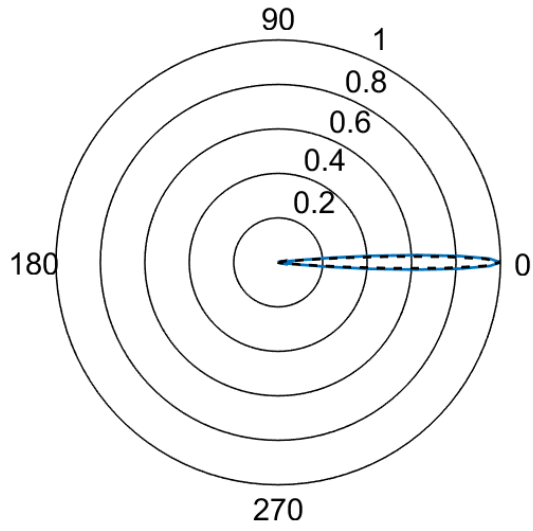


(a)

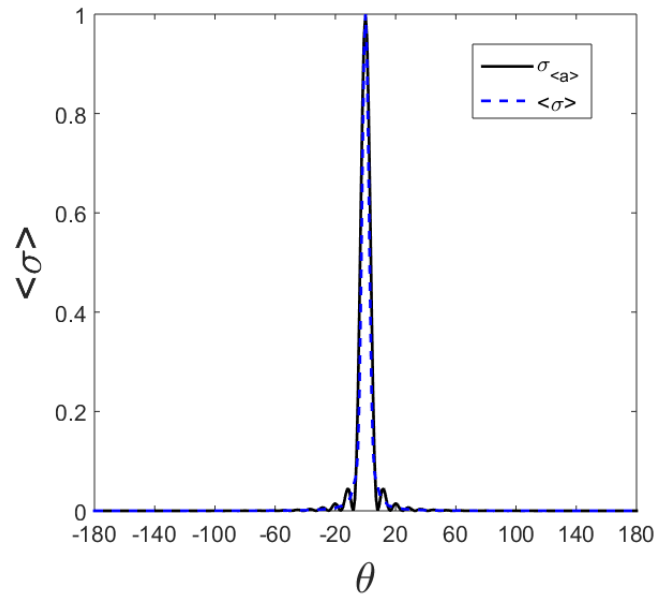


(b)

Figure 3.5: Cross polarized scattering cross section (normalized) of a small PEMC cylinder of random radius with uniform distribution where  $a_1 = 0.1\lambda$  and  $a_2 = 0.6\lambda$ .

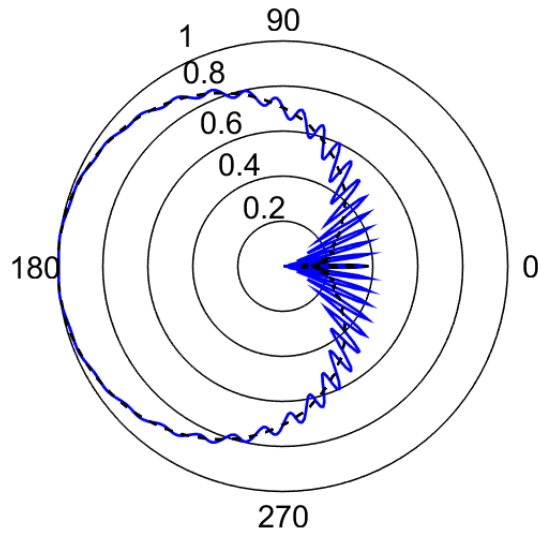


(a)

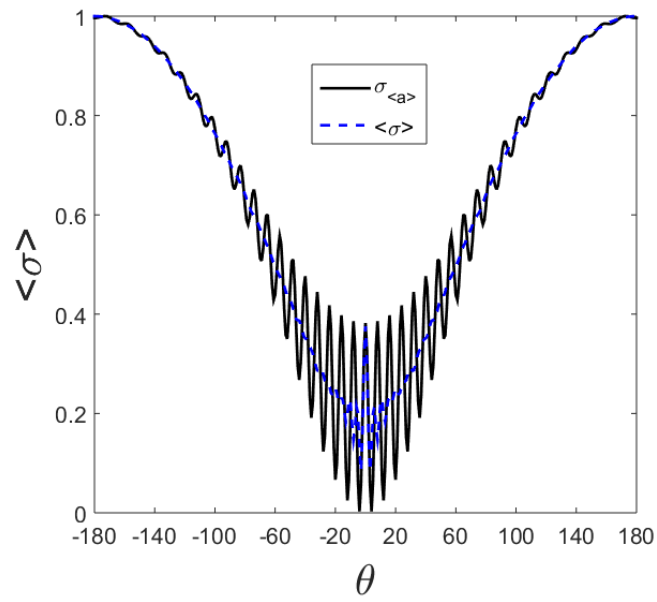


(b)

Figure 3.6: Co polarized scattering cross section (normalized) of a large PEMC cylinder of random radius with uniform distribution where  $a_1 = 1\lambda$  and  $a_2 = 6\lambda$ .

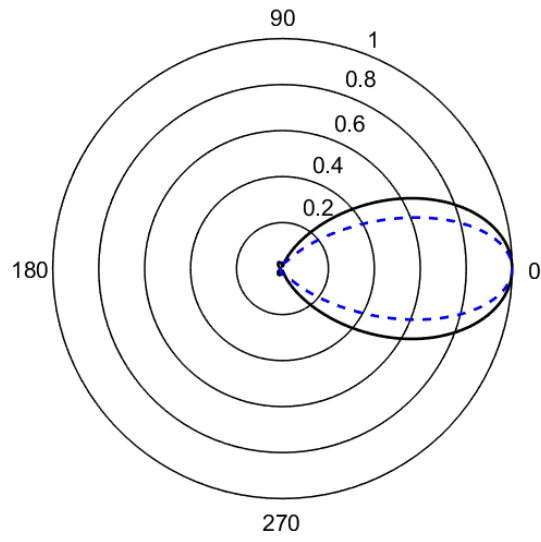


(a)

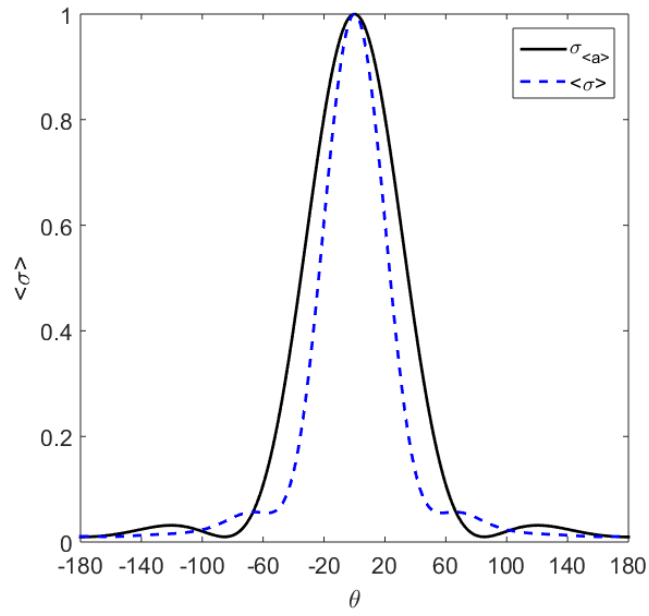


(b)

Figure 3.7: Cross polarized scattering cross section (normalized) of a large PEMC cylinder of random radius with uniform distribution where  $a_1 = 1\lambda$  and  $a_2 = 6\lambda$ .



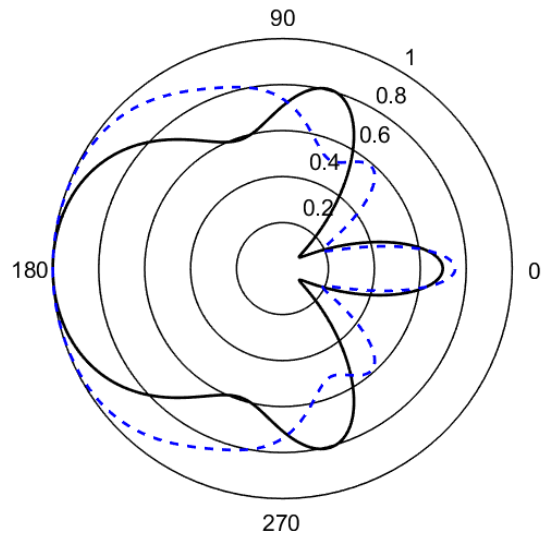
(a)



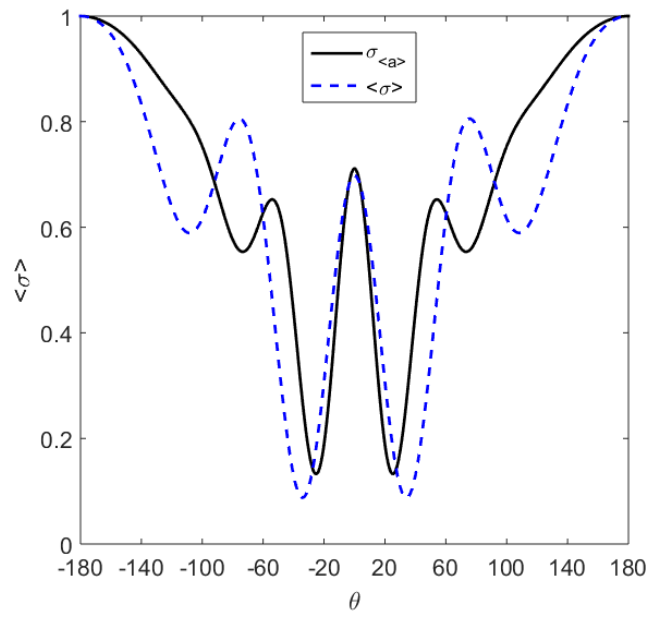
(b)

Figure 3.8: Same as Figure (3.4) except that normal distribution with  $s_a = 0.25$  is considered.



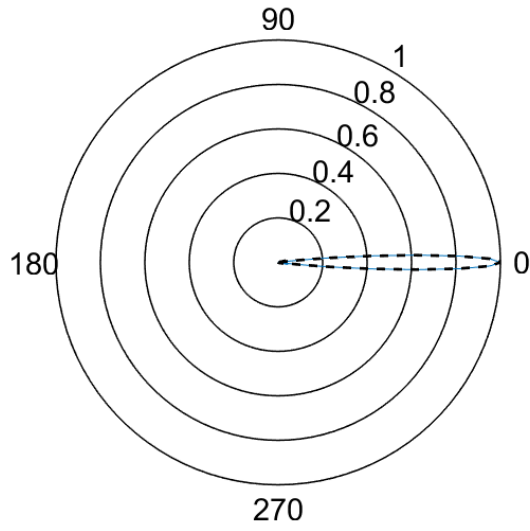


(a)

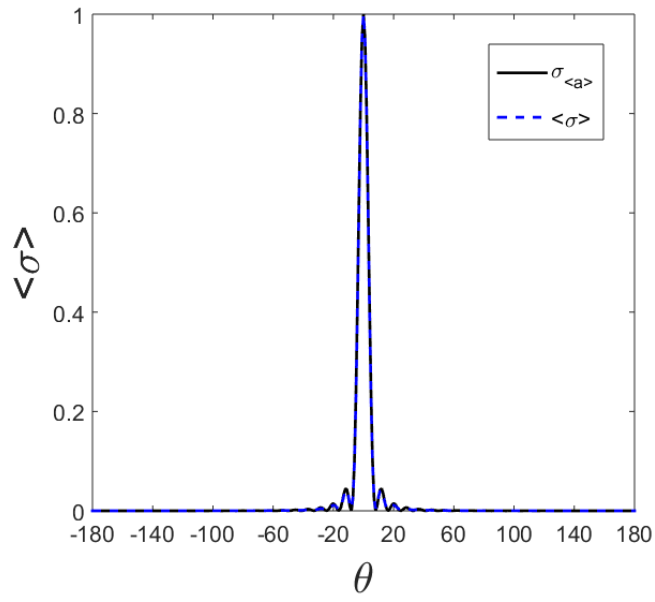


(b)

Figure 3.9: Same as Figure (3.5) except that normal distribution with  $s_a = 0.25$  is considered.

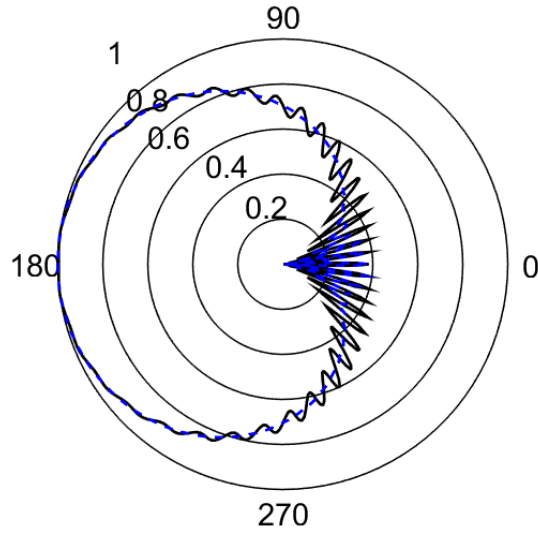


(a)

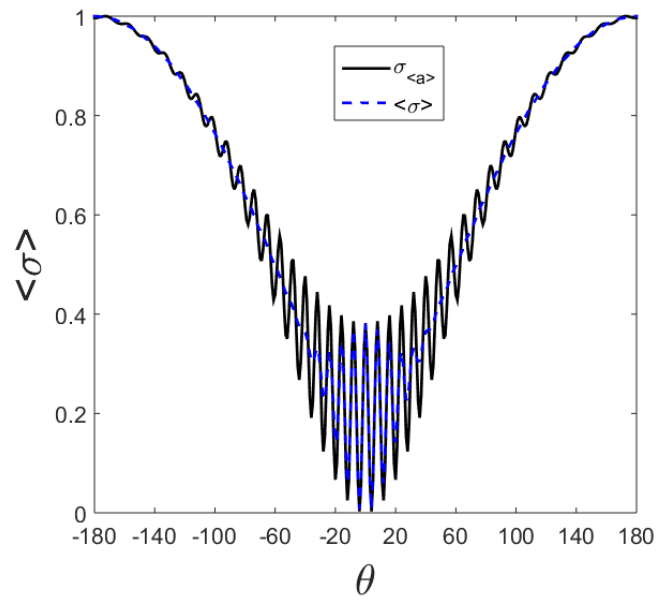


(b)

Figure 3.10: Same as Figure (3.6) except that normal distribution with  $s_a = 0.25$  is considered.

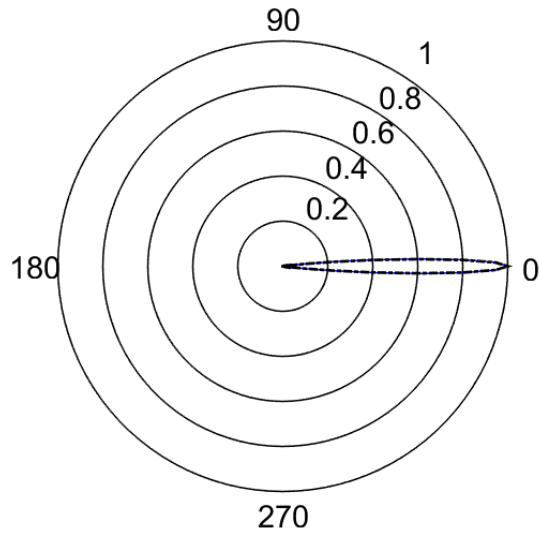


(a)

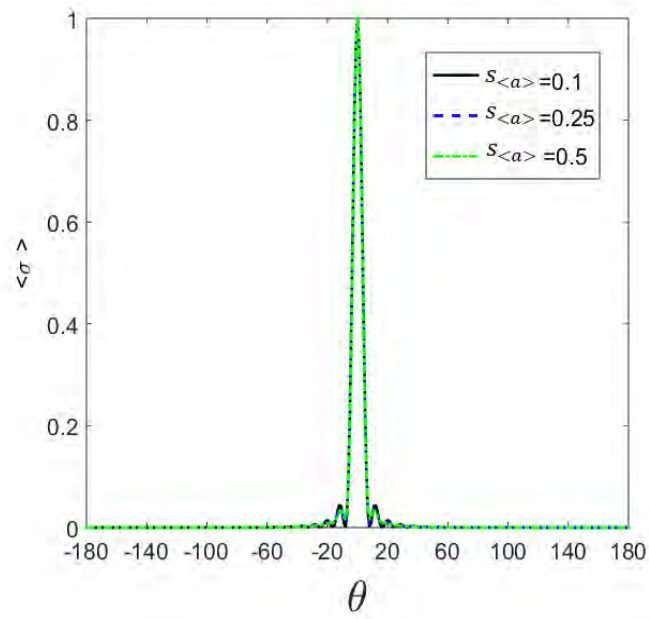


(b)

Figure 3.11: Same as Figure (3.7) except that normal distribution with  $s_a = 0.25$  is considered.



(a)



(b)

Figure 3.12: Co polarized scattering cross section (normalized) of a PEMC cylinder of random radius with normal distribution for different values of standard deviation.

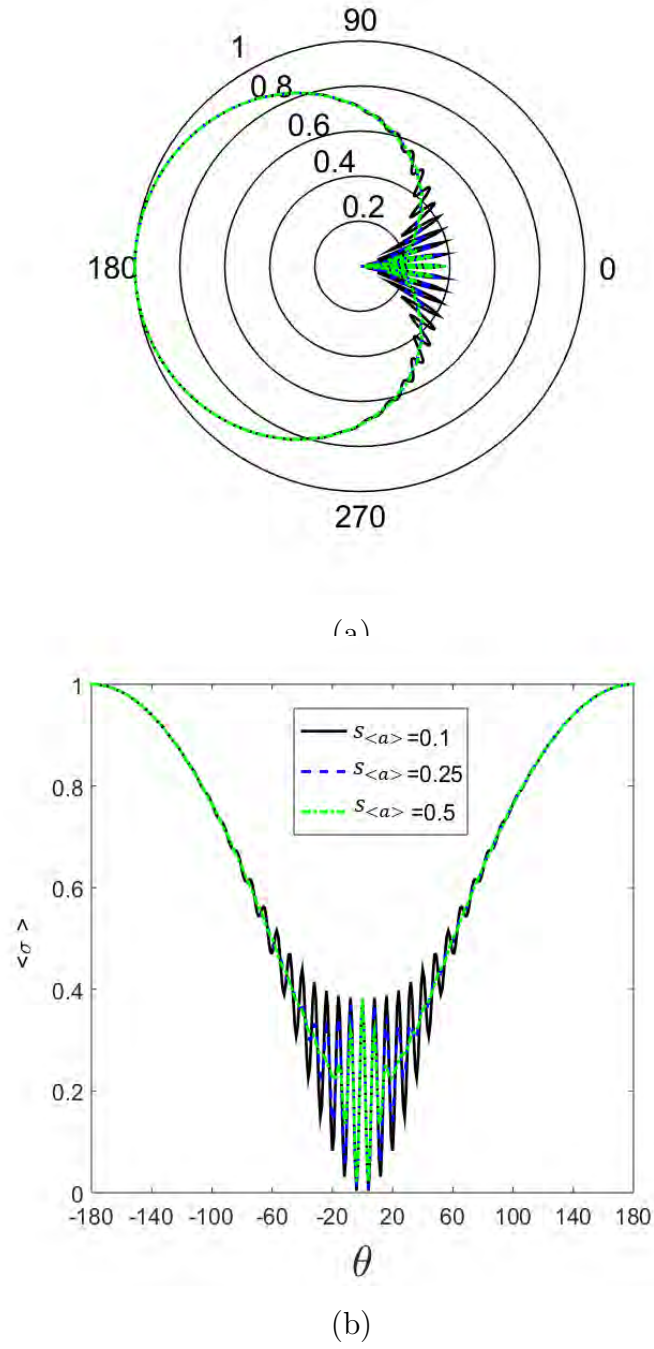


Figure 3.13: Cross polarized scattering cross section (normalized) of a PEMC cylinder of random radius with normal distribution for different values of standard deviation.

## Chapter 4

# Scattered field from a random PEC cylinder with arbitrary shape using the perturbation theory

In this chapter, scattering from a random PEC cylinder having shape perturbations is discussed. An effort has been made to relate the PT conditions with the RC generation. This is very important as the conditions for the PT to be valid must not be violated in the generation of the random cylinder. Both the TM and TE polarized incident fields are assumed. The solution is verified by implementing the well known MOM. Problem formulation is given in Section 4.1 and the numerical results are presented in Section 4.2. The time dependency is taken as  $e^{j\omega t}$ .

### 4.1 Problem formulation

A random PEC cylinder with an arbitrary cross section is assumed as shown in Figure (4.1). It is assumed that the cylinder is infinite in z-direction and the problem is two dimensional. All the mediums are linear, homogeneous and isotropic. A plane wave is made incident to illuminate the scatterer. In polar coordinates, the radius of the random cylinder in terms of unperturbed cylinder radius  $a$  and perturbation constant  $B$  are expressed as

$$\rho' = a + Bp(\theta) \tag{4.1.1}$$

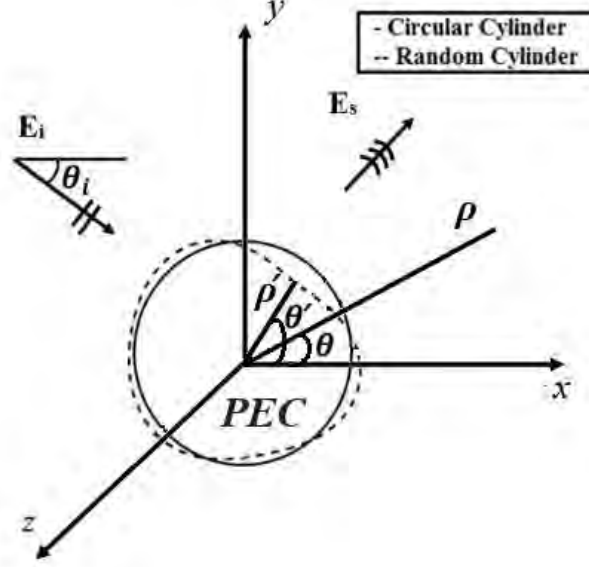


Figure 4.1: A circular random PEC cylinder illuminated by TM/TE polarized incident field.

where  $B$  satisfy the relation  $B \ll \lambda$ . The TM or TE polarized incident field is denoted by  $V_i$  which represents electric or magnetic field component, respectively. It is given by

$$V_i = \sum_{n=-\infty}^{+\infty} V_0 (-j)^n J_n(k\rho) e^{jn(\theta-\theta_i)} \quad (4.1.2)$$

where  $V_0^{TE} = \frac{E_0}{\omega\mu_0}$  and  $V_0^{TM} = \frac{E_0}{k_0}$ . By writing perturbation series, the scattered field can be represented as [35]

$$V_s = \sum_{n=-\infty}^{+\infty} V_0 (-j)^n (c_n^0 + c_n^1 kB + c_n^2 (kB)^2 + \dots) H_n^{(2)}(k\rho) e^{jn(\theta-\theta_i)} \quad (4.1.3)$$

where  $c_n^0$ ,  $c_n^1$  etc are the unknown coefficients and can be found by imposing the boundary conditions at the perturbed cylinder surface.

### 4.1.1 Solution for TM Polarization

To find the unknown scattering coefficients, the following boundary conditions will be applied at the surface of the cylinder as [34]

$$V_z^i + V_z^s = 0 \quad (4.1.4)$$

After putting the expressions for the incident and scattered fields into boundary condition, we get

$$\begin{aligned} & \sum_{n=-\infty}^{+\infty} (-j)^n J_n(ka) e^{jn(\theta-\theta_i)} \\ & + \sum_{n=-\infty}^{+\infty} (-j)^n (c_n^0 + c_n^1 kB + c_n^2 (kB)^2 + \dots) H_n^{(2)}(ka) e^{jn(\theta-\theta_i)} = 0 \end{aligned} \quad (4.1.5)$$

The Taylor series expansion of Bessel and Hankel functions about  $ka$  can be written as

$$F_n(k\rho') = F_n\{k(a + Bp(\theta))\} = F_n(ka) + F_n'(ka)kBp(\theta) + \dots \quad (4.1.6)$$

Putting the above equation in equation (4.1.5), we get

$$\begin{aligned} & \sum_{n=-\infty}^{+\infty} (-j)^n [J_n(ka) + J_n'(ka)kBp(\theta) + \dots] e^{jn\theta} \\ & + \sum_{n=-\infty}^{+\infty} (-j)^n \left[ H_n^{(2)}(ka) + H_n^{(2)'}(ka)kBp(\theta) + \dots \right] \\ & (c_n^0 + c_n^1 kB + c_n^2 (kB)^2 + \dots) e^{jn\theta} = 0 \end{aligned} \quad (4.1.7)$$

Comparing the coefficients of the zeroth order terms the following expression is obtained for  $c_n^0$

$$c_n^0 = -\frac{J_n(ka)}{H_n^{(2)}(ka)} \quad (4.1.8)$$

For  $B = 0$ , there is no perturbation and the resultant scattered field will be that of an unperturbed circular cylinder given by [1]

$$V_s = - \sum_{n=-\infty}^{+\infty} V_0 (-j)^n \frac{J_n(ka)}{H_n^{(2)}(ka)} H_n^{(2)}(k\rho) e^{jn(\theta-\theta_i)} \quad (4.1.9)$$



The first order scattering coefficient  $c_n^1$  can be calculated by comparing the first order terms as

$$\sum_{n=-\infty}^{+\infty} (-j)^n c_n^1 H_n^{(2)}(ka) e^{jn\theta} = \frac{2jp(\theta)}{\pi ka} \sum_{n=-\infty}^{+\infty} (-j)^n \frac{e^{jn\theta}}{H_n^{(2)}(ka)} \quad (4.1.10)$$

The higher terms of  $(kB)^2$  can be neglected as  $kB \ll 1$ . The Fourier series representation of  $p(\theta)$  is

$$p(\theta) = Re \left[ \sum_{m=-\infty}^{+\infty} Y_m e^{j(m\theta + \psi_m)} \right] \quad (4.1.11)$$

Putting the above equation in equation (4.1.10) we get the solution for  $c_n^1$ ,

$$c_n^1 = \frac{2j^{n+1}}{\pi ka H_n^{(2)}(ka)} \sum_{q=-\infty}^{+\infty} (-j)^q \frac{Y_{n-q} e^{j\psi_{n-q}}}{H_q^{(2)}(ka)} \quad (4.1.12)$$

The scattered field up to first order is given by

$$V_s = \sum_{n=-\infty}^{+\infty} V_0 (-j)^n \left[ -\frac{J_n(ka)}{H_n^{(2)}(ka)} + \frac{2j^{n+1}}{\pi ka H_n^{(2)}(ka)} \sum_{q=-\infty}^{+\infty} (-j)^q \frac{Y_{n-q} e^{j\psi_{n-q}}}{H_q^{(2)}(ka)} kB \right] H_n^{(2)}(k\rho) e^{jn(\theta - \theta_i)} \quad (4.1.13)$$

In the next section, the unknown coefficients for the TE polarization will be derived.

#### 4.1.2 Solution for TE Polarization

In the TM case, it is seen that the electric field  $E_z$  is always tangent to the surface of the cylinder while for the TE case,  $E_\phi$  is always tangent to the cylinder boundary. So, the tangential electric field component will be found using the unit tangent vector defined by [35]

$$\hat{t} = \frac{\zeta \hat{\rho}}{\sqrt{1 + \zeta^2}} + \frac{\hat{\phi}}{\sqrt{1 + \zeta^2}} \quad (4.1.14)$$

where  $\zeta = \frac{B \partial p(\theta)}{a + B p(\theta)}$  and  $\partial p(\theta) = \frac{\partial p(\theta)}{\partial \theta}$ . Using the tangential components of the electric field, the boundary condition is given by

$$V_{tan}^i + V_{tan}^s = 0 \quad (4.1.15)$$

The tangent electric field can be calculated using the Maxwell's equation as [35]

$$V_{tan}^i = \frac{1}{j\omega\epsilon} \sum_{n=-\infty}^{+\infty} j^{-n} \frac{1}{\sqrt{1+\zeta^2}} \left[ \frac{\zeta j n}{\rho'} J_n(k\rho') - k J_n'(k\rho') \right] e^{jn(\theta-\theta_i)} \quad (4.1.16)$$

and

$$V_{tan}^s = \frac{1}{j\omega\epsilon} \sum_{n=-\infty}^{+\infty} j^{-n} (c_n^0 + c_n^1 k B + c_n^2 (kB)^2 + \dots) \frac{1}{\sqrt{1+\zeta^2}} \left[ \frac{\zeta j n}{\rho'} H_n^{(2)}(k\rho') - k H_n'^{(2)}(k\rho') \right] e^{jn(\theta-\theta_i)} \quad (4.1.17)$$

Substituting the expressions for the tangential incident and scattered fields in equation (4.1.15), we obtain

$$\begin{aligned} & -\frac{1}{j\omega\epsilon} \sum_{n=-\infty}^{+\infty} j^{-n} \frac{1}{\sqrt{1+\zeta^2}} \left[ \frac{\zeta j n}{\rho'} \{J_n(ka) + J_n'(ka) k B p(\theta) + \dots\} \right. \\ & \left. - k \{J_n'(ka) + J_n''(ka) k B p(\theta) + \dots\} \right] e^{jn\theta} \\ & -\frac{1}{j\omega\epsilon} \sum_{n=-\infty}^{+\infty} j^{-n} (c_n^0 + c_n^1 k B + c_n^2 (kB)^2 + \dots) \frac{1}{\sqrt{1+\zeta^2}} \\ & \left[ \frac{\zeta j n}{\rho'} \{H_n^{(2)}(ka) + H_n'^{(2)}(ka) k B p(\theta) + \dots\} \right. \\ & \left. - k \{H_n'^{(2)}(ka) + H_n''^{(2)}(ka) k B p(\theta) + \dots\} \right] e^{jn\theta} = 0 \end{aligned} \quad (4.1.18)$$

In the above equation, the Taylor series expansion of the Hankel functions is used. Balancing the zeroth order terms of the equation (4.1.18), the unknown scattering coefficient  $c_n^0$  can be obtained as

$$c_n^0 = -\frac{J_n'(ka)}{H_n'^{(2)}(ka)} \quad (4.1.19)$$

The resultant scattered field for the unperturbed circular cylinder can be written as

$$V_s = \sum_{n=-\infty}^{+\infty} j^{-n} \left[ -\frac{J_n'(ka)}{H_n'^{(2)}(ka)} \right] H_n^{(2)}(k\rho) e^{jn(\theta-\theta_i)} \quad (4.1.20)$$

To calculate  $c_n^1$ , we equate the first order terms of equation (4.1.18)

$$\sum_{n=-\infty}^{+\infty} j^{-n} H_n^{(2)}(ka) c_n^1 e^{jn\theta} = \sum_{n=-\infty}^{+\infty} j^{-n} \left[ \frac{p(\theta) T_n}{H_n^{(2)}(ka)} - \frac{p'(\theta) 2n}{\pi(ka)^3 H_n^{(2)}(ka)} \right] e^{jn\theta} \quad (4.1.21)$$

where  $T_n = J_n''(ka) H_n^{(2)}(ka) - J_n'(ka) H_n''^{(2)}(ka)$ . The expression for the  $p'(\theta)$  is given by

$$p'(\theta) = \text{Re} \left[ \sum_{m=-\infty}^{+\infty} j m Y_m e^{j(m\theta + \psi_m)} \right] \quad (4.1.22)$$

Substituting the above equation in equation (4.1.21),  $c_n^1$  can be written as

$$c_n^1 = \frac{j^n}{H_n^{(2)}(ka)} \sum_{q=-\infty}^{+\infty} j^{-q} \frac{Y_{n-q} e^{j\psi_{n-q}}}{H_q^{(2)}(ka)} \left[ T_q - \frac{j2(n-q)q}{\pi(ka)^3} \right] \quad (4.1.23)$$

The resultant scattered field is given by

$$V_s = \frac{1}{j\omega\epsilon} \sum_{n=-\infty}^{+\infty} j^{-n} \left[ -\frac{J_n'(ka)}{H_n^{(2)}(ka)} + \frac{j^n}{H_n^{(2)}(ka)} \sum_{q=-\infty}^{+\infty} j^{-q} \frac{Y_{n-q} e^{j\psi_{n-q}}}{H_q^{(2)}(ka)} \right. \\ \left. \left\{ T_q - \frac{j2(n-q)q}{\pi(ka)^3} \right\} k B \right] H_n^{(2)}(k\rho) e^{jn(\theta - \theta_i)} \quad (4.1.24)$$

From equation (4.1.23), it is seen that the function  $p'(\theta)$  is not required, only coefficients are required.

## 4.2 RC Generation and Results

In this section, the RC generation is discussed and relationship to the PT is developed. For the PT to be valid, the conditions are given by

$$|kp(\theta)| < 1 \quad (4.2.1)$$

and

$$\left| \frac{\partial p(\theta)}{\partial \theta} \right| < 1 \quad (4.2.2)$$

In [38], the finite term Fourier series is used to generate a random cylinder and it is given by

$$p(\theta) = \sum_{n=1}^N Y_n \cos(n\theta + \psi_n) \quad (4.2.3)$$

It is assumed that the random amplitude  $Y_n$  and phase  $\psi_n$  are independent and identically distributed uniformly between  $[-B, B]$  and  $[-\pi, \pi]$  respectively. In this model,  $p(\theta)$  is zero mean and its variance is  $NB^2/6$  where  $N$  denotes the number of terms. The maximum value of the sum of the series is  $|NB|$ . Putting the maximum value of  $p(\theta)$  in the first condition defined in equation (4.2.1), we get

$$|kNB| << 1 \quad (4.2.4)$$

The derivative of  $p(\theta)$  can be expressed as

$$\frac{\partial p(\theta)}{\partial \theta} = \sum_{n=1}^N nY_n \sin(n\theta + \psi_n) \quad (4.2.5)$$

The maximum value of the sum of the above series is

$$S = \frac{N(N+1)B}{2} \quad (4.2.6)$$

From equations (4.2.5), (4.2.6) and the second condition given in equation (4.2.2), we get

$$\left| \frac{N(N+1)B}{2} \right| << 1 \quad (4.2.7)$$

From equations (4.2.4) and (4.2.7), the conditions for RC generation can be written as

$$|kNB| << 1, \quad \left| \frac{N(N+1)B}{2} \right| << 1 \quad (4.2.8)$$

For  $N < (4\pi/\lambda - 1)$ , the first condition dominates while the second condition dominates when  $N > (4\pi/\lambda - 1)$ . It means that the perturbations must be small and the condition for gentle slope will be automatically satisfied for smaller values of  $N$ . For our simulations,  $N$  is a small number and only the condition given in equation (4.2.4) must satisfy. Figure (4.2) shows the random cylinder generated by using equation (4.2.3). In Figure (4.2a),  $N$  is kept constant while  $B$  is kept constant in Figure (4.2b). It can be noticed that the randomness of the cylinder varies as the value of  $B$  or  $N$  is changed.

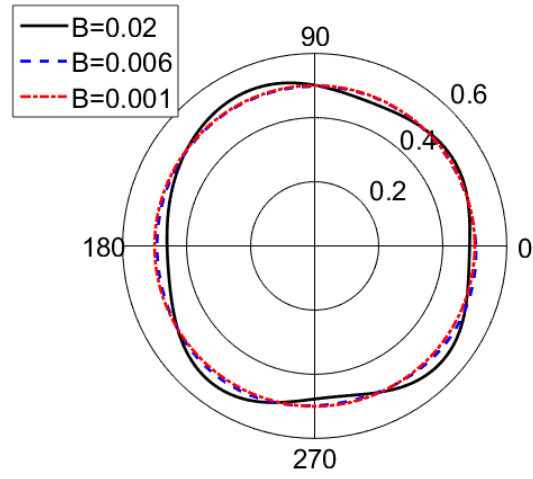
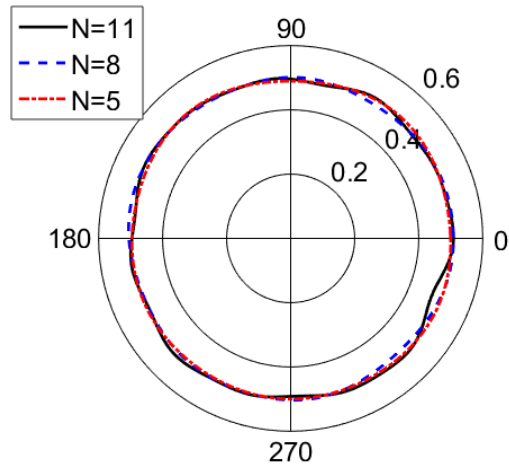
Figures (4.3) and (4.4) show the scattering cross section of a random PEC cylinder obtained using the PT and MoM for  $a = 0.5\lambda$  and  $a = 1\lambda$  respectively. The other

parameters are  $B = 0.005$  and  $N = 5$ . Result obtained using the MoM compared well with that obtained by the PT for a slightly perturbed cylinder.

The scattered field from a circular cylinder is obtained by selecting perturbation parameter  $B = 0$ . We consider a PEC cylinder with mean radius  $a = 0.5\lambda$  and  $B = 0.005$ ,  $N = 5$ . The near zone scattered field for normal incidence is obtained as shown in Figure (4.5). A large cylinder with mean radius  $a = 1\lambda$  is considered in Figure (4.6). These two dimensional field plots show that the scattered field in near zone from a perturbed PEC cylinder varies considerably while compared with the scattered field from a circular cylinder ( $B = 0$ ). The difference between the scattered fields in forward and backward directions for TE and TM polarized incident fields is also very much clear.

Figures (4.7) and (4.8) show the scattered field from a perturbed PEC cylinder where  $a = 0.5\lambda$  and  $N = 5$ . For reference, result for a circular cylinder having  $a = 0.5\lambda$  is also shown. For a circular cylinder  $B = 0$  and for a random cylinder  $B = 0.005$ . A large cylinder with  $a = 1\lambda$  is considered in Figures (4.9) and (4.10). It is noted that for the small value of the perturbation parameter  $B$ , the scattered field from the random cylinder is almost equal to that of the circular cylinder.

Figures (4.11) and (4.12) show the scattering cross section of a perturbed PEC cylinder with different value of the perturbation parameter where  $N=5$ . When  $B$  is kept small, a little variation in the scattered field is observed while the large variations can be found when  $B$  is increased. Figures (4.13) and (4.14) show the scattering cross section from a perturbed cylinder with different values of  $N$  where  $B = 0.005$ . Small variations in the scattered field is observed when  $N$  is kept small while the large variations can be seen when  $N$  is increased. Scattering for TE polarized field is more sensitive to the change in  $B$  and  $N$  than TM case. Figures (4.15) and (4.16) show the scattering cross section of a perturbed PEC cylinder with different value of radius where  $B = 0.005$  and  $N = 5$ . As radius of the cylinder is increased large variations are noticed.

(a)RC for  $N = 5$ (b)RC for  $B = 0.005$ Figure 4.2: Generation of the random cylinder with  $a = 0.5\lambda$ .

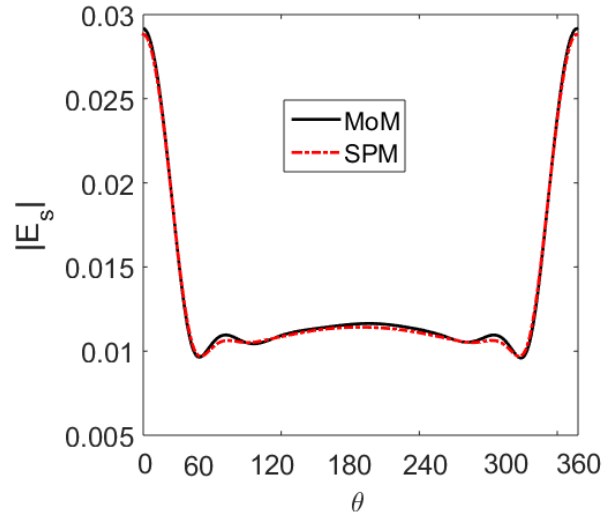


Figure 4.3: Comparison of scattered field from a perturbed PEC cylinder using the PT with that obtained using the MoM where  $a = 0.5\lambda$ ,  $B = 0.005$  and  $N = 5$ .

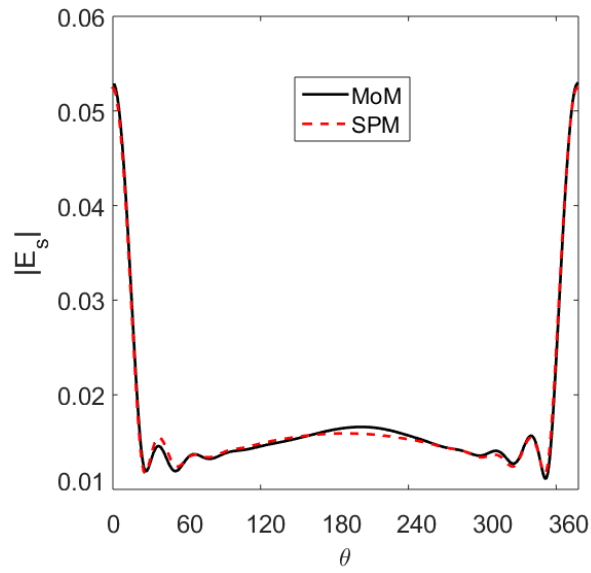


Figure 4.4: Same as figure (4.3) except that radius  $a = 1\lambda$  is assumed.

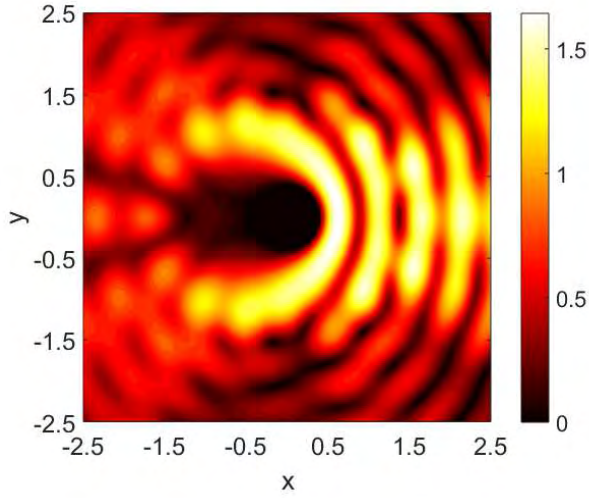
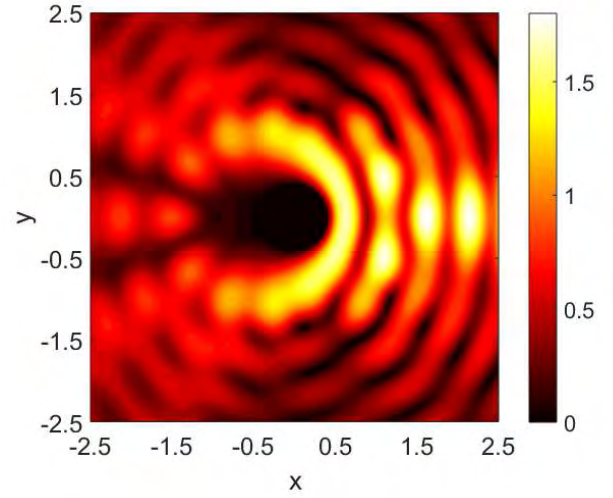
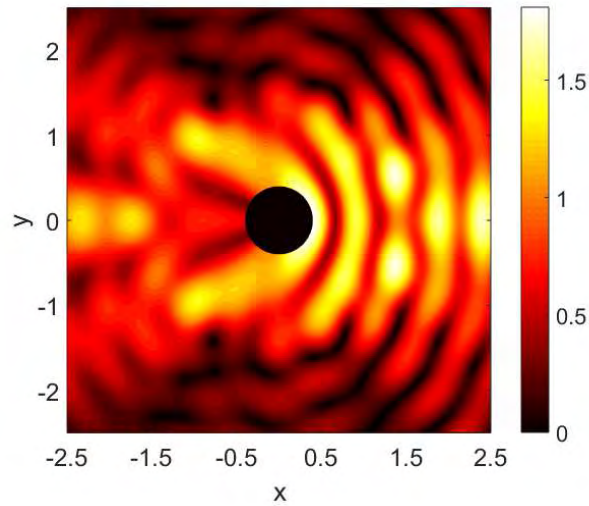
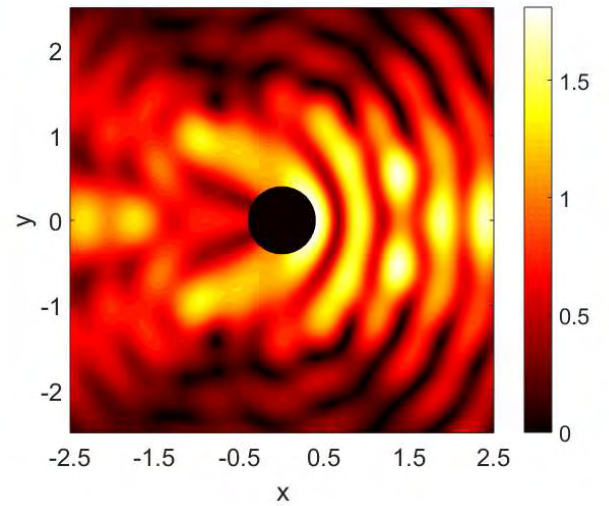
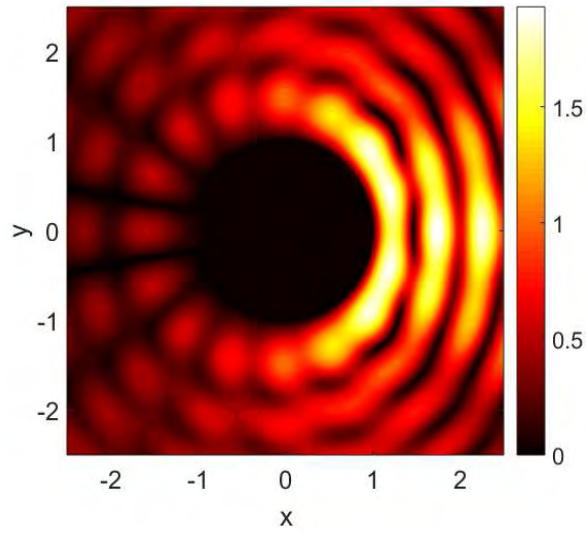
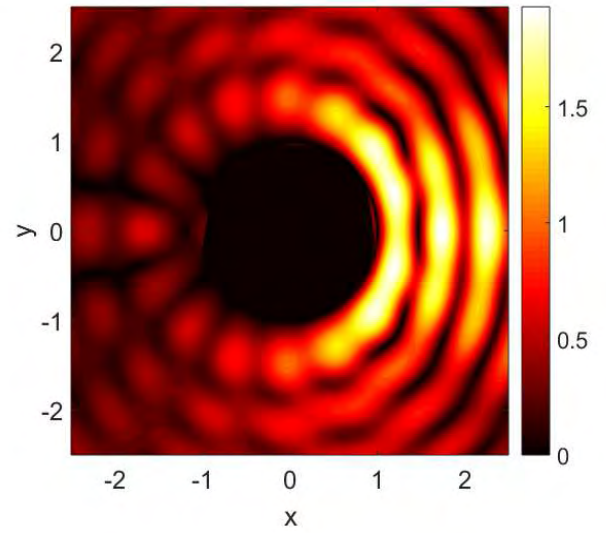
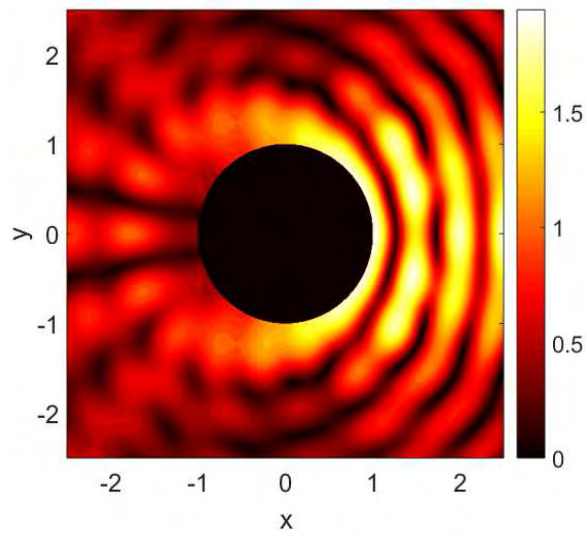
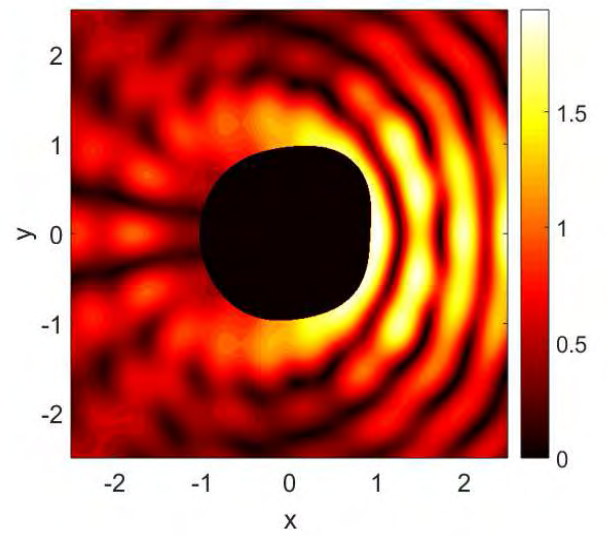
(a) Circular cylinder  $B = 0$ , TM polarization(b) Perturbed cylinder  $B = 0.005$ , TM polarization(c) Circular cylinder  $B = 0$ , TE polarization(d) Perturbed cylinder  $B = 0.005$ , TE polarization

Figure 4.5: Scattered field from a perturbed PEC cylinder with mean radius  $a = 0.5\lambda$  and  $N = 5$ .



(a) Circular cylinder  $B = 0$ , TM polarization(b) Perturbed cylinder  $B = 0.005$ , TM polarization(c) Circular cylinder  $B = 0$ , TE polarization(d) Perturbed cylinder  $B = 0.005$ , TE polarizationFigure 4.6: Same as Figure (4.5) except that  $a = 1\lambda$  is assumed.

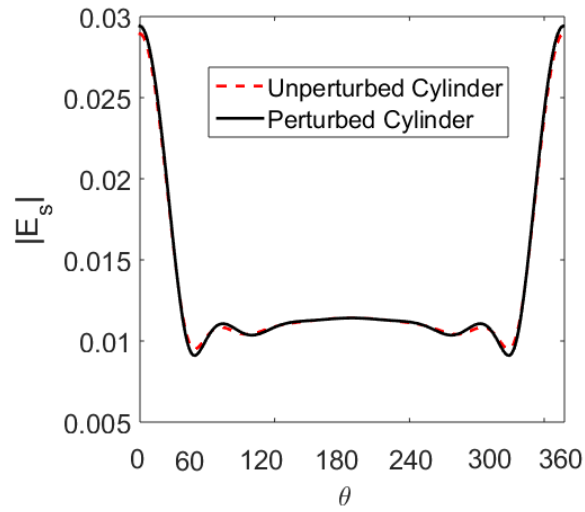


Figure 4.7: Scattered field from a perturbed PEC cylinder for TM polarization where  $a = 0.5\lambda$  and  $B = 0.005$ .

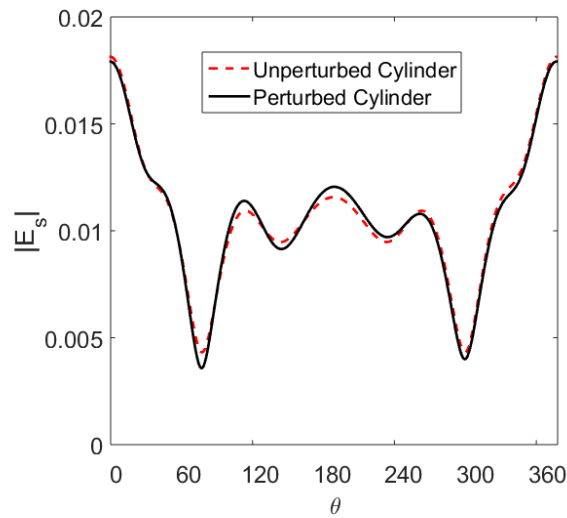


Figure 4.8: Same as Figure (4.7) except that TE polarization is assumed.

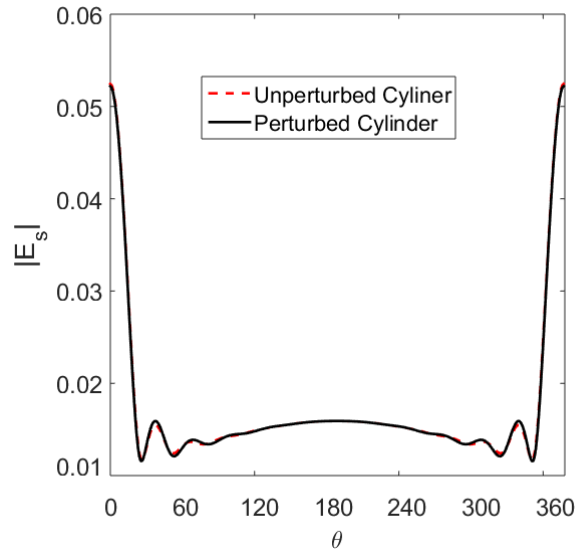


Figure 4.9: Scattered field from a perturbed PEC cylinder for TM polarization where  $a = 1\lambda$  and  $B = 0.005$ .

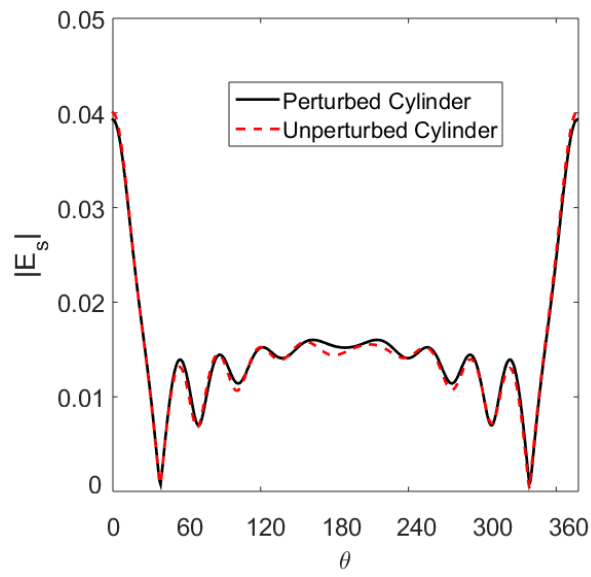


Figure 4.10: Same as Figure (4.9) except that TE polarization is assumed.

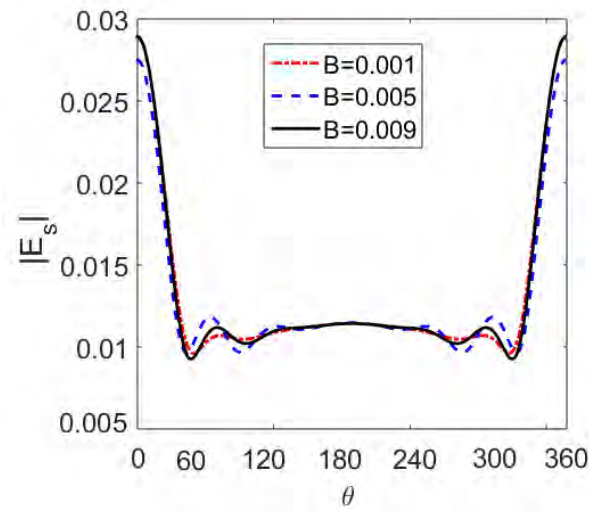


Figure 4.11: Scattered field from a perturbed PEC cylinder for different values of  $B$  where  $a = 0.5\lambda$  and TM polarized incident field is assumed.

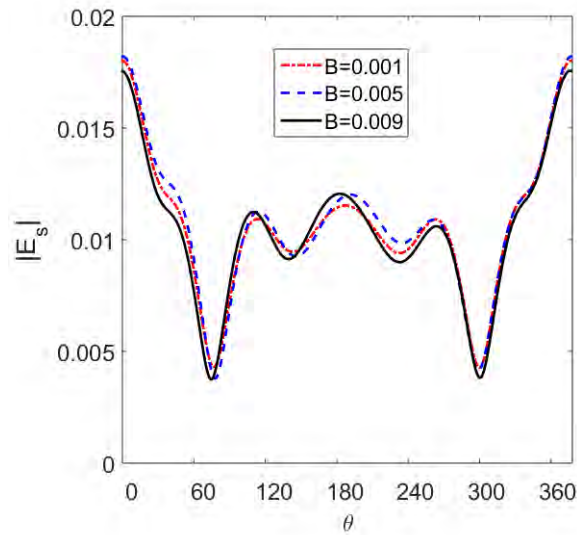


Figure 4.12: Same as Figure (4.11) except that TE polarized incident field is assumed.

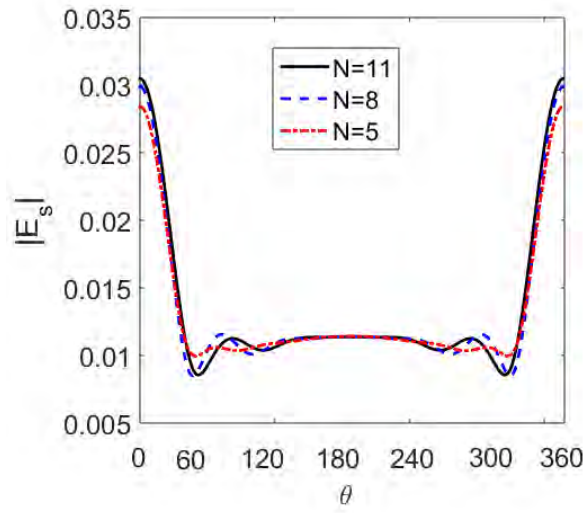


Figure 4.13: Scattered field from a perturbed PEC cylinder for different values of  $N$  where  $a = 0.5\lambda$  and TM polarized incident field is assumed.

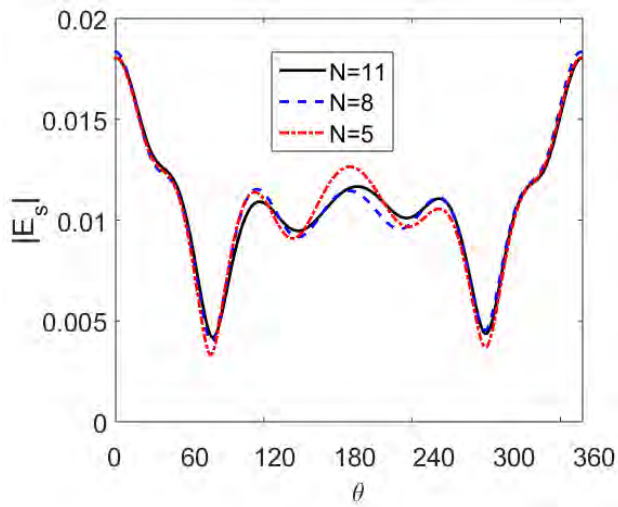


Figure 4.14: Same as Figure (4.13) except that TE polarized incident field is assumed.

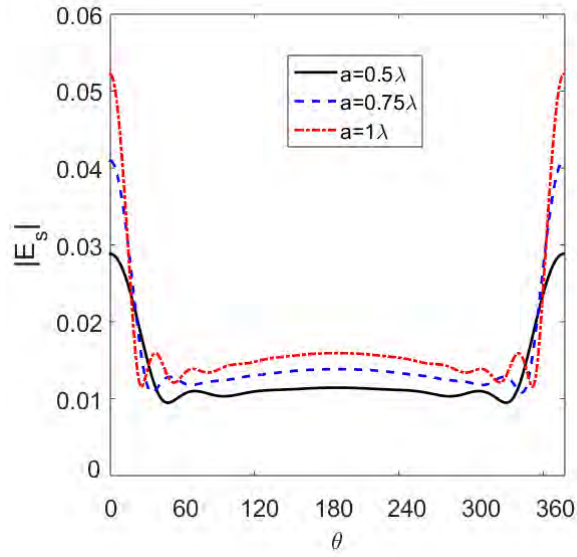


Figure 4.15: Scattered field from a perturbed PEC cylinder for different values of 'a' where  $B = 0.005$ ,  $N = 5$  and TM polarized incident field is assumed.

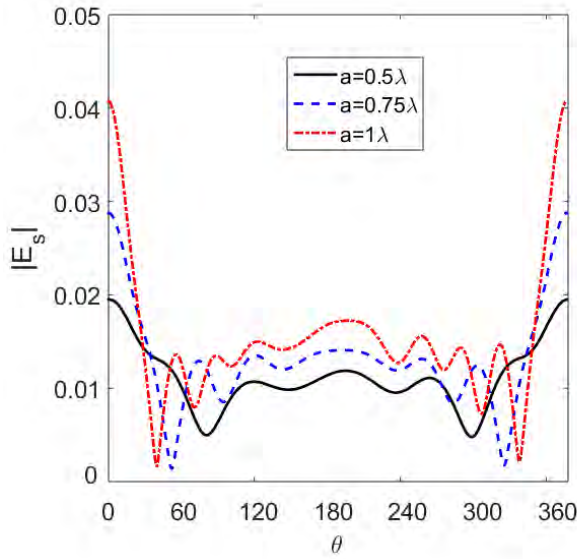


Figure 4.16: Same as Figure (4.15) except that TE polarized incident field is assumed.

## Chapter 5

# Scattered field from a random PEMC cylinder with arbitrary shape using the perturbation theory

In this chapter, a random PEMC cylinder is considered and the scattered field is calculated using the PT. First, perturbed cylinder generation and the related PT conditions for the method to be valid are described in Section 5.1. Moreover, the detailed calculations for the zeroth and the first order solution are evaluated. Numerical simulations are performed in Section 5.2. The time dependency is taken as  $e^{j\omega t}$ .

### 5.1 Problem formulation

Consider figure 5.1, a random cylinder (RC) is generated using the model expressed in [38]. It is assumed that the cylinder is infinite in z-direction and the problem is two dimensional. All the mediums are linear, homogeneous and isotropic. The mathematical description in terms of  $Y_n$  (random amplitude) independent and identical uniformly distributed between  $[-B, B]$  and  $\psi_n$  (phase) distributed between  $[-\pi, \pi]$  is expressed as

$$p(\theta) = \sum_{n=1}^N Y_n \cos(n\theta + \psi_n) \quad (5.1.1)$$

The perturbation on the cylinder's surface can be expressed as [34],

$$\rho' = a + Bp(\theta) \quad (5.1.2)$$

where  $a$  is the unperturbed radius and  $B$  is the perturbation constant satisfying  $B \ll \lambda$ . The validity conditions for PT are reported as [39],

$$|kNB| \ll 1 \quad (5.1.3)$$

$$\left| \frac{N(N+1)B}{2} \right| \ll 1 \quad (5.1.4)$$

### 5.1.1 TM polarization

A TM polarized electric field is incident upon the cylinder and is given by

$$E_z^i = \sum_{n=-\infty}^{n=\infty} j^{-n} J_n(k_0 \rho) e^{jn\theta} \quad (5.1.5)$$

Since the scattered electric and magnetic fields will have both the co and cross

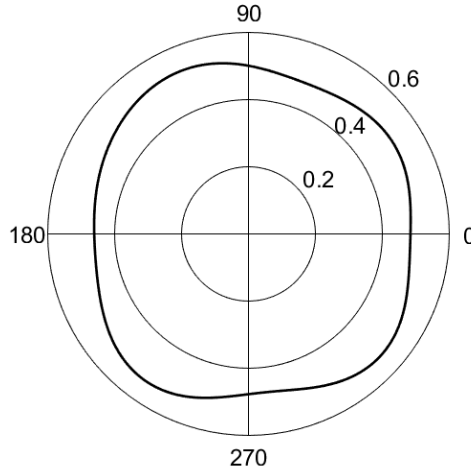


Figure 5.1: A random PEMC cylinder with radius  $a = 0.5\lambda$ .

polarized components. It is worth mentioning that for a perturbed cylinder, the z-component of the field is always tangent to the surface of the cylinder satisfying the



following boundary condition

$$ME_z^i + ME_z^s + H_z^s = 0 \quad (5.1.6)$$

where

$$E_z^s = \sum_{n=-\infty}^{n=\infty} j^{-n} a_n H_n^{(2)}(k_0 \rho) e^{jn\theta} \quad (5.1.7)$$

$$H_z^s = -\frac{1}{j\eta_0} \sum_{n=-\infty}^{n=\infty} j^{-n} b_n H_n^{(2)}(k_0 \rho) e^{jn\theta} \quad (5.1.8)$$

In the above equations, the co polarized unknown scattering coefficient is described by  $a_n$  while the cross polarized unknown coefficient is described by  $b_n$ . The  $\phi$  component is no more tangential to the surface of a perturbed cylinder. The other tangential components are obtained by taking the dot product with the tangent vector reported in [35]. The expression can be written as

$$\hat{t} = \frac{\zeta \hat{\rho}}{\sqrt{1 + \zeta^2}} + \frac{\hat{\phi}}{\sqrt{1 + \zeta^2}} \quad (5.1.9)$$

where  $\zeta = \frac{Bp'(\theta)}{a+Bp(\theta)}$  and  $p'(\theta) = \frac{\partial}{\partial \theta} r(\theta)$ . Hence, the boundary condition for the tangential component is given by,

$$H_{tan}^i + ME_{tan}^s + H_{tan}^s = 0 \quad (5.1.10)$$

Using the following relation

$$H_{tan} = \frac{1}{j\omega\mu_0} \left( \nabla \times E_z \hat{z} \right) \cdot \hat{t} \quad (5.1.11)$$

the incident and scattered fields in terms of the tangential component can be evaluated as,

$$H_{tan}^i = -\frac{1}{j\eta_0} \sum_{n=-\infty}^{n=\infty} \frac{1}{\sqrt{1 + \zeta^2}} j^{-n} \left[ \frac{\zeta j n}{k_0 \rho'} J_n(k_0 \rho') - J_n'(k_0 \rho') \right] e^{jn\theta} \quad (5.1.12)$$

$$H_{tan}^s = -\frac{1}{j\eta_0} \sum_{n=-\infty}^{n=\infty} \frac{1}{\sqrt{1 + \zeta^2}} j^{-n} a_n \left[ \frac{\zeta j n}{k_0 \rho'} H_n^{(2)}(k_0 \rho') - H_n'^{(2)}(k_0 \rho') \right] e^{jn\theta} \quad (5.1.13)$$

$$E_{tan}^s = \sum_{n=-\infty}^{n=\infty} \frac{1}{\sqrt{1 + \zeta^2}} j^{-n} b_n \left[ \frac{\zeta j n}{k_0 \rho'} H_n^{(2)}(k_0 \rho') - H_n'^{(2)}(k_0 \rho') \right] e^{jn\theta} \quad (5.1.14)$$

To find the unknown coefficients from the boundary condition in equations (5.1.6) and (5.1.10), the PT is applied. The first step is to expand the unknown coefficients into the perturbation series as

$$a_n = a_n^0 + a_n^1 k_0 B + a_n^2 (k_0 B)^2 + \dots \quad (5.1.15)$$

$$b_n = b_n^0 + b_n^1 k_0 B + b_n^2 (k_0 B)^2 + \dots \quad (5.1.16)$$

Moreover, the cylindrical wave functions are expanded into Taylor series about  $k_0 a$  as [35],

$$F_n(k_0 \rho') = F_n \left\{ k_0 (a + B p(\theta)) \right\} = F_n(k_0 a) + F_n'(k_0 a) k_0 B p(\theta) + \dots \quad (5.1.17)$$

By substituting the equations (5.1.15)-(5.1.17) in the field expressions defined in the equations (5.1.5), (5.1.7) and (5.1.8) and using the boundary condition in the equation (5.1.6) we get,

$$\begin{aligned} & \sum_{n=-\infty}^{n=\infty} j^{-n} \{ J_n(k_0 a) + k_0 B p(\theta) J_n'(k_0 a) \} e^{jn\theta} \\ & + \sum_{n=-\infty}^{n=\infty} j^{-n} (a_n^0 + a_n^1 k_0 B + a_n^2 (k_0 B)^2 + \dots) \\ & \{ H_n^{(2)}(k_0 a) + k_0 B p(\theta) H_n'^{(2)}(k_0 a) \} e^{jn\theta} \\ & - \frac{1}{j M \eta_0} \sum_{n=-\infty}^{n=\infty} j^{-n} (b_n^0 + b_n^1 k_0 B + b_n^2 (k_0 B)^2 + \dots) \\ & \{ H_n^{(2)}(k_0 a) + k_0 B p(\theta) H_n'^{(2)}(k_0 a) \} e^{jn\theta} = 0 \end{aligned} \quad (5.1.18)$$

Similarly, putting the equations (5.1.15)-(5.1.17) in the field expressions defined in the equations (5.1.12)-(5.1.14) and using the boundary conditions in the equation

(5.1.10) we get,

$$\begin{aligned}
& -\frac{n\zeta}{k_0\rho'M\eta_0} \sum_{n=-\infty}^{n=\infty} j^{-n} \{J_n(k_0a) + k_0Bp(\theta)J'_n(k_0a)\}e^{jn\theta} \\
& + \frac{1}{jM\eta_0} \sum_{n=-\infty}^{n=\infty} j^{-n} \{J'_n(k_0a) + k_0Bp(\theta)J''_n(k_0a)\}e^{jn\theta} \\
& - \frac{n\zeta}{k_0\rho'M\eta_0} \sum_{n=-\infty}^{n=\infty} j^{-n} (a_n^0 + a_n^1 k_0B + a_n^2 (k_0B)^2 + \dots) \\
& \{H_n^{(2)}(k_0a) + k_0Bp(\theta)H_n'^{(2)}(k_0a)\}e^{jn\theta} \\
& + \frac{1}{jM\eta_0} \sum_{n=-\infty}^{n=\infty} j^{-n} (a_n^0 + a_n^1 k_0B + a_n^2 (k_0B)^2 + \dots) \\
& \{H_n'^{(2)}(k_0a) + k_0Bp(\theta)H_n''^{(2)}(k_0a)\}e^{jn\theta} \\
& + \frac{jn\zeta}{k_0\rho'} \sum_{n=-\infty}^{n=\infty} j^{-n} (b_n^0 + b_n^1 k_0B + b_n^2 (k_0B)^2 + \dots) \\
& \{H_n^{(2)}(k_0a) + k_0Bp(\theta)H_n'^{(2)}(k_0a)\}e^{jn\theta} \\
& - \sum_{n=-\infty}^{n=\infty} j^{-n} (b_n^0 + b_n^1 k_0B + b_n^2 (k_0B)^2 + \dots) \\
& \{H_n'^{(2)}(k_0a) + k_0Bp(\theta)H_n''^{(2)}(k_0a)\}e^{jn\theta} = 0
\end{aligned} \tag{5.1.19}$$

Putting the values of  $\zeta$  and  $\rho'$  in the above equations and comparing the zeroth order terms, the following expressions are obtained as,

$$a_n^0 H_n^{(2)}(k_0a) - \frac{1}{jM\eta_0} b_n^0 H_n'^{(2)}(k_0a) = -J_n(k_0a) \tag{5.1.20}$$

$$a_n^0 H_n'^{(2)}(k_0a) - jM\eta_0 b_n^0 H_n''^{(2)}(k_0a) = -J'_n(k_0a) \tag{5.1.21}$$

The above expressions can be solved to find unknown coefficients  $a_n^0$  and  $b_n^0$  as,

$$a_n^0 = -\frac{H_n^{(2)}(k_0a)J'_n(k_0a) - M^2\eta_0^2 J_n(k_0a)H_n'^{(2)}(k_0a)}{(1 + M^2\eta_0^2)H_n^{(2)}(k_0a)H_n'^{(2)}(k_0a)} \tag{5.1.22}$$

$$b_n^0 = -\frac{2M\eta_0}{(1 + M^2\eta_0^2)\pi k_0a H_n^{(2)}(k_0a)H_n'^{(2)}(k_0a)} \tag{5.1.23}$$

Equations (5.1.22) and (5.1.23) are similar to the expressions as reported by Rupp in [2]. The first order terms from the equations (5.1.18) and (5.1.19) can be written as

$$\sum_{n=-\infty}^{n=\infty} j^{-n} a_n^1 H_n^{(2)}(k_0 a) - \frac{1}{jM\eta_0} \sum_{n=-\infty}^{n=\infty} j^{-n} b_n^1 H_n^{(2)}(k_0 a) = -l_1 \quad (5.1.24)$$

$$\sum_{n=-\infty}^{n=\infty} j^{-n} a_n^1 H_n'^{(2)}(k_0 a) - jM\eta_0 \sum_{n=-\infty}^{n=\infty} j^{-n} b_n^1 H_n'^{(2)}(k_0 a) = -jM\eta_0 l_2 \quad (5.1.25)$$

where

$$l_1 = p(\theta) \sum_{n=-\infty}^{n=\infty} \left\{ J_n'(k_0 a) + a_n^0 H_n'^{(2)}(k_0 a) - \frac{1}{jM\eta_0} b_n^0 H_n'^{(2)}(k_0 a) \right\} \quad (5.1.26)$$

$$\begin{aligned} l_2 = p'(\theta) \sum_{n=-\infty}^{n=\infty} \left\{ -\frac{jn}{(k_0 a)^2} J_n(k_0 a) - \frac{nM\eta_0}{(k_0 a)^2} b_n^0 H_n^{(2)}(k_0 a) \right. \\ \left. - \frac{jn}{(k_0 a)^2} a_n^0 H_n^{(2)}(k_0 a) \right\} + p(\theta) \left\{ \frac{2}{k_0 a} J_n'(k_0 a) + J_n''(k_0 a) \right. \\ \left. + a_n^0 H_n''(k_0 a) - jM\eta_0 b_n^0 H_n''(k_0 a) + \frac{2}{k_0 a} a_n^0 H_n'(k_0 a) \right. \\ \left. - \frac{2jM\eta_0}{k_0 a} b_n^0 H_n'(k_0 a) \right\} \end{aligned} \quad (5.1.27)$$

The higher terms of  $(kB)^2$  can be neglected as  $kB \ll 1$ . From the equation (5.1.1) the expressions for  $p'(\theta)$  can be written as,

$$p'(\theta) = Re \left[ \sum_{m=-\infty}^{+\infty} jm Y_m e^{j(m\theta + \psi_m)} \right] \quad (5.1.28)$$

Putting the values of  $p(\theta)$  and  $p'(\theta)$  from equations (5.1.1) and (5.1.28) in the equations (5.1.26) and (5.1.27), the following expressions are obtained

$$\begin{aligned} l_1 = \sum_{m=-\infty}^{+\infty} Y_m e^{j(m\theta + \psi_m)} \sum_{n=-\infty}^{n=\infty} \left\{ J_n'(k_0 a) + a_n^0 H_n'^{(2)}(k_0 a) \right. \\ \left. - \frac{1}{jM\eta_0} b_n^0 H_n'^{(2)}(k_0 a) \right\} \end{aligned} \quad (5.1.29)$$

$$\begin{aligned}
l_2 = & \sum_{m=-\infty}^{+\infty} jmY_me^{i(m\theta+\psi_m)} \sum_{n=-\infty}^{n=\infty} \left\{ -\frac{jn}{(k_0a)^2} J_n(k_0a) - \frac{nM\eta_0}{(k_0a)^2} b_n^0 H_n^{(2)}(k_0a) \right. \\
& - \frac{jn}{(k_0a)^2} a_n^0 H_n^{(2)}(k_0a) \left. \right\} + \sum_{m=-\infty}^{+\infty} Y_me^{j(m\theta+\psi_m)} \sum_{n=-\infty}^{n=\infty} \left\{ \frac{2}{k_0a} J'_n(k_0a) \right. \\
& + J''_n(k_0a) + a_n^0 H''_n(k_0a) - jM\eta_0 b_n^0 H''_n(k_0a) + \frac{2}{k_0a} a_n^0 H'_n(k_0a) \\
& \left. - \frac{2jM\eta_0}{k_0a} b_n^0 H'_n(k_0a) \right\} \quad (5.1.30)
\end{aligned}$$

Equations (5.1.24) and (5.1.25) can be solved simultaneously using the orthogonality condition to find the unknown coefficients  $a_n^1$  and  $b_n^1$  as,

$$a_n^1 = -\frac{jM\eta_0 L_2 H_n^{(2)}(k_0a) - M^2\eta_0^2 L_1 H_n'^{(2)}(k_0a)}{(1 + M^2\eta_0^2) H_n^{(2)}(k_0a) H_n'^{(2)}(k_0a)} \quad (5.1.31)$$

$$b_n^1 = jM\eta_0 \left\{ \frac{-jM\eta_0 L_2 H_n^{(2)}(k_0a) + L_1 H_n'^{(2)}(k_0a)}{(1 + M^2\eta_0^2) H_n^{(2)}(k_0a) H_n'^{(2)}(k_0a)} \right\} \quad (5.1.32)$$

where

$$L_1 = \sum_{q=-\infty}^{+\infty} Y_{n-q} e^{j\psi_{n-q}} \left\{ J'_q(k_0a) + a_q^0 H_q'^{(2)}(k_0a) - \frac{1}{jM\eta_0} b_q^0 H_q'^{(2)}(k_0a) \right\} \quad (5.1.33)$$

$$\begin{aligned}
L_2 = & \sum_{q=-\infty}^{+\infty} j(n-q) Y_{n-q} e^{j(\psi_{n-q})} \left\{ -\frac{jq}{(k_0a)^2} J_q(k_0a) - \frac{qM\eta_0}{(k_0a)^2} b_q^0 H_q^{(2)}(k_0a) \right. \\
& - \frac{jq}{(k_0a)^2} a_q^0 H_q^{(2)}(k_0a) \left. \right\} + \sum_{q=-\infty}^{+\infty} Y_{n-q} e^{j(\psi_{n-q})} \left\{ \frac{2}{k_0a} J'_q(k_0a) + J''_q(k_0a) \right. \\
& + a_q^0 H''_q(k_0a) - jM\eta_0 b_q^0 H''_q(k_0a) + \frac{2}{k_0a} a_q^0 H'_q(k_0a) - \frac{2jM\eta_0}{k_0a} b_q^0 H'_q(k_0a) \left. \right\} \quad (5.1.34)
\end{aligned}$$

The zeroth and the first order coefficients can be used to represent the scattered field as,

$$\begin{aligned}
E_s = & \sum_{n=-\infty}^{+\infty} E_0(-j)^n \left[ \hat{z}(a_n^0 + a_n^1 k_0 B) H_n^{(2)}(k_0\rho) + \right. \\
& \left. \hat{\rho}, \hat{\phi}(b_n^0 + b_n^1 k_0 B) H_n'^{(2)}(k_0\rho) \right] e^{jn(\theta-\theta_i)} \quad (5.1.35)
\end{aligned}$$

### 5.1.2 TE polarization

The TE polarized incident magnetic field is given by

$$H_z^i = -\frac{1}{j\eta_0} \sum_{n=-\infty}^{n=\infty} j^{-n} J_n(k_0\rho) e^{jn\theta} \quad (5.1.36)$$

The boundary condition for the z-component is expressed as,

$$H_z^i + H_z^s + ME_z^s = 0 \quad (5.1.37)$$

where

$$H_z^s = -\frac{1}{j\eta_0} \sum_{n=-\infty}^{n=\infty} j^{-n} c_n H_n^{(2)}(k_0\rho) e^{jn\theta} \quad (5.1.38)$$

$$E_z^s = \sum_{n=-\infty}^{n=\infty} j^{-n} d_n H_n^{(2)}(k_0\rho) e^{jn\theta} \quad (5.1.39)$$

where  $c_n$  and  $d_n$  are the co and cross polarized unknown coefficients. The boundary condition for the tangential component can be written as,

$$ME_{tan}^i + ME_{tan}^s + H_{tan}^s = 0 \quad (5.1.40)$$

The tangential component of the incident and scattered field can be written using the equation (5.1.11) as,

$$E_{tan}^i = \sum_{n=-\infty}^{n=\infty} \sqrt{1 + \zeta^2} j^{-n} \left[ \frac{\zeta j n}{k_0 \rho'} J_n(k_0 \rho') - J_n'(k_0 \rho') \right] e^{jn\theta} \quad (5.1.41)$$

$$E_{tan}^s = \sum_{n=-\infty}^{n=\infty} \sqrt{1 + \zeta^2} j^{-n} c_n \left[ \frac{\zeta j n}{k_0 \rho'} H_n^{(2)}(k_0 \rho') - H_n'^{(2)}(k_0 \rho') \right] e^{jn\theta} \quad (5.1.42)$$

$$H_{tan}^s = -\frac{1}{j\eta_0} \sum_{n=-\infty}^{n=\infty} \sqrt{1 + \zeta^2} j^{-n} d_n \left[ \frac{\zeta j n}{k_0 \rho'} H_n^{(2)}(k_0 \rho') - H_n'^{(2)}(k_0 \rho') \right] e^{jn\theta} \quad (5.1.43)$$

By substituting the equations (5.1.15)-(5.1.17) in the field expressions defined in the equations (5.1.38) and (5.1.39) and using the boundary conditions in the equation

(5.1.37) we get,

$$\begin{aligned}
& - \sum_{n=-\infty}^{n=\infty} j^{-n} \{J_n(k_0 a) + k_0 B p(\theta) J'_n(k_0 a)\} e^{jn\theta} \\
& - \sum_{n=-\infty}^{n=\infty} j^{-n} (c_n^0 + c_n^1 k_0 B + c_n^2 (k_0 B)^2 + \dots) \\
& \{H_n^{(2)}(k_0 a) + k_0 B p(\theta) H_n'^{(2)}(k_0 a)\} e^{jn\theta} \\
& + j M \eta_0 \sum_{n=-\infty}^{n=\infty} j^{-n} (d_n^0 + d_n^1 k_0 B + d_n^2 (k_0 B)^2 + \dots) \\
& \{H_n^{(2)}(k_0 a) + k_0 B p(\theta) H_n'^{(2)}(k_0 a)\} e^{jn\theta} = 0
\end{aligned} \tag{5.1.44}$$

Similarly, putting the equations (5.1.15)-(5.1.17) in the field expressions defined in the equations (5.1.41)-(5.1.43) and using the boundary conditions in the equation (5.1.40) we get,

$$\begin{aligned}
& + \frac{j n \zeta}{k_0 \rho'} \sum_{n=-\infty}^{n=\infty} j^{-n} \{J_n(k_0 a) + k_0 B p(\theta) J'_n(k_0 a)\} e^{jn\theta} \\
& - \sum_{n=-\infty}^{n=\infty} j^{-n} \{J'_n(k_0 a) + k_0 B p(\theta) J''_n(k_0 a)\} e^{jn\theta} \\
& + \frac{j n \zeta}{k_0 \rho'} \sum_{n=-\infty}^{n=\infty} j^{-n} (c_n^0 + c_n^1 k_0 B + c_n^2 (k_0 B)^2 + \dots) \\
& \{H_n'^{(2)}(k_0 a) + k_0 B p(\theta) H_n''^{(2)}(k_0 a)\} e^{jn\theta} \\
& - \sum_{n=-\infty}^{n=\infty} j^{-n} (c_n^0 + c_n^1 k_0 B + c_n^2 (k_0 B)^2 + \dots) \\
& \{H_n'^{(2)}(k_0 a) + k_0 B p(\theta) H_n''^{(2)}(k_0 a)\} e^{jn\theta}
\end{aligned}$$

$$\begin{aligned}
& -\frac{n\zeta}{M\eta_0 k_0 \rho'} \sum_{n=-\infty}^{n=\infty} j^{-n} (d_n^0 + d_n^1 k_0 B + d_n^2 (k_0 B)^2 + \dots) \\
& \{H_n^{(2)}(k_0 a) + k_0 B p(\theta) H_n''^{(2)}(k_0 a)\} e^{jn\theta} \\
& + \frac{1}{jM\eta_0} \sum_{n=-\infty}^{n=\infty} j^{-n} (d_n^0 + d_n^1 k_0 B + d_n^2 (k_0 B)^2 + \dots) \\
& \{H_n^{(2)}(k_0 a) + k_0 B p(\theta) H_n''^{(2)}(k_0 a)\} e^{jn\theta} = 0
\end{aligned} \tag{5.1.45}$$

Putting the values of  $\zeta$  and  $\rho'$  in the above equation and solving the equations (5.1.44) and (5.1.45) for the zeroth order terms, the following expressions are obtained

$$c_n^0 H_n^{(2)}(k_0 a) - jM\eta_0 d_n^0 H_n^{(2)}(k_0 a) = -J_n(k_0 a) \tag{5.1.46}$$

$$c_n^0 H_n'^{(2)}(k_0 a) - \frac{1}{jM\eta_0} d_n^0 H_n'^{(2)}(k_0 a) = -J_n'(k_0 a) \tag{5.1.47}$$

The above expressions can be solved to find the unknown coefficients  $c_n^0$  and  $d_n^0$  as,

$$c_n^0 = -\frac{J_n(k_0 a) H_n'^{(2)}(k_0 a) - M^2 \eta_0^2 H_n^{(2)}(k_0 a) J_n'(k_0 a)}{(1 + M^2 \eta_0^2) H_n^{(2)}(k_0 a) H_n'^{(2)}(k_0 a)} \tag{5.1.48}$$

$$d_n^0 = \frac{2M\eta_0}{(1 + M^2 \eta_0^2) \pi k_0 a H_n^{(2)}(k_0 a) H_n'^{(2)}(k_0 a)} \tag{5.1.49}$$

Equations (5.1.48) and (5.1.49) are similar to the expressions reported by Rupp in [2]. The first order terms from the equations (5.1.44) and (5.1.45) can be written as

$$\sum_{n=-\infty}^{n=\infty} j^{-n} c_n^1 H_n^{(2)}(k_0 a) + jM\eta_0 \sum_{n=-\infty}^{n=\infty} j^{-n} d_n^1 H_n^{(2)}(k_0 a) = -l_1 \tag{5.1.50}$$

$$\sum_{n=-\infty}^{n=\infty} j^{-n} c_n^1 H_n'^{(2)}(k_0 a) + \frac{1}{jM\eta_0} \sum_{n=-\infty}^{n=\infty} j^{-n} d_n^1 H_n'^{(2)}(k_0 a) = -l_2 \tag{5.1.51}$$

where

$$l_1 = p(\theta) \sum_{n=-\infty}^{n=\infty} \left\{ -J_n'(k_0 a) - c_n^0 H_n'^{(2)}(k_0 a) + jM\eta_0 d_n^0 H_n^{(2)}(k_0 a) \right\} \tag{5.1.52}$$



$$\begin{aligned}
l_2 = & p'(\theta) \sum_{n=-\infty}^{n=\infty} \left\{ \frac{jnM\eta_0}{(k_0a)^2} J_n(k_0a) + \frac{jn}{(k_0a)^2} d_n^0 H_n^{(2)}(k_0a) \right. \\
& - \frac{nM\eta_0}{(k_0a)^2} c_n^0 H_n^{(2)}(k_0a) \left. \right\} - p(\theta) \sum_{n=-\infty}^{n=\infty} \left\{ \frac{2jM\eta_0}{k_0a} J'_n(k_0a) \right. \\
& + jM\eta_0 J''_n(k_0a) + jM\eta_0 c_n^0 H''_n(k_0a) + d_n^0 H''_n(k_0a) \\
& \left. + \frac{2jM\eta_0}{k_0a} c_n^0 H'_n(k_0a) + \frac{2}{k_0a} d_n^0 H'_n(k_0a) \right\} \quad (5.1.53)
\end{aligned}$$

Putting the values of  $p(\theta)$  and  $p'(\theta)$  from the equations (5.1.1) and (5.1.28) in the equations (5.1.52) and (5.1.53), the following equations are obtained,

$$\begin{aligned}
l_1 = & \sum_{m=-\infty}^{+\infty} Y_m e^{j(m\theta+\psi_m)} \sum_{n=-\infty}^{n=\infty} \left\{ J'_n(k_0a) + c_n^0 H_n^{(2)}(k_0a) \right. \\
& \left. + jM\eta_0 d_n^0 H_n^{(2)}(k_0a) \right\} \quad (5.1.54)
\end{aligned}$$

$$\begin{aligned}
l_2 = & \sum_{m=-\infty}^{+\infty} jmY_m e^{j(m\theta+\psi_m)} \sum_{n=-\infty}^{n=\infty} \left\{ \frac{jnM\eta_0}{(k_0a)^2} J_n(k_0a) + \frac{jn}{k_0a} d_n^0 H_n^{(2)}(k_0a) \right. \\
& - \frac{nM\eta_0}{k_0a} c_n^0 H_n^{(2)}(k_0a) \left. \right\} - \sum_{m=-\infty}^{+\infty} Y_m e^{j(m\theta+\psi_m)} \sum_{n=-\infty}^{n=\infty} \left\{ \frac{2jM\eta_0}{k_0a} J'_n(k_0a) \right. \\
& + jM\eta_0 J''_n(k_0a) + jM\eta_0 c_n^0 H''_n(k_0a) + d_n^0 H''_n(k_0a) \\
& \left. + \frac{2jM\eta_0}{k_0a} c_n^0 H'_n(k_0a) + \frac{2}{k_0a} d_n^0 H'_n(k_0a) \right\} \quad (5.1.55)
\end{aligned}$$

The higher terms of  $(kB)^2$  can be neglected as  $kB \ll 1$ . Equations (5.1.50) and (5.1.51) can be solved to find the unknown coefficients  $c_n^1$  and  $d_n^1$  as,

$$c_n^1 = - \frac{M^2 \eta_0^2 L_2 H_n^{(2)}(k_0a) - L_1 H_n'^{(2)}(k_0a)}{(1 + M^2 \eta_0^2) H_n^{(2)}(k_0a) H_n'^{(2)}(k_0a)} \quad (5.1.56)$$

$$d_n^1 = jM\eta_0 \left\{ \frac{-L_2 H_n^{(2)}(k_0a) + L_1 H_n'^{(2)}(k_0a)}{(1 + M^2 \eta_0^2) H_n^{(2)}(k_0a) H_n'^{(2)}(k_0a)} \right\} \quad (5.1.57)$$

where

$$L_1 = \sum_{q=-\infty}^{+\infty} Y_{n-q} e^{j\psi_{n-q}} \left\{ J'_q(k_0 a) + c_q^0 H_q^{(2)}(k_0 a) + jM\eta_0 d_q^0 H_q^{(2)}(k_0 a) \right\} \quad (5.1.58)$$

$$\begin{aligned} L_2 = & \sum_{q=-\infty}^{+\infty} j(n-q) Y_{n-q} e^{j\psi_{n-q}} \left\{ -\frac{qM\eta_0}{(k_0 a)^2} J_q(k_0 a) - \frac{q}{k_0 a} d_q^0 H_q^{(2)}(k_0 a) \right. \\ & + \frac{jqM\eta_0}{k_0 a} c_q^0 H_q^{(2)}(k_0 a) \left. \right\} - \sum_{q=-\infty}^{+\infty} Y_{n-q} e^{j\psi_{n-q}} \left\{ \frac{jM\eta_0}{k_0 a} J'_q(k_0 a) \right. \\ & - jM\eta_0 J''_q(k_0 a) - jM\eta_0 c_q^0 H''_q(k_0 a) - d_q^0 H''_q(k_0 a) \\ & \left. + \frac{2jM\eta_0}{k_0 a} c_q^0 H'_q(k_0 a) - \frac{2}{k_0 a} d_n^0 H'_n(k_0 a) \right\} \end{aligned} \quad (5.1.59)$$

The zeroth and the first order coefficients can be used to represent the scattered field as,

$$\begin{aligned} E_s = & \sum_{n=-\infty}^{+\infty} E_0(-j)^n \left[ \hat{\rho}, \hat{\phi}(c_n^0 + c_n^1 k_0 B) H_n^{(2)}(k_0 \rho) + \right. \\ & \left. \hat{z}(d_n^0 + d_n^1 k_0 B) H_n^{(2)}(k_0 \rho) \right] e^{jn(\theta-\theta_i)} \end{aligned} \quad (5.1.60)$$

It is noteworthy that for  $M\eta_0 = \infty$ , the coefficients  $a_n^1$ ,  $c_n^1$  in the equations (5.1.31) and (5.1.56) reduce to the coefficients reported in [39] for both the TM and TE polarizations. It validates that the scattered field from a perturbed PEC cylinder can be extracted from that of the perturbed PEMC cylinder.

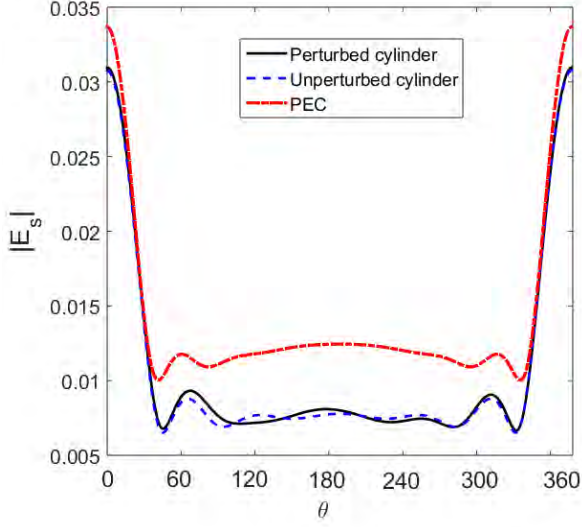
## 5.2 Numerical Results

In this section, equation (5.1.35) is implemented to obtain the results for the TM polarization while the results for the TE polarization are obtained by implementing the equation (5.1.60). Far zone scattered field from a PEMC perturbed cylinder is shown in Figures (5.2) and (5.3) for  $a = 0.5\lambda$  and  $a = 1\lambda$  respectively. The angular behavior shows very small difference between the co and cross scattered field from the PEMC perturbed cylinder and that scattered from the circular cylinder. For reference, scattered field from a PEC cylinder is also presented. To get more details,

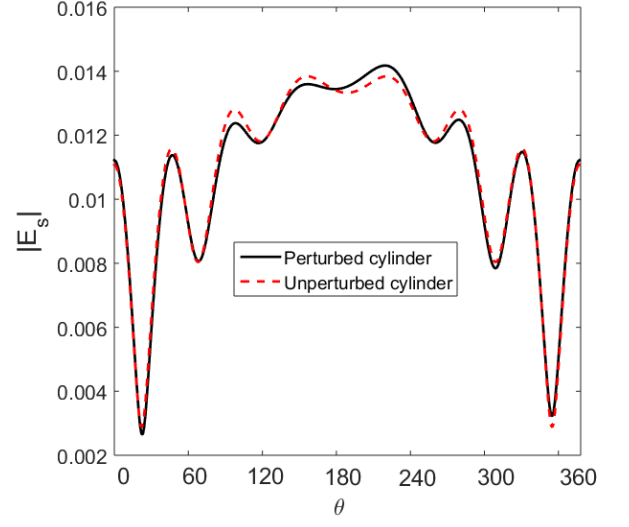
near field is shown in Figures (5.4) and (5.5) for  $a = 0.5\lambda$  and  $a = 1\lambda$  respectively where a TM polarized incident field while results for TE polarized field are shown in Figures (5.6) and (5.7) respectively. The distinctions due to perturbation are more pronounced now in co as well in cross polarized components.

The degree to which the object is perturbed can be controlled by both the perturbation parameter  $B$  and the number of terms in Fourier series  $N$ . Small values of  $N$  and  $B$  introduce small perturbations while the large values of  $N$  and  $B$  give considerable perturbations. Far zone scattered field as a function of perturbation parameter  $B$  is presented in Figures (5.8) and (5.9). The significant variation in co and cross polarized component is noted. The effect of perturbation on near zone forward and backward scattered fields is shown in Figures (5.10) and (5.11) for TM and TE polarizations, respectively. The scattered field for TM polarization is different from that for TE polarization.

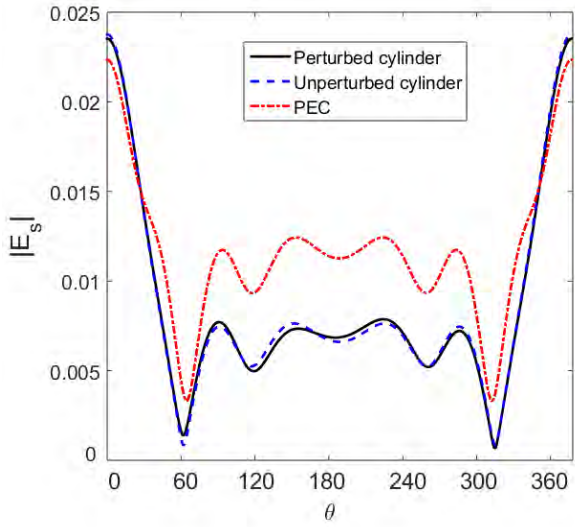
Figures (5.12) and (5.13) show the far zone scattered field for different values of  $N$ . Near zone scattered field is presented in Figures (5.14) and (5.15) for TM and TE polarizations, respectively. Comparing these results with those presented in Figures (5.10) and (5.11), it can be seen that the large value of  $N$  introduces significant variation in the shape of the cylinder and the scattering properties. Moreover, the forward and backward scattering is also different for both the TM and TE polarized incidence. In Figures (5.16) and (5.17), scattered field as a function of the admittance  $M$  is shown where  $a = 0.5\lambda$ ,  $B = 0.005$  and  $N = 5$ . The scattered field from a PEC cylinder is also plotted for reference. It can be noted that co polarized scattered field from a PEMC cylinder is smaller than that for a PEC cylinder due to presence of cross polarized field which decreases as admittance is increased.



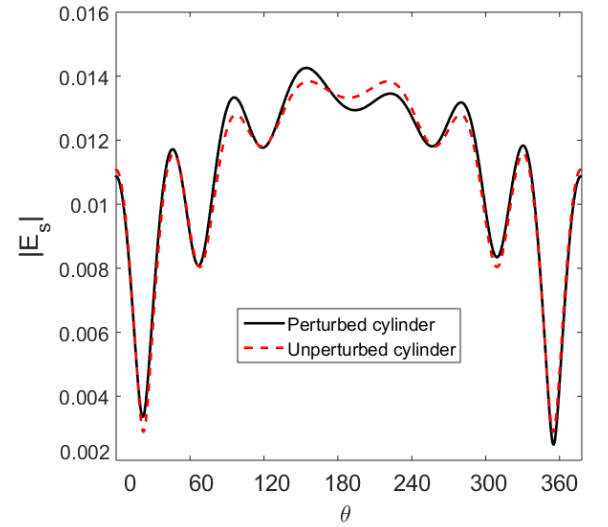
(a) Co polarized component, TM polarization



(b) Cross polarized component, TM polarization

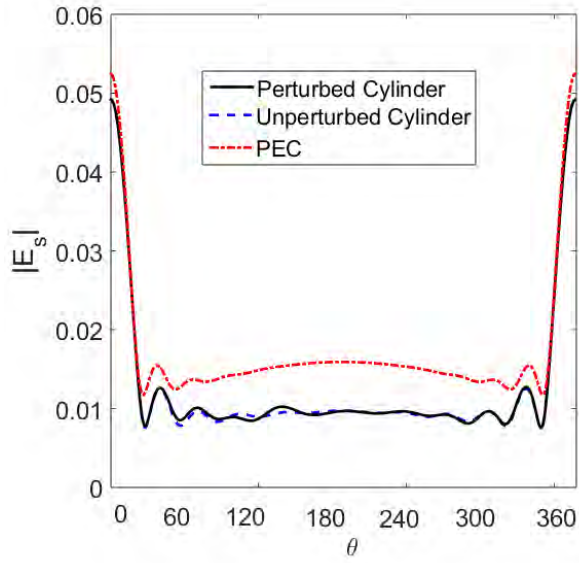


(c) Co polarized component, TE polarization

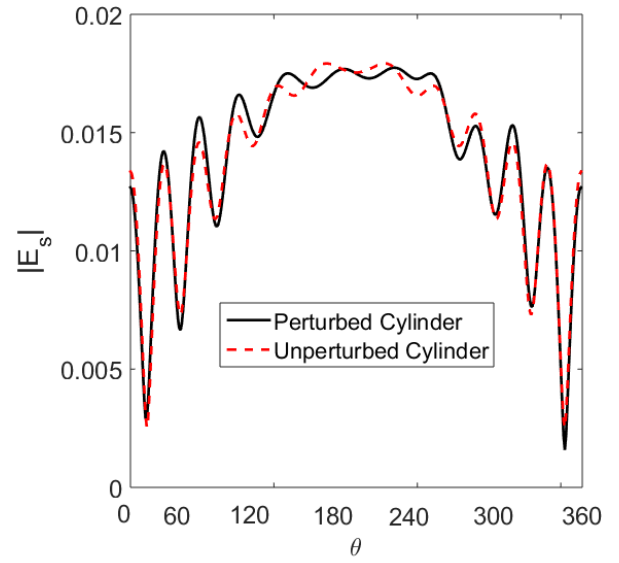


(d) Cross polarized component, TE polarization

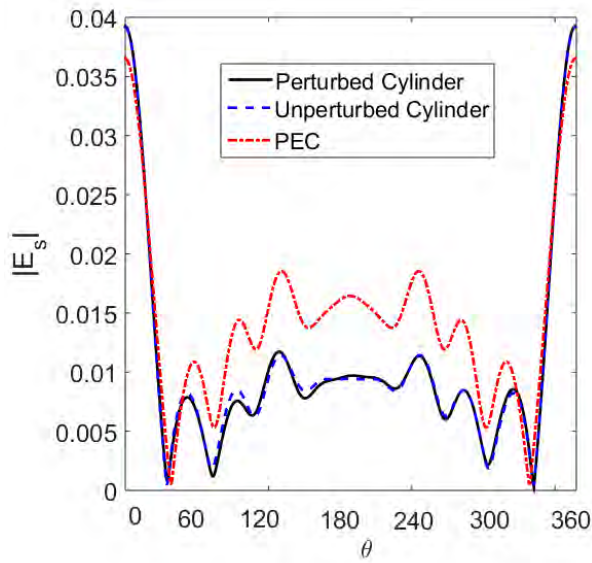
Figure 5.2: Scattered field from a perturbed PEMC cylinder with mean radius  $a = 0.5\lambda$ ,  $B=0.005$ ,  $M_{\eta_0} = 2$  and  $N=5$ .



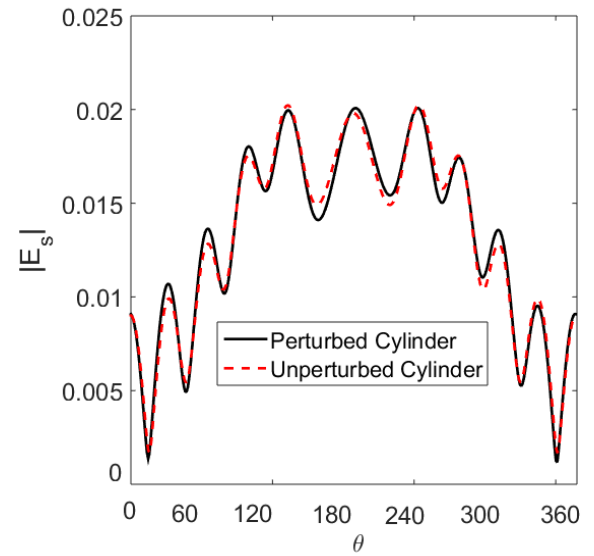
(a) Co polarized component, TM polarization



(b) Cross polarized component, TM polarization



(c) Co polarized component, TE polarization



(d) Cross polarized component, TE polarization

Figure 5.3: Same as Figure (5.2) except that a perturbed PEMC cylinder with mean radius  $a = 1\lambda$  is assumed.

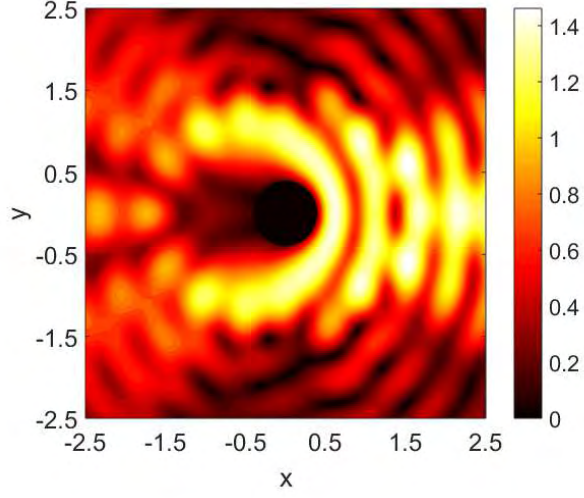
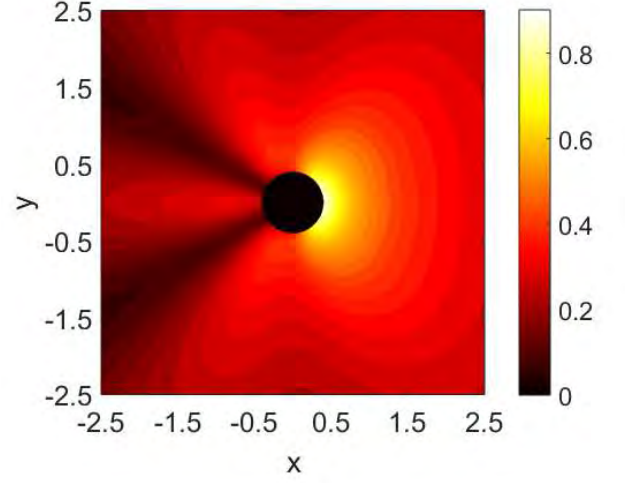
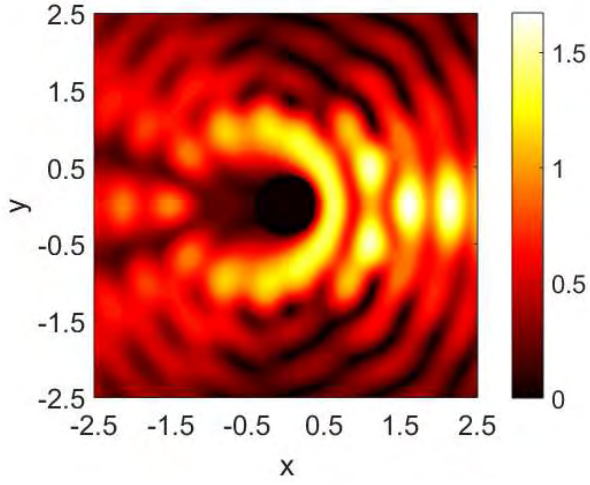
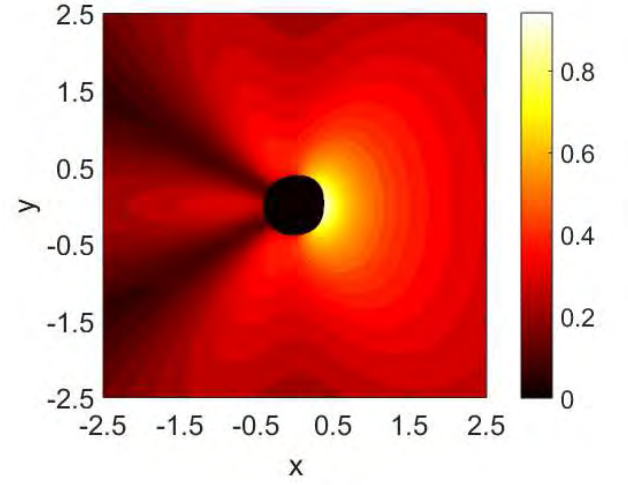
(a) Co polarized component,  $B = 0$ (b) Cross polarized component,  $B = 0$ (c) Co polarized component,  $B = 0.005$ .(d) Cross polarized component,  $B = 0.005$ .

Figure 5.4: Two dimensional field map of the scattered field from a perturbed PEMC cylinder with mean radius  $a = 0.5\lambda$ ,  $N = 5$  and  $M\eta_0 = 2$ . A TM polarized field is normally incident on the cylinder.

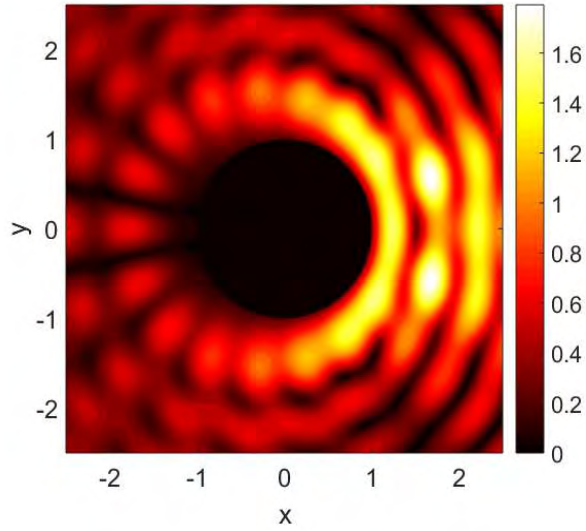
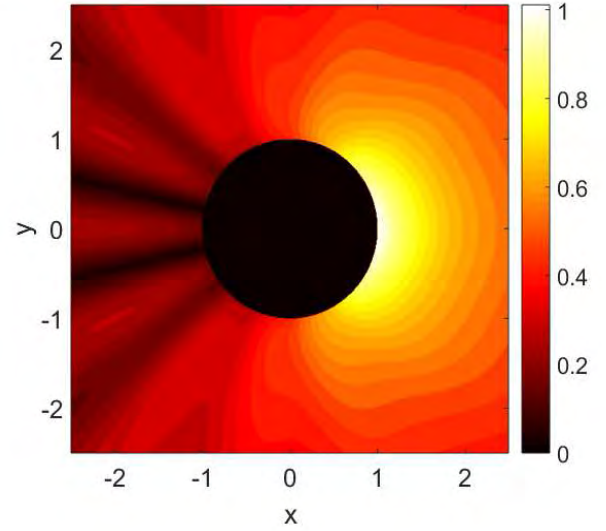
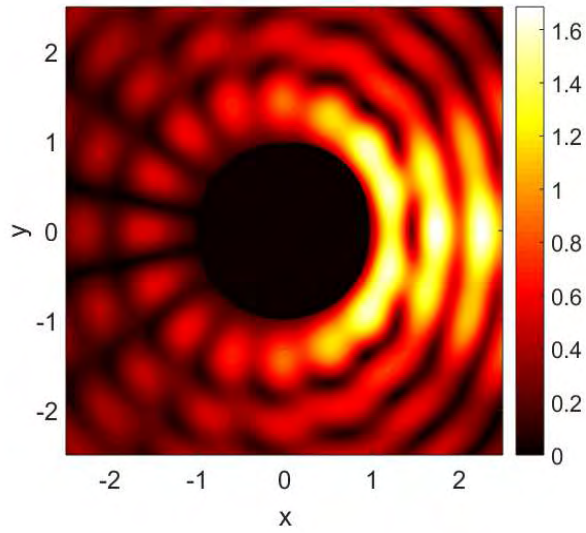
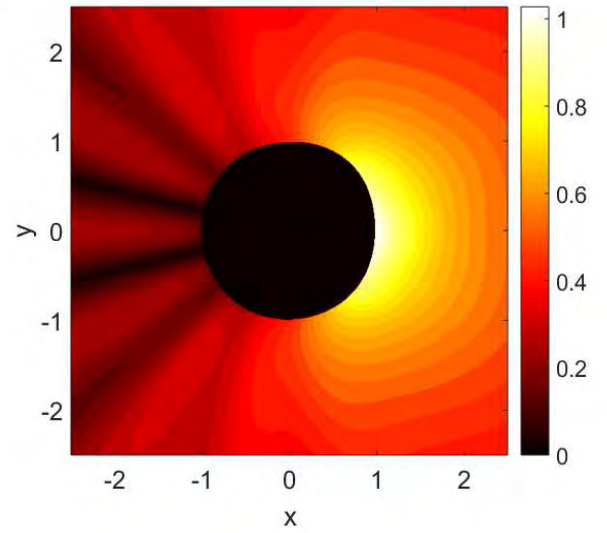
(a) Co polarized component,  $B = 0$ (b) Cross polarized component,  $B = 0$ (c) Co polarized component,  $B = 0.005$ .(d) Cross polarized component,  $B = 0.005$ .

Figure 5.5: Same as Figure (5.4) except that a perturbed PEMC cylinder with mean radius  $a = 1\lambda$  is assumed.



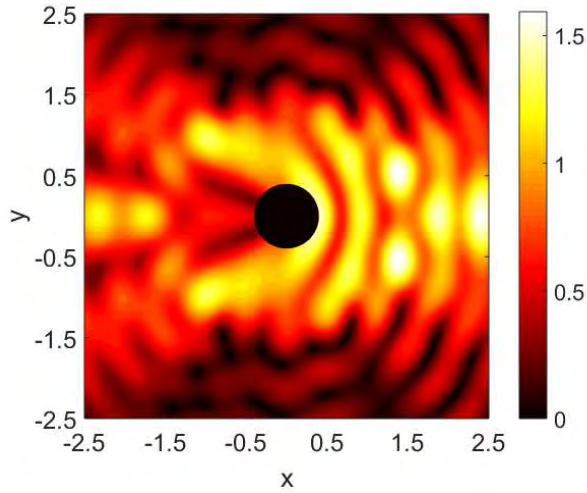
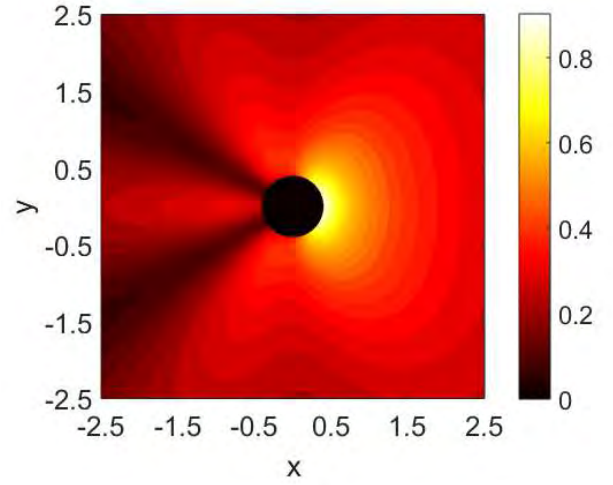
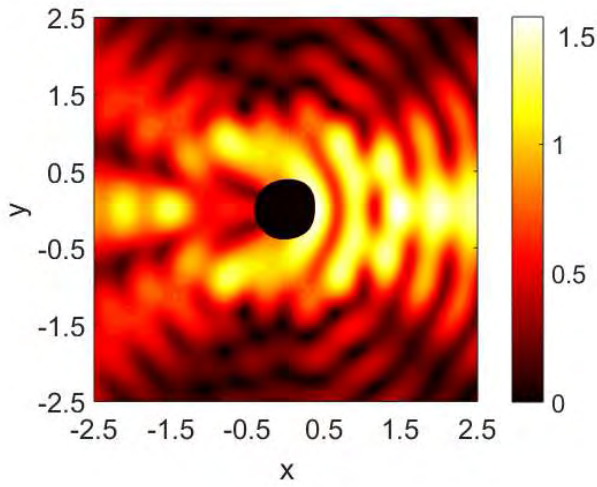
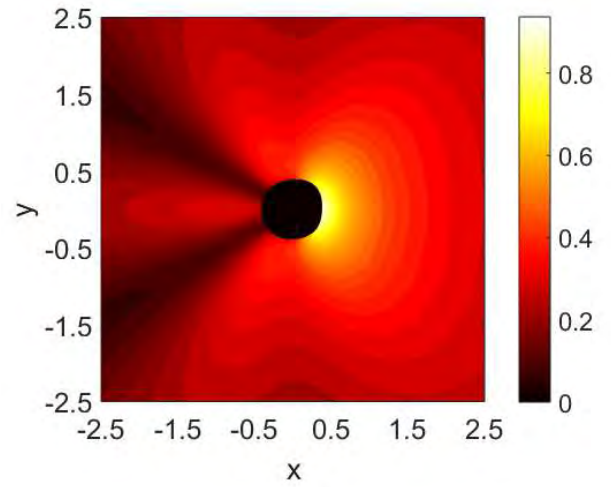
(a) Co polarized component,  $B = 0$ (b) Cross polarized component,  $B = 0$ (c) Co polarized component,  $B = 0.005$ .(d) Cross polarized component,  $B = 0.005$ .

Figure 5.6: Two dimensional field map of the scattered field from a perturbed PEMC cylinder with mean radius  $a = 0.5\lambda$ ,  $N = 5$  and  $M\eta_0 = 2$ . A TE polarized field is normally incident on the cylinder.



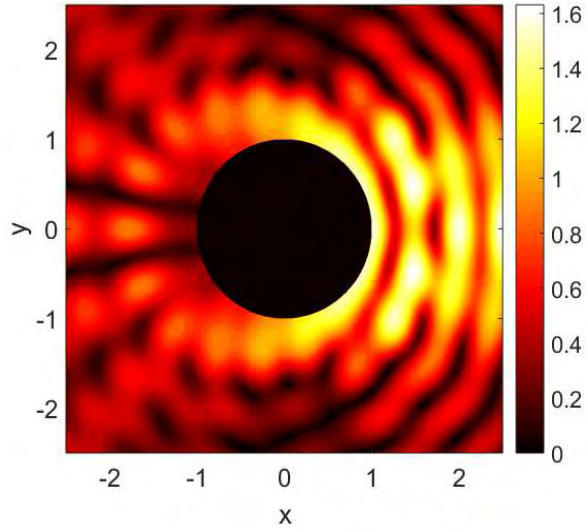
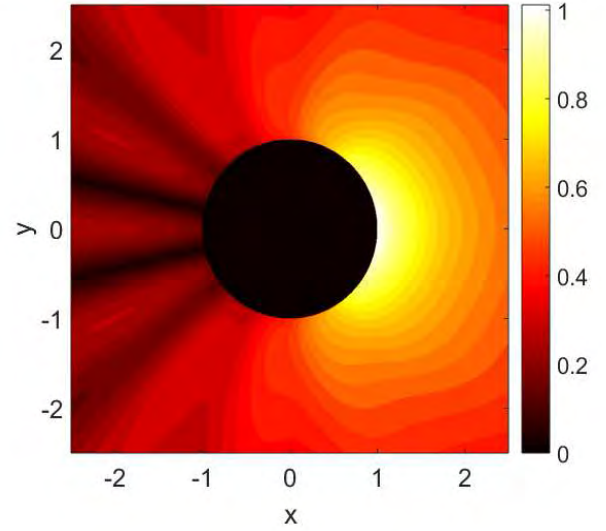
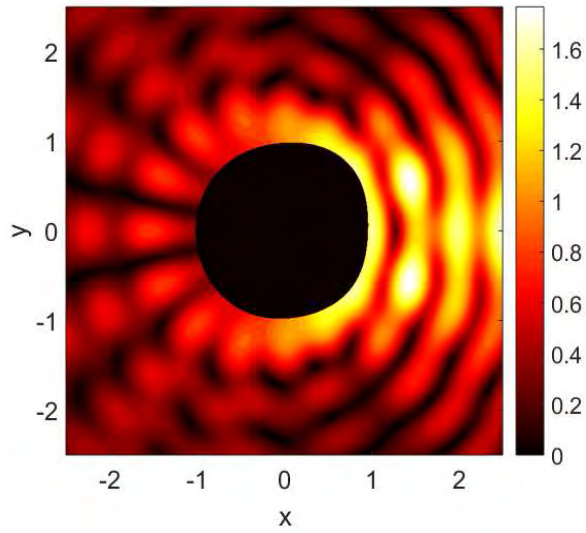
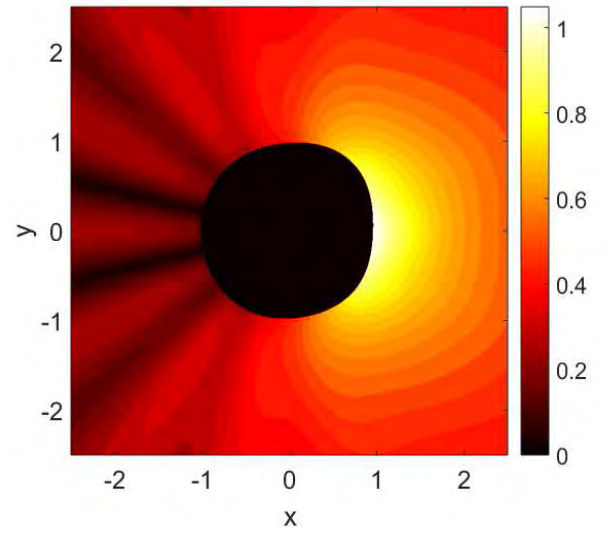
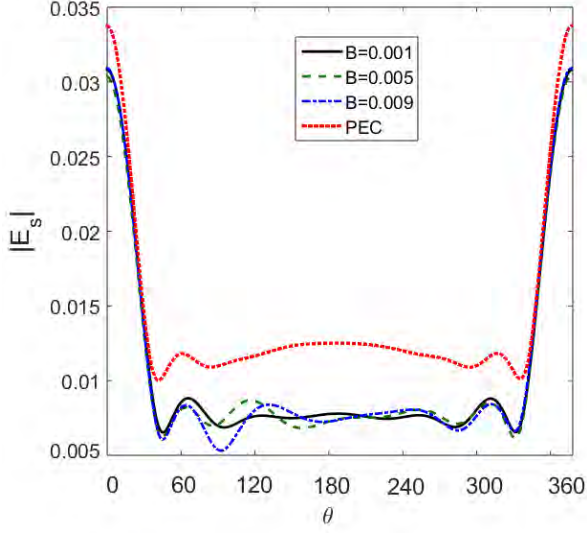
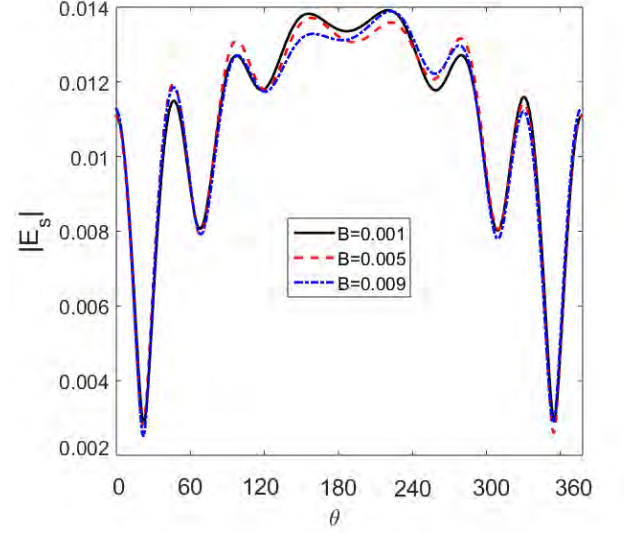
(a) Co polarized component,  $B = 0$ (b) Cross polarized component,  $B = 0$ (c) Co polarized component,  $B = 0.005$ .(d) Cross polarized component,  $B = 0.005$ .

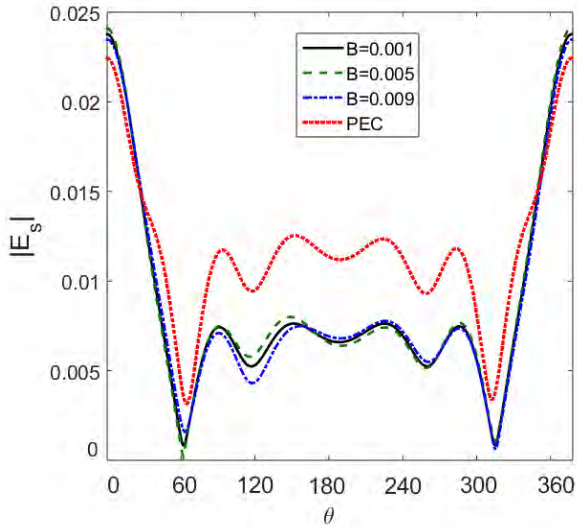
Figure 5.7: Same as Figure (5.6) except that a perturbed PEMC cylinder with mean radius  $a = 1\lambda$  is considered.



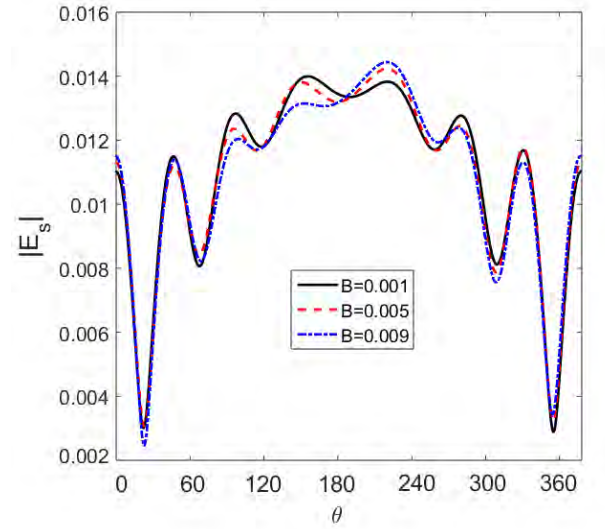
(a) Co polarized component, TM polarization



(b) Cross polarized component, TM polarization

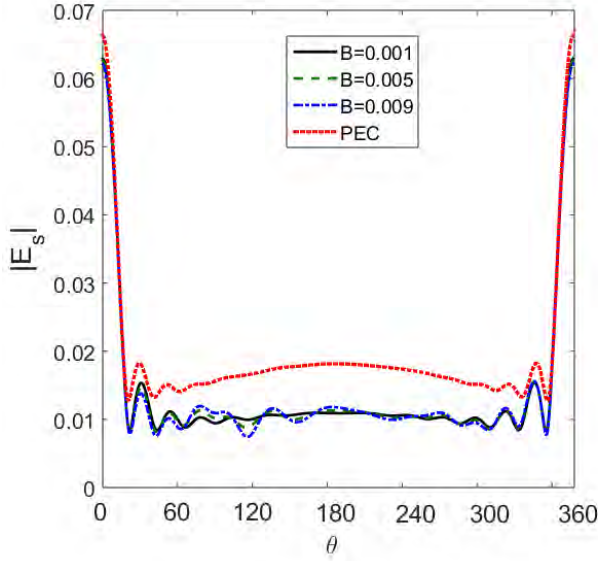


(c) Co polarized component, TE polarization

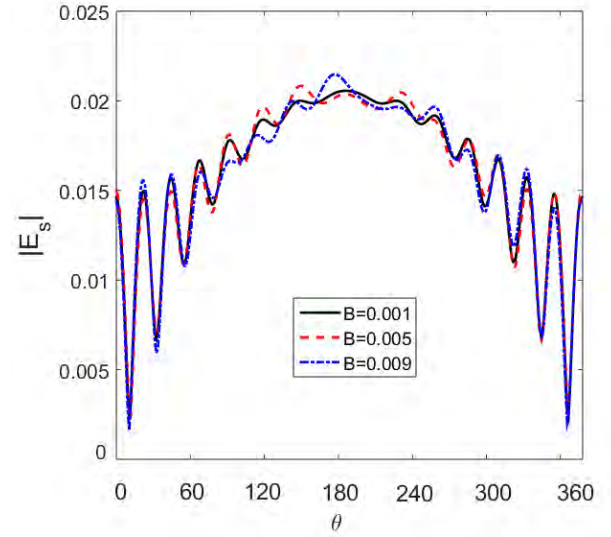


(d) Cross polarized component, TE polarization

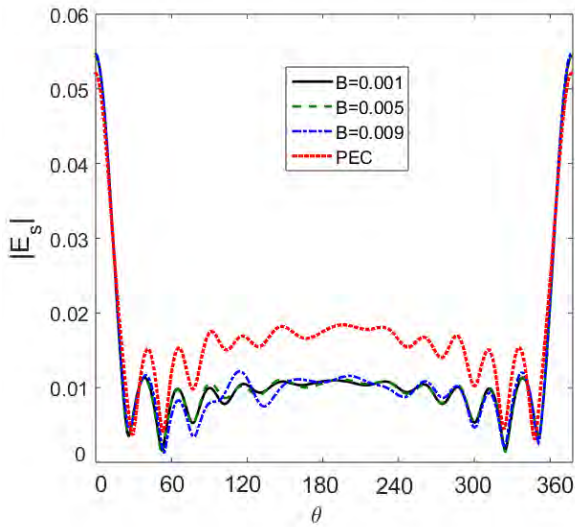
Figure 5.8: Scattered field from a perturbed PEMC cylinder for different values of the perturbation parameter  $B$  with mean radius  $a = 0.5\lambda$ ,  $M\eta_0 = 2$  and  $N=5$ .



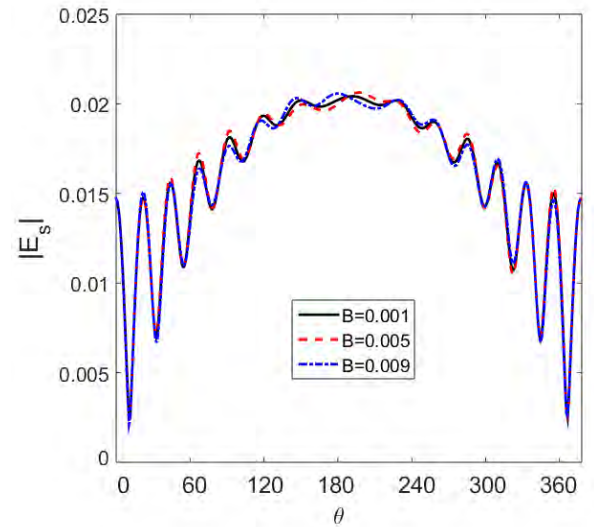
(a) Co polarized component, TM polarization



(b) Cross polarized component, TM polarization



(c) Co polarized component, TE polarization



(d) Cross polarized component, TE polarization

Figure 5.9: Same as Figure (5.8) except that a perturbed PEMC cylinder with mean radius  $a = 1\lambda$  is considered.

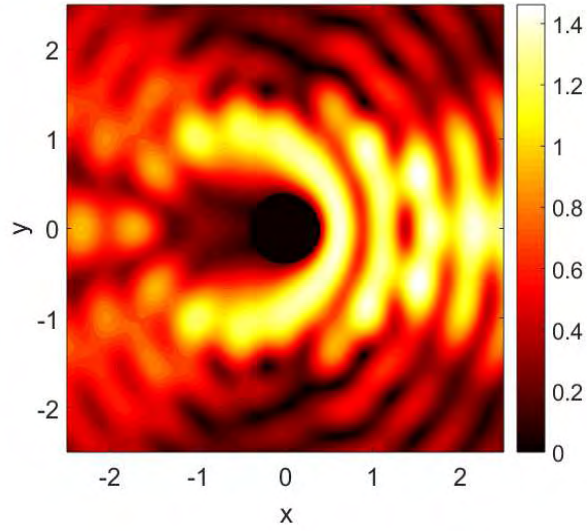
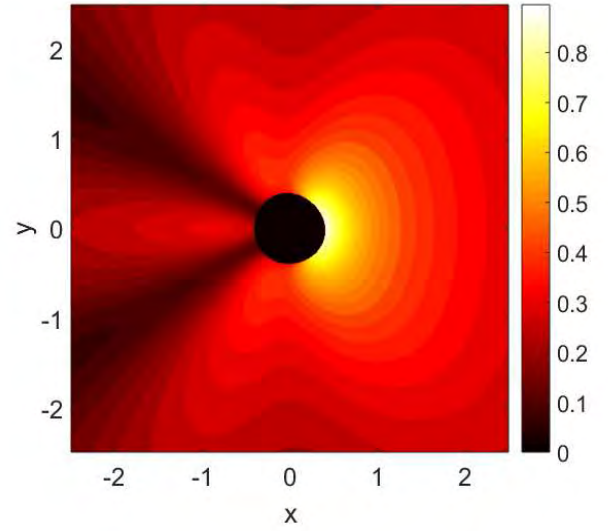
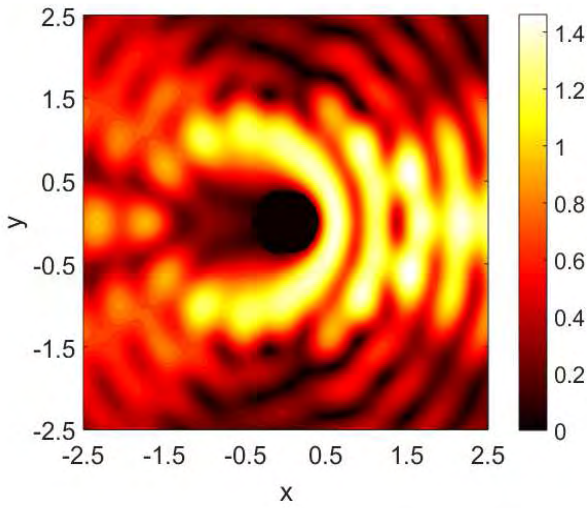
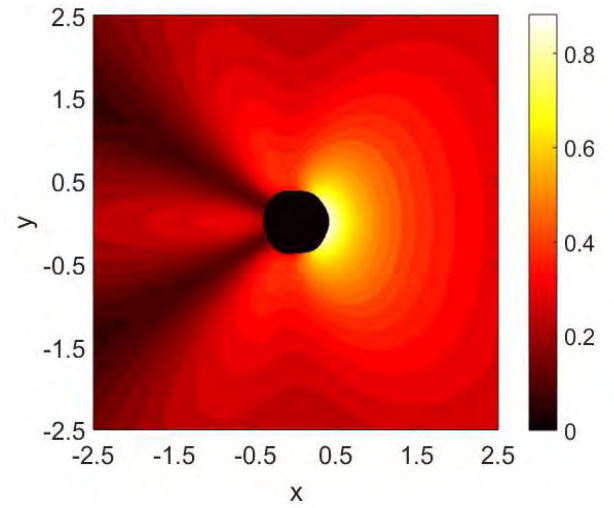
(a) Co polarized,  $B=0.001$ (b) Cross polarized,  $B=0.001$ (c) Co polarized,  $B=0.009$ (d) Cross polarized,  $B=0.009$ 

Figure 5.10: Two dimensional field map of the scattered field from a perturbed PEMC cylinder for different values of  $B$  with mean radius  $a = 0.5\lambda$ ,  $N = 5$  and  $M\eta_0 = 2$ . A TM polarized field is normally incident on the cylinder.



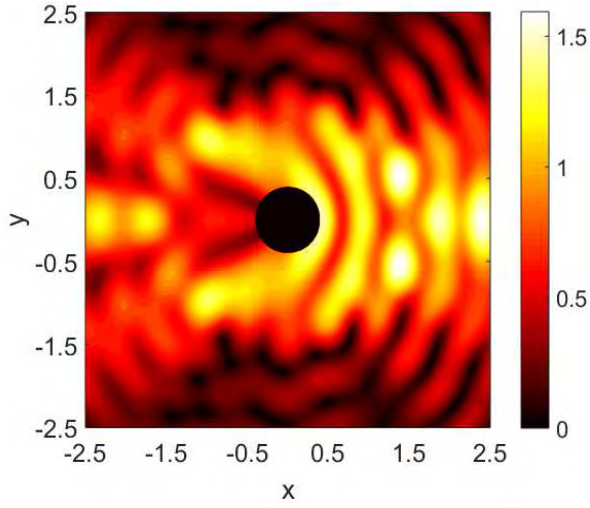
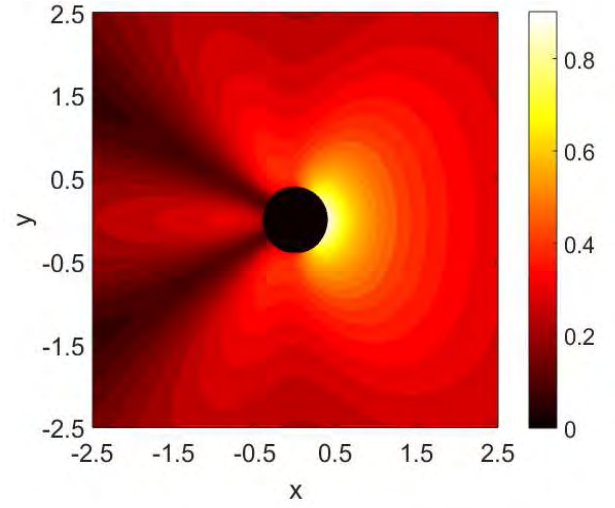
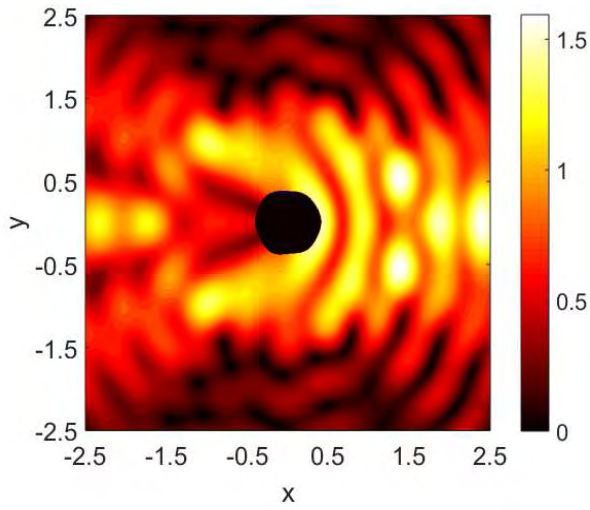
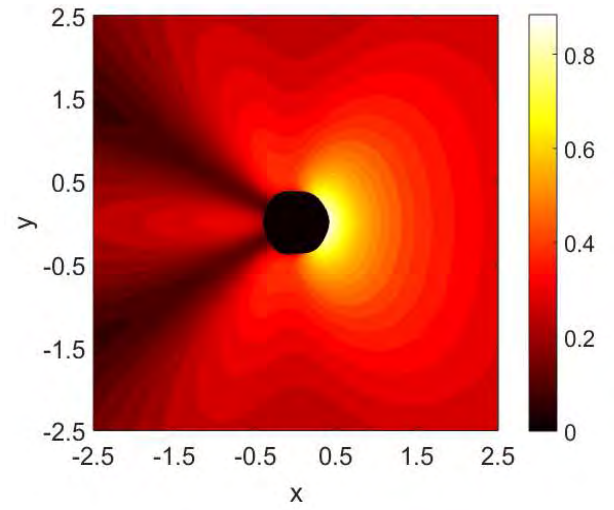
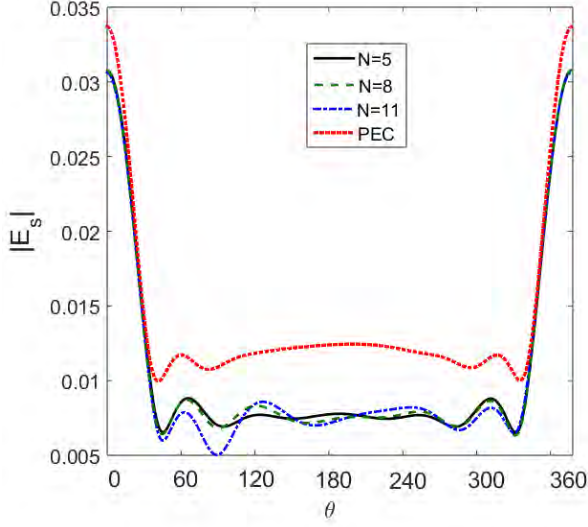
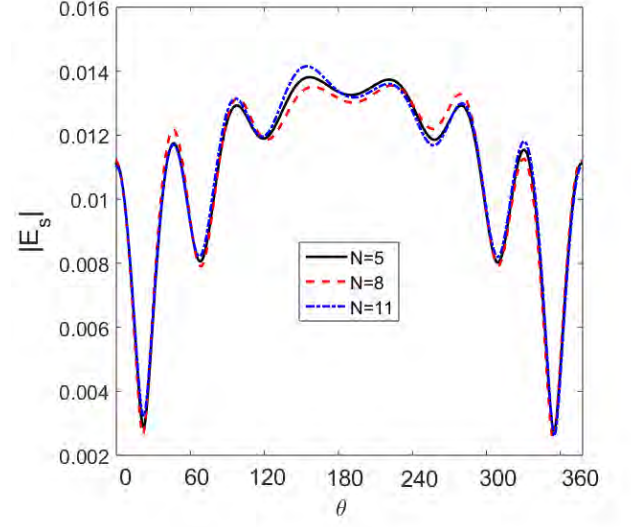
(a) Co polarized,  $B=0.001$ (b) Cross polarized,  $B=0.001$ (c) Co polarized,  $B=0.009$ (d) Cross polarized,  $B=0.009$ 

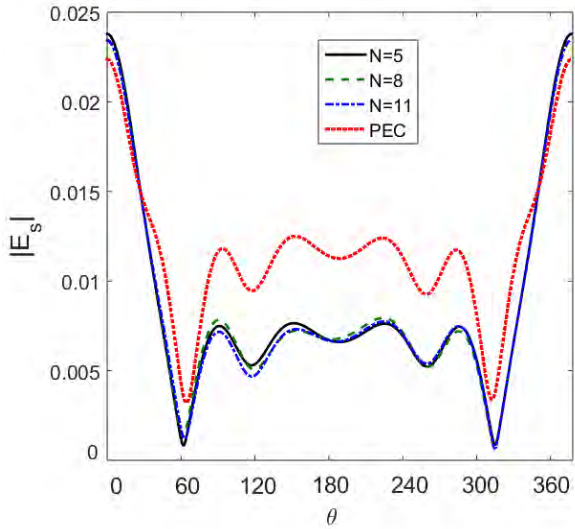
Figure 5.11: Same as figure (5.10) except that a TE polarized field is incident on the cylinder.



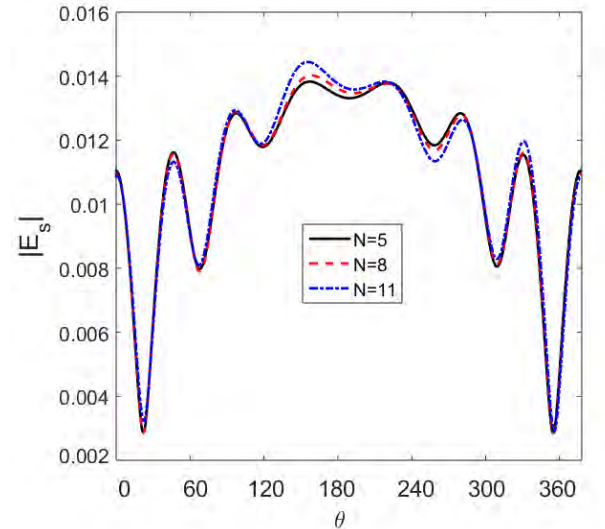
(a) Co polarized component, TM polarization



(b) Cross polarized component, TM polarization

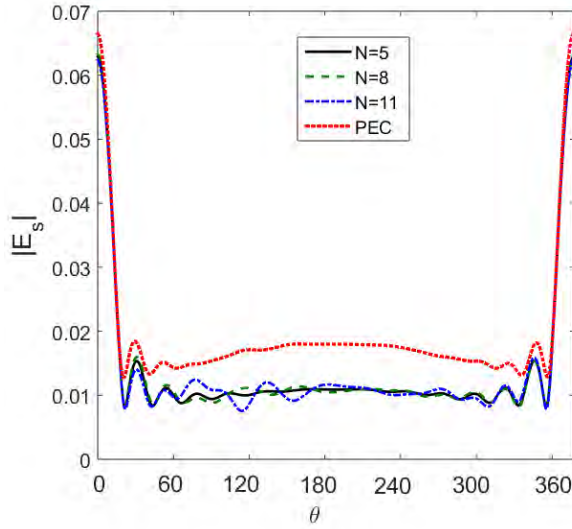


(c) Co polarized component, TE polarization

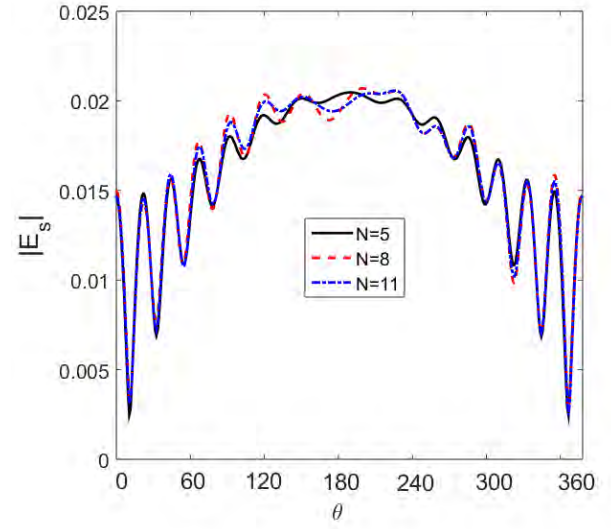


(d) Cross polarized component, TE polarization

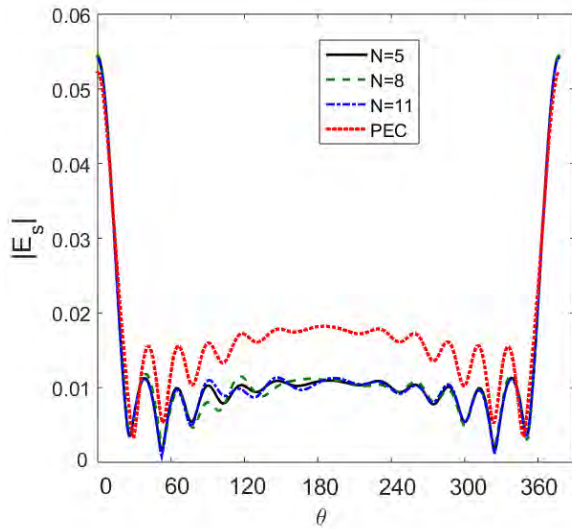
Figure 5.12: Scattered field from a perturbed PEMC cylinder for different values of  $N$  with mean radius  $a = 0.5\lambda$ ,  $M\eta_0 = 2$  and  $B=0.005$ .



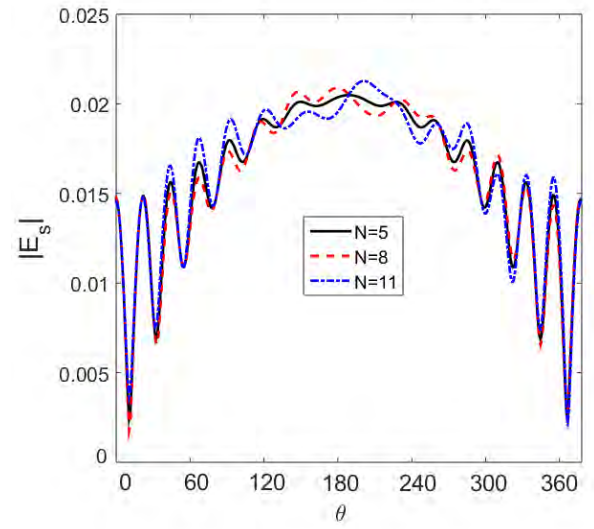
(a) Co polarized component, TM polarization



(b) Cross polarized component, TM polarization

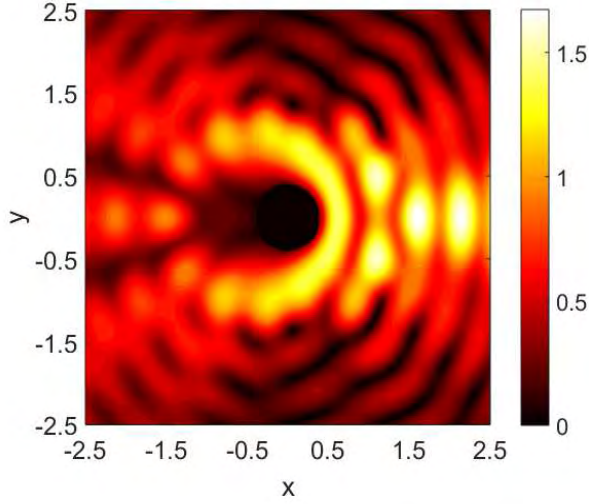


(c) Co polarized component, TE polarization

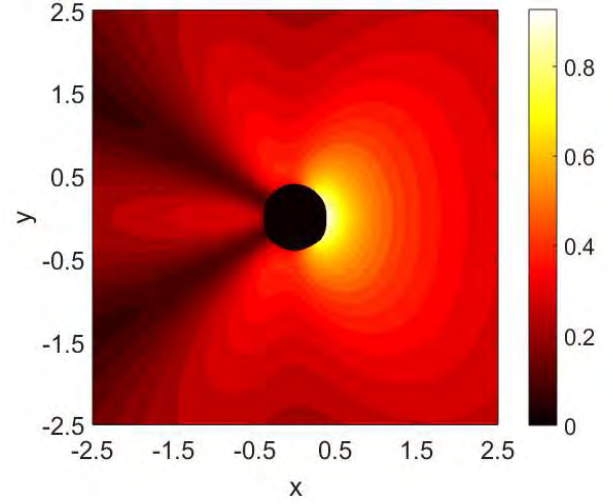


(d) Cross polarized component, TE polarization

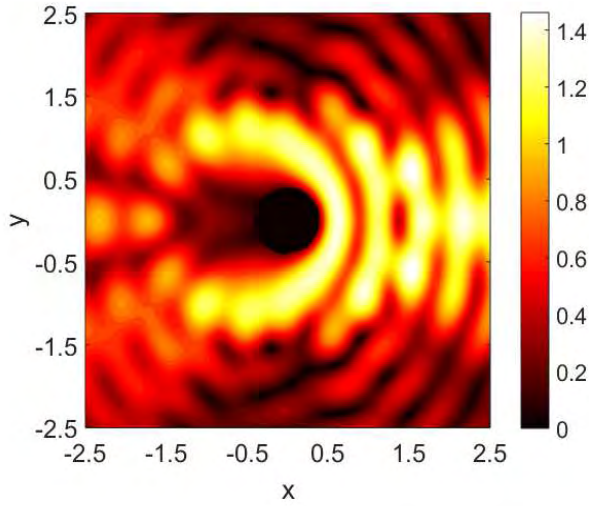
Figure 5.13: Same as Figure (5.12) except that a perturbed PEMC cylinder with mean radius  $a = 1\lambda$  is considered.



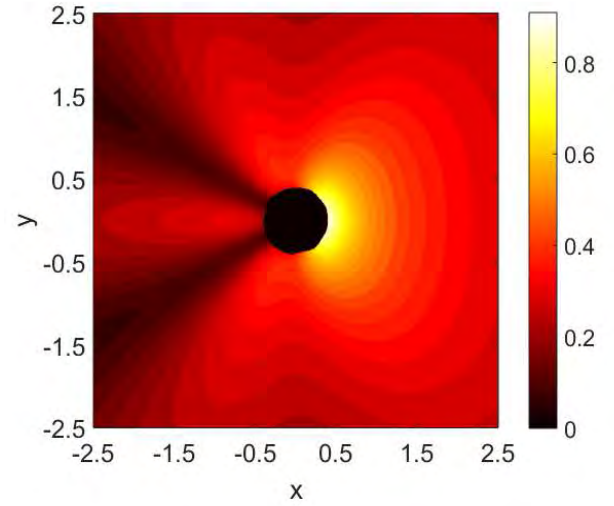
(a) Co polarized, N=8



(b) Cross polarized, N=8



(c) Co polarized, N=11



(d) Cross polarized, N=11

Figure 5.14: Two dimensional field map of the scattered field from a perturbed PEMC cylinder for different values of  $N$  with mean radius  $a = 0.5\lambda$ ,  $B = 0.005$  and  $M\eta_0 = 2$ . A TM polarized field is normally incident on the cylinder.



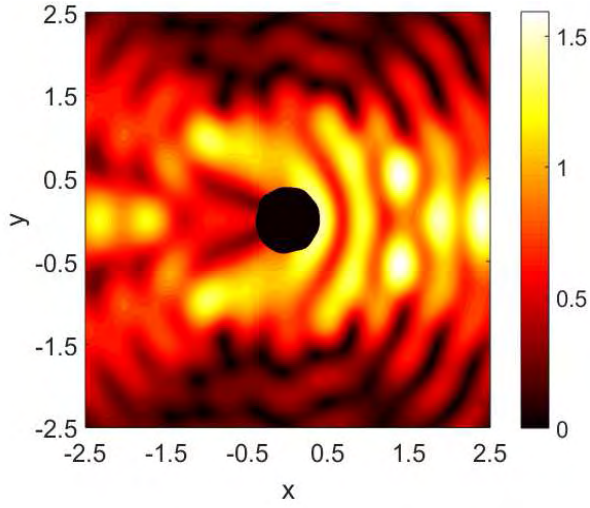
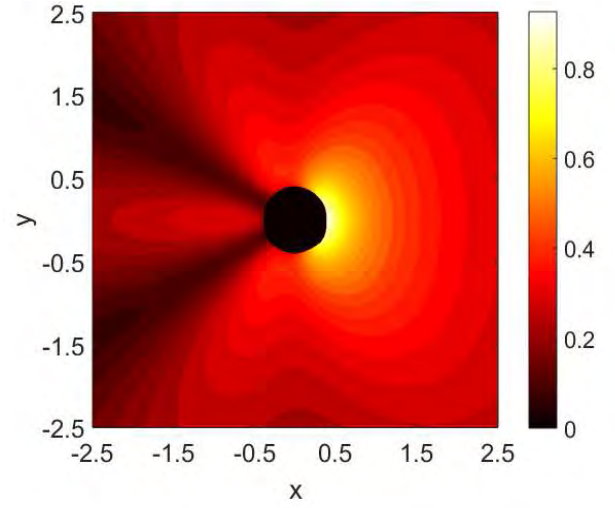
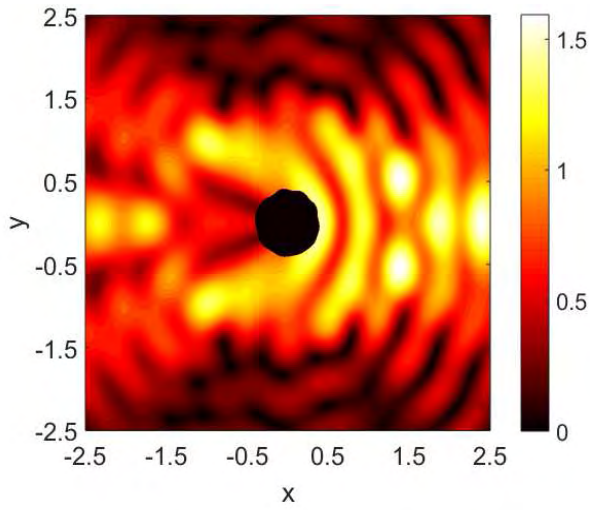
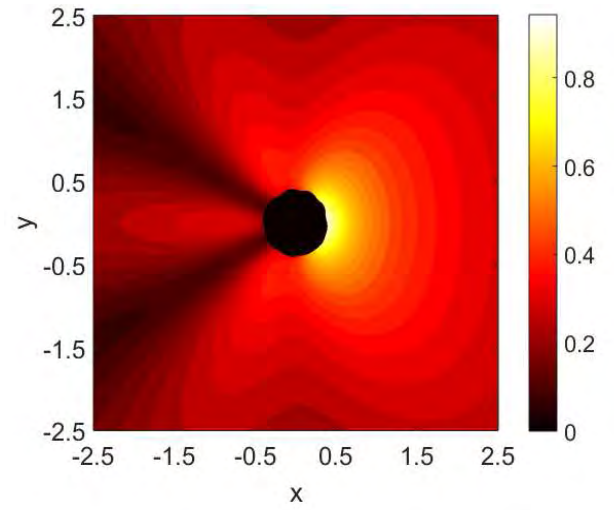
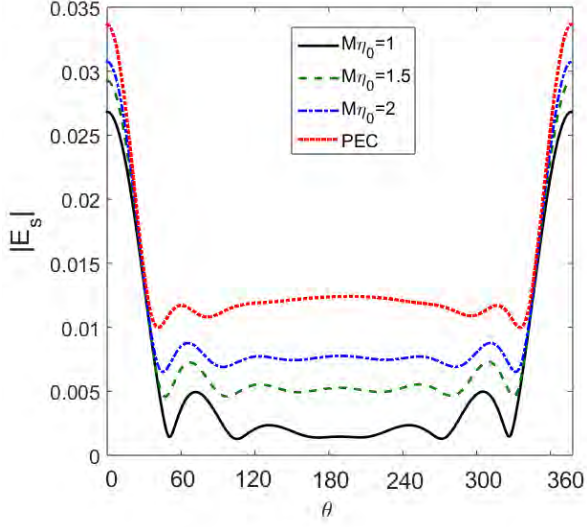
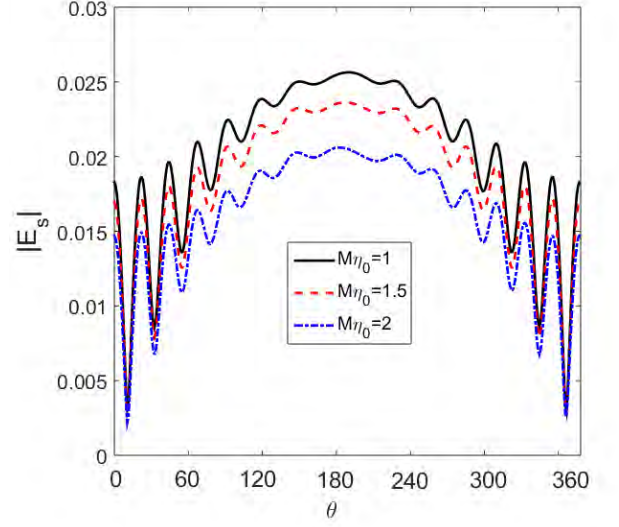
(a) Co polarized,  $N=8$ (b) Cross polarized,  $N=8$ (c) Co polarized,  $N=11$ (d) Cross polarized,  $N=11$ 

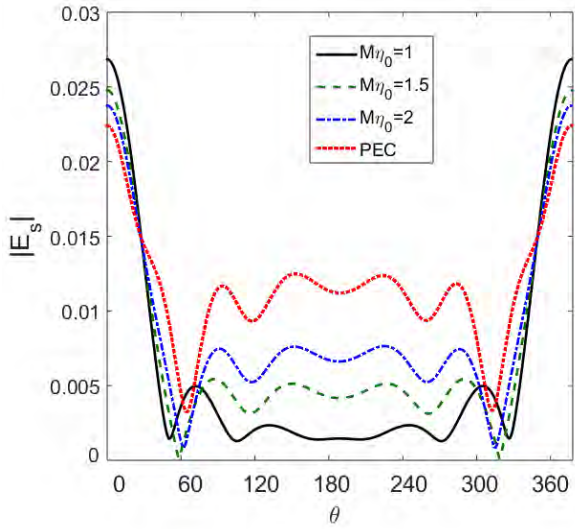
Figure 5.15: Same as figure (5.14) except that a TE polarized field is normally incident on the cylinder.



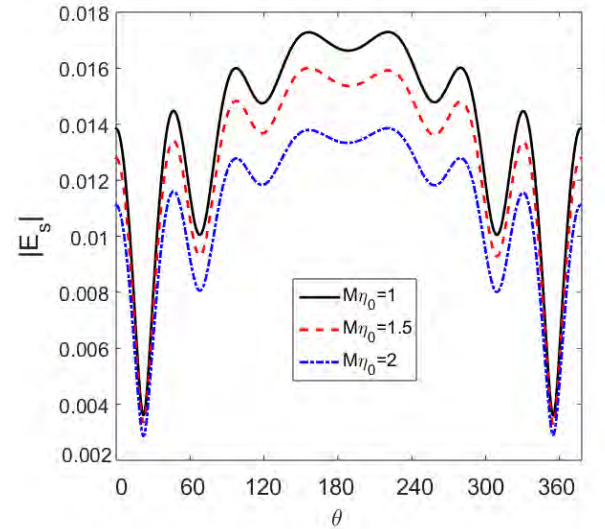
(a) Co polarized component, TM polarization



(b) Cross polarized component, TM polarization

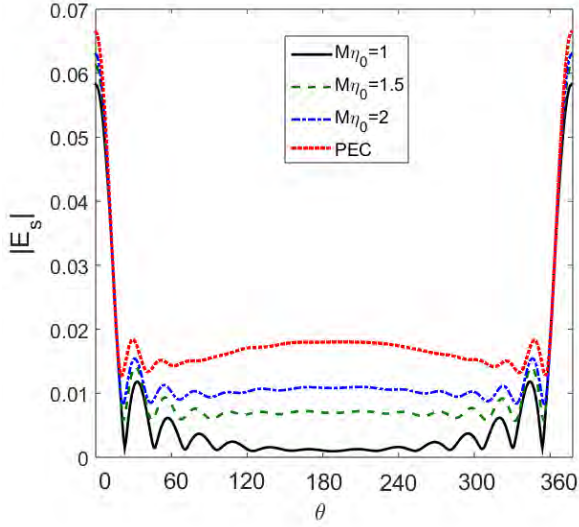


(c) Co polarized component, TE polarization

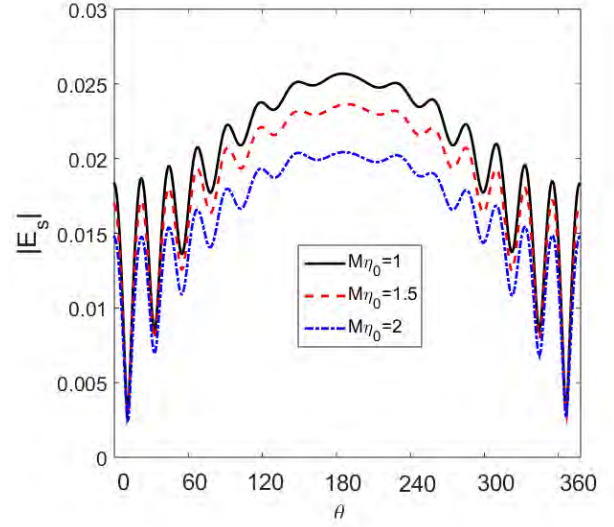


(d) Cross polarized component, TE polarization

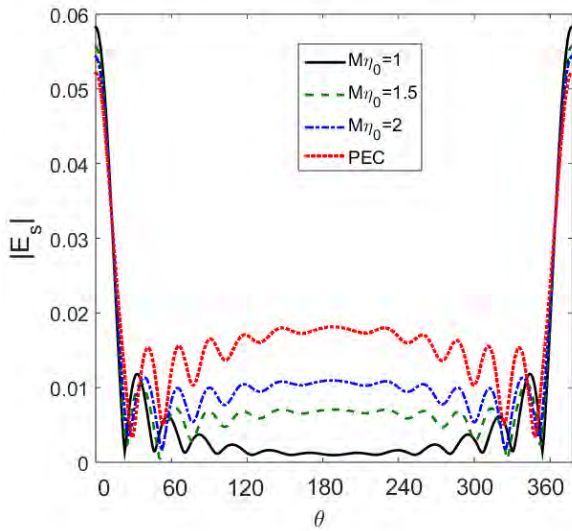
Figure 5.16: Scattered field from a perturbed PEMC cylinder for different values of  $M\eta_0$  with mean radius  $a = 0.5\lambda$ ,  $B = 0.005$  and  $N=5$ .



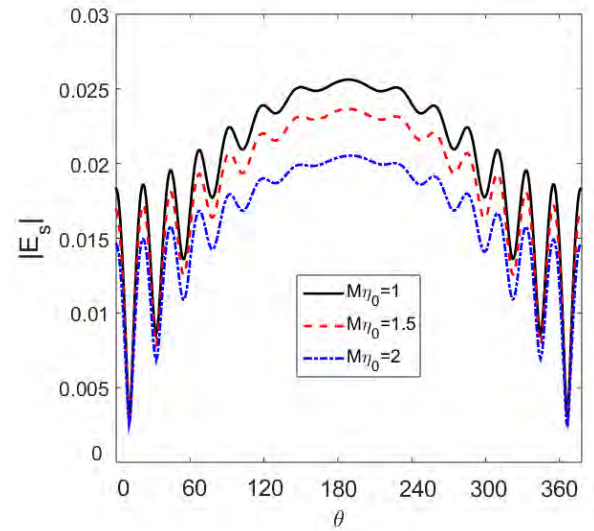
(a) Co polarized component, TM polarization



(b) Cross polarized component, TM polarization



(c) Co polarized component, TE polarization



(d) Cross polarized component, TE polarization

Figure 5.17: Same as Figure (5.16) except that a perturbed PEMC cylinder with mean radius  $a = 1\lambda$  is considered.

# Chapter 6

## Conclusion

First, average scattered field from a PEC/ PEMC cylinder of random radius with uniform and normal distribution is studied. Analysis is done for both TE and TM polarizations. Analytical expressions of average scattered field are derived for a very small cylinder and are also verified using numerical evaluation. It is shown that the average scattered field of a very small PEMC cylinder can be obtained by average scattered field from a very small PEC cylinder. For admittance  $M = 1/\eta_0$ , the co polarized scattered field is equal to  $\langle b_0 \rangle$  only and higher terms do not contribute i.e.,  $b_n \rightarrow 0 \forall, n \neq 0$ . In case of small and large cylinder, only numerical results can be obtained. This study shows that  $\langle \sigma \rangle$  for large PEC cylinder does not differ from  $\sigma_{\langle a \rangle}$  with uniform distribution. Difference is noticed for small cylinder. For large PEMC cylinder,  $\langle \sigma \rangle$  and  $\sigma_{\langle a \rangle}$  are almost the same for both co and cross polarized scattered fields. Very small difference is observed for cross polarized scattered field for small cylinder. In case of normal distribution of radius,  $\langle \sigma \rangle$  and  $\sigma_{\langle a \rangle}$  for both PEC and PEMC are same.

Secondly, scattering from a random PEC cylinder is studied using the relationship between the PT and RC generation model for shape perturbation. The numerical results obtained using the PT are compared well with the MoM. The variations are small for small values of  $B$  and  $N$  while an increase in the value of  $N$  and  $B$  results in large variations in the scattered field. Scattered field for TE polarized incidence is more sensitive to  $B$  and  $N$  as compared to TM polarized incidence. Near zone

scattering properties are observed in case of a perturbed PEMC cylinder. Near zone forward and backward scattering properties of the perturbed cylinder are compared with that of the circular cylinder and distinctions are pronounced. It is observed that the far field angular behavior of the scattered field shows little difference and near zone scattering pattern is more insightful to understand the scattering phenomenon. Finally, the variations of the co and cross polarized scattered field as a function of perturbation parameter  $B$  and admittance parameter  $M$  are noted. It is noticed that both  $N$  and  $B$  control the amount of roughness and affect the scattered field from the random cylinder.

# Chapter 7

## Appendix

### 7.1 Taylor series of $\frac{1}{z(a^2)}$ about $a = \langle a \rangle$

$$\begin{aligned} \frac{1}{z(a^2)} &= \frac{1}{\left(z(\langle a \rangle)\right)^2} + \frac{2(a - \langle a \rangle)\left(\frac{2i}{\pi}\right)}{\langle a \rangle \left(z(\langle a \rangle)\right)^3} \\ &+ \frac{(a - \langle a \rangle)^2 \left[ \frac{2i}{\pi} \left( -1 + \frac{2i}{\pi} (3 + \ln(k_0 \langle a \rangle)) \right) \right]}{\langle a \rangle^2 \left(z(\langle a \rangle)\right)^4} + \dots \end{aligned}$$

### 7.2 Evaluation of integral $I_1$

$$I_1 = \int_{a_1}^{a_2} \frac{A_c}{1 - \frac{2i}{\pi} \ln(k'_0 a)} da$$

$$u = 1 - \frac{2i}{\pi} \ln(k'_0 a)$$

$$da = -a \frac{\pi}{2i} du$$

$$a = \frac{1}{k'_0} e^{\frac{\pi}{2i}(1-u)}$$

$$z(a_1) = 1 - \frac{2i}{\pi} \ln(k'_0 a_1)$$

$$z(a_2) = 1 - \frac{2i}{\pi} \ln(k'_0 a_2)$$

$$I_1 = \frac{-\pi A_c e^{\frac{\pi}{2i}}}{2i} \int_{z(a_1)}^{z(a_2)} \frac{e^{\frac{-\pi u}{2i}}}{k'_0 u} da$$

$$I_1 = \frac{\pi^2 A_c e^{\frac{-i\pi}{2}}}{4k'_0} \int_{z(a_1)}^{z(a_2)} \frac{e^{\frac{-\pi u}{2i}}}{\frac{\pi u}{2i}} da$$

$$I_1 = -\frac{A_c e^{\frac{\pi}{2i}}}{k'_0} \left\{ E_1[z(a_2)] - E_1[z(a_1)] - \gamma \right\}$$

$E_1(z)$  can be calculated by the following relation given in [45]

$$E_1(z) = E_i(z) - \ln z - \gamma$$

where  $\gamma = 1.781$  and  $E_i(z)$  is the exponential integral defined as

$$E_i(z) = - \int_0^z \frac{1 - e^{-t}}{t} dt$$

### 7.3 Evaluation of integral $I_2$

$$I_2 = \int_{a_1}^{a_2} \frac{A_c}{\left[1 - \frac{2i}{\pi} \ln(k'_0 a)\right]^2} da$$

$$\left[ \frac{1}{1 - \frac{2i}{\pi} \ln(k'_0 a)} \right]' = \frac{2i}{a\pi} \frac{1}{\left[1 - \frac{2i}{\pi} \ln(k'_0 a)\right]^2}$$

Putting the above relation, we get

$$I_2 = \frac{\pi A_c}{2i} \int_{a_1}^{a_2} a \left[ \frac{1}{1 - \frac{2i}{\pi} \ln(k'_0 a)} \right]' da$$

$$I_2 = \frac{\pi A_c}{2i} \left[ \frac{a_2}{1 - \frac{2i}{\pi} \ln(k'_0 a_2)} - \frac{a_1}{1 - \frac{2i}{\pi} \ln(k'_0 a_1)} + \frac{i\pi}{2A_c} I_1 \right]$$

# References

- [1] C. A. Balanis, *Advanced Engineering Electromagnetics*, Wiley, New York, 2012.
- [2] R. Ruppin, “Scattering of electromagnetic radiation by a perfect electromagnetic conductor cylinder,” *Journal of Electromagnetic Waves and Applications*, Vol. 20, 1853-1860, 2006.
- [3] I. V. Lindell and A. H. Sihvola, “Realization of PEMC boundary,” *IEEE Transactions on Antennas and Propagation*, Vol. 53, 3012-3018, 2005.
- [4] I. V. Lindell and A. H. Sihvola, “Electromagnetic boundary and its realization with anisotropic metamaterial,” *Physical Review*, Vol. 79, 1-7, 2009.
- [5] N. Montaseri, M. Soleimani and A. Abdolali, “Realization of the perfect electromagnetic conductor circular cylinder using anisotropic media,” *Progress In Electromagnetics Research*, Vol. 25, 173-184, 2012.
- [6] A. Shahvarpour, T. Koderá, A. Parsa and C. Caloz, “Arbitrary electromagnetic conductor boundaries using Faraday rotation in a grounded ferrite slab,” *IEEE Transactions on Microwave Theory and Techniques*, Vol. 58, 2781-2793, 2010.
- [7] C. Caloz, A. Shahvarpour, D. L. Sounas, T. Koderá, B. Gurlek and N. Chamanara, “Practical realization of perfect electromagnetic conductor (PEMC) boundaries using ferrites, magnet-less non reciprocal metamaterials (MNMs) and graphene,” *In Proceedings of 2013 URSI, International Symposium on Electromagnetic Theory*, 652- 655, 2013.



- [8] J. R. Wait, "Scattering of a plane wave from a circular dielectric cylinder at oblique incidence," *Canadian Journal of Physics*, Vol. 33, 189-195, 1955.
- [9] A. Z. Elsherbeni and M. Hamid, "Scattering by parallel conducting circular cylinders," *IEEE transactions on antennas and propagation*, Vol. 35, 355-358, 1987.
- [10] K. Hongo, "Multiple scattering by two conducting cylinders," *IEEE transactions on antennas and propagation*, Vol. 26, 748-751, 1978.
- [11] A. Z. Elsherbeni, M. Hamid, and G. Tian, "Iterative scattering of a gaussian beam by an array of circular conducting and dielectric cylinders," *Journal of Electromagnetic Waves and Applications*, Vol. 7, 1323-1342, 1993.
- [12] A. Z. Elsherbeni, "A comparative study of two-dimensional multiple scattering techniques," *Radio Science*, Vol. 29, 1023-1033, 1994.
- [13] W. Y. Yin, L. W. Li, and M. S. Leong, "Scattering from multiple bi-anisotropic cylinders and their modeling of cylindrical objects of arbitrary cross-section," *Progress In Electromagnetics Research*, Vol. 27, 159-184, 2000.
- [14] B. H. Henin, A. Z. Elsherbeni and M. Al. Sharkawy, "Oblique incidence plane wave scattering from an array of circular dielectric cylinders," *Progress In Electromagnetics Research*, Vol. 68, 261-279, 2007.
- [15] A. K. Hamid and F. R. Cooray, "Scattering by a Perfect Electromagnetic Conducting Elliptic Cylinder," *Progress In Electromagnetics Research Letters*, Vol. 10, 59-67, 2009.
- [16] A. Shooshtari and A. R. Sebak, "Electromagnetic scattering by parallel metamaterial cylinders," *Progress In Electromagnetics Research*, Vol. 57, 165-177, 2006.
- [17] S. Ahmed and Q. A. Naqvi, "Electromagnetic scattering from a perfect electromagnetic conductor circular cylinder coated with a metamaterial having negative permittivity and/or permeability," *Optics Communications*, Vol. 281, 5664-5670, 2008.

- [18] S. Ahmed, F. Manan, A. Shahzad and Q. A. Naqvi, "Electromagnetic scattering from a chiral-coated PEMC cylinder," *Progress In Electromagnetics Research*, Vol. 19, 239-250, 2011.
- [19] F. R. Cooray and A. K. Hamid, "Scattering from a coated perfect electromagnetic conducting elliptic cylinder," *International Journal of Electronics and Communications*, Vol. 66, 472-479, 2012.
- [20] N. Montaseri, A. Abdolali, M. Soleimani, and V. Nayyeri, "Plane wave scattering by a circular PEMC cylinder coated with anisotropic media," *International Journal of RF and Microwave Computer-Aided Engineering*, Vol. 23, 225-231, 2013.
- [21] A. Ghaffar, M. Z. Yaqoob, M. A. Alkanhal, M. Sharif, and Q. A. Naqvi, "Electromagnetic scattering from anisotropic plasma-coated perfect electromagnetic conductor cylinders," *International Journal of Electronics and Communications*, Vol. 68, 767-772, 2014.
- [22] F. Frezza, L. Pajewski and G. Schettini, "A spectral-domain solution for the scattering problem of a circular cylinder buried in a dielectric half-space," *Progress In Electromagnetics Research*, Vol. 38, 223-52, 2002.
- [23] M. D. Vico, F. Frezza, L. Pajewski and G. Schettini, "Scattering by buried dielectric cylindrical structures," *Radio Science*, Vol. 40, 1-11, 2005.
- [24] M. D. Vico, F. Frezza, L. Pajewski and G. Schettini, "Scattering by a finite set of perfectly conducting cylinders buried in a dielectric half-space: a spectral-domain solution," *IEEE Transactions on Antennas and Propagation*, Vol. 53, 719-727, 2005.
- [25] C. Ponti and S. Vellucci, "Scattering by conducting cylinders below a dielectric layer with a fast noniterative approach," *IEEE Transactions on Microwave Theory and Techniques*, Vol. 63, 30-39, 2014.

- [26] S. Ahmed and Q. A. Naqvi, "Electromagnetic scattering from a perfect electromagnetic conductor cylinder buried in a dielectric half space," *Progress In Electromagnetics Research*, Vol. 78, 25-38, 2008.
- [27] M. A. Fiaz and M. A. Ashraf, "Scattering of two-dimensional field from a PEMC cylinder buried beneath slightly rough surface," *Journal of Electromagnetic Waves and Applications*, Vol. 28, 470-484, 2014.
- [28] A. Ahmad and M. A. Fiaz, "Scattered field from a PEMC cylinder buried below rough interface using extended boundary condition method," *Optik*, Vol. 193, 162572, 2019.
- [29] S. O. Rice, "Reflection of electromagnetic waves from slightly rough surfaces," *Communications on Pure and Applied Mathematics*, Vol. 4, 351-378, 1951.
- [30] D. E. Cartwright and M. S. L. Higgins, "The statistical distribution of the maxima of a random function, proceedings of the royal society of London," *Series A, Mathematical and Physical Sciences*, Vol. 237, 212-232, 1956.
- [31] D. Liang, P. Xu, L. Tsang, Z. Gui, and K. S. Chen, "Electromagnetic scattering by rough surfaces with large heights and slopes with applications to microwave remote sensing of rough surface over layered media," *Progress In Electromagnetics Research*, Vol. 95, 199-218, 2009.
- [32] Z. Lin, X. Zhang, and G. Fang, "Theoretical model of electromagnetic scattering from 3D multi-layer dielectric media with slightly rough surfaces," *Progress In Electromagnetics Research*, Vol. 96, 37-62, 2009.
- [33] G. Mittal and D. Singh, "Critical analysis of microwave scattering response on roughness parameter and moisture content for periodic rough surfaces and its retrieval," *Progress In Electromagnetics Research*, Vol. 100, 129-152, 2010.
- [34] D. E. Lawrence and K. Sarabandi, "Acoustic and electromagnetic wave interaction: estimation of doppler spectrum from an acoustically vibrated metallic

- circular cylinder,” *IEEE Transactions on Antennas and Propagation*, Vol. 51, 1499-1507, 2003.
- [35] D. E. Lawrence and K. Sarabandi, “Acoustic and electromagnetic wave interaction: Analytical formulation for acousto-electromagnetic scattering behavior of a dielectric cylinder,” *IEEE Transactions on Antennas and Propagation*, Vol. 49, 1382-1392, 2001.
  - [36] A. Ditkowski and Y. Harness, “Wave scattering by randomly shaped objects,” *Applied Numerical Mathematics*, Vol. 62, 1819-1836, 2012.
  - [37] R. Trivedi and U. K. Khankhoje, “A perturbative solution to plane wave scattering from a rough dielectric cylinder,” *IEEE Transactions on Antennas and Propagation*, Vol. 63, 4069-4080, 2015.
  - [38] M. A. Ashraf and A. A. Rizvi, “Electromagnetic scattering from a random cylinder by moments method ,” *Journal of Electromagnetic Waves and Applications*, Vol. 25, 467-480, 2011
  - [39] F. Masood, U. Amin, M. A. Fiaz and M. A. Ashraf, “On relating the perturbation theory and random cylinder generation to study scattered field,” *Physical Communication*, Vol. 39, 101003, 2020.
  - [40] M. A. Fiaz, M. A. Ashraf and A. A. Rizvi, “Average scattered field from a random PEC cylinder buried below a slightly rough surface,” *Waves in Random and Complex Media*, Vol. 0, 1-16, 2017.
  - [41] F. Masood and M. A. Fiaz, “Evaluation of average cross-polarised scattered field from a PEMC cylinder of the random radius with uniform/normal distribution,” *IET Microwaves, Antennas and Propagation*, Vol. 13, 804-812, 2019.
  - [42] F. Masood, M. A. Fiaz and M. A. Ashraf, “On applying the perturbation theory for the evaluation of near zone scattering properties of a perturbed PEMC cylinder,” *Accepted for publication in Optik*, 2021.

- [43] C. Eftimiu, “Electromagnetic scattering by rough conducting circular cylinders I: Angular corrugation; II: Axial corrugation.” *IEEE Transactions on Antennas and Propagation*, Vol. 36, 651–658, 659–663, 1988.
- [44] H. Ogura and H. Nakayama, “Scattering of waves from a random cylindrical surface.” *Mathematical Physics*, Vol. 29, 851–860, 1988.
- [45] M. Abramowitz, I. A. Stegun, *Handbook of mathematical functions with formulas, graphs, and mathematical tables*. Washington (DC): U.S. Government Printing Offices; 1972.

# Turnitin Originality Report

Average Scattered Field From a PEMC Cylinder With Random Rastina  
Masood

by Fahad



From DRSM (DRSM L)

- Processed on 27-Sep-2021 11:17 PKT
- ID: 1658523314
- Word Count: 13193

Similarity Index

12%

Similarity by Source

Internet Sources:

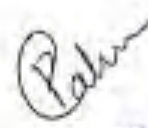
1%

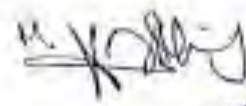
Publications:

11%

Student Papers:

1%

  
Focal Person (Turnitin)  
Quaid-I-Azam University  
Islamabad

  
Assistant Professor  
Department of Electronics  
Quaid-I-Azam University  
Islamabad

sources:

- 1 4% match (publications)  
Muhammad Arshad Fiaz, Muhammad Aqueel Ashraf, Azhar Abbas Rizvi, "Average scattered field from a random PEC cylinder buried below a slightly rough surface", Waves in Random and Complex Media, 2017
- 2 1% match (publications)  
Ashfaq Ahmad, Muhammad Arshad Fiaz, "Near zone scattering and extinction properties of a left-handed material cylinder buried in a semi infinite medium with rough interface", Journal of Modern Optics, 2019
- 3 1% match (publications)  
Ashfaq Ahmad, Muhammad Arshad Fiaz, "Scattered field from a PEMC cylinder buried below rough interface using extended boundary condition method", Optik, 2019
- 4 1% match (publications)  
Gu Xu, "DIAGONAL HORN GAUSSIAN EFFICIENCY ENHANCEMENT BY DIELECTRIC LOADING FOR SUBMILLIMETER WAVE APPLICATION AT 150 GHz", Progress In Electromagnetics Research, 2011
- 5 1% match (publications)  
M. A. Ashraf, A. A. Rizvi, "Electromagnetic Scattering from a Random Cylinder by Moment Method", Journal of Electromagnetic Waves and Applications, 2012
- 6 < 1% match (student papers from 01-Oct-2016)  
Submitted to Higher Education Commission Pakistan on 2016-10-01

< 1% match (student papers from 01-Oct-2016)

C:\Users\Dr Arshad Fiaz\Downloads\Turnitin\_Originality\_Report.html